Analysis of Different Structures of Patch Antennas

Bashar Bahaa Noori Qas Elias

Submitted to the
Institute of Graduate Studies and Research
in partial fulfillment of the requirements for the Degree of

Master of Science
in
Electrical and Electronic Engineering

Eastern Mediterranean University
January 2014
Gazimağusa, North Cyprus

Approval of the Institute of Graduate Studies and Research

Prof. Dr. Elvan Yılmaz
Director

I certify that this thesis satisfies the requirements as a thesis for the degree of Master of Science in Electrical and Electronic Engineering.

Prof. Dr. Aykut Hocanın
Chair, Department of Electrical and Electronic Engineering

We certify that we have read this thesis and that in our opinion it is fully adequate in scope and quality as a thesis for the degree of Master of Science in Electrical and Electronic Engineering.

Assist. Prof. Dr. Rasime Uyguroğlu
Supervisor

Examining Committee

1. Prof. Dr. Şener Uysal
2. Assoc. Prof. Dr. Hasan Demirel
3. Asst. Prof. Dr. Rasime Uyguroğlu

ABSTRACT

In this thesis, Method of Moment (MoM) based FEKO software version 5.5 was used to simulate patch antennas in different structures. For patch antennas, some of the fields are in the substrate and some of them in air. Due to this reason, it is necessary to calculate the effective dielectric constant which affects the resonant frequency and the wavelength of the wave in the substrate. Simulations were carried out to compute the value of effective dielectric constant of a single substrate layer which has a relative permittivity equal to 2.2 by making use of the standing wave pattern (SWP) generated by FEKO. After that, microstrip patch antennas were simulated based on multi-substrate layers instead of a single layer. Square, circular and triangular patches were simulated by FEKO and the resonant frequencies obtained were compared with other published (experimental, analytical, simulations by other methods) works. The results are close (from 1 to 3GHz difference) for different modes of the circular patch, while they were equal at 4.02 GHz and 7.03 GHz for the triangular and square patches respectively.

Slot antennas are used to enhance the bandwidths, but slots may affect the relative permittivity. i.e. the effective permittivity. Triangular and square shape slot antennas were simulated by FEKO and the results were compared among themselves and with the published result for the triangular slot. The results very close.

Slots on the patch are widely used. Here a triangular slot for various heights was simulated by FEKO for the rectangular patch. If has been observed that the resonance frequency reduces by the increase of the height. The optimum height for

the given design was recorded. Also, circular slots were applied inside the circular patch to improve the return loss, voltage standing wave ratio and the bandwidth.

Defected ground structures (DGS) in different shapes (rectangular, phi-shape, c-shape and plus-shape) were used to solve the surface wave problem which is a drawback for patch antennas. The use of this method resulted in gain enhancement.

Gain was enhanced by using patch antenna array topology. In this thesis, a 4 element array antenna was designed at 2 GHz and simulated by FEKO. A maximum gain of 13.1dB dB was achieved.

Keywords: Effective Dielectric Constant, Gain, return loss, Patch Antenna, Patch Array Antenna.

ÖZ

Bu tez çalışmasında Moment Metodu temelli FEKO yazılım programı kullanılarak, değişik yama antenlerin simülasyonu yapılmıştır. Yama antenlerde, sıçramadan ötürü elektrik alanının bir kısmı dielektrik içerisinde iken, bir kısmı havaya sıçradığından , efektif dielektrik sabiti, bağıl permitivite değerinden farklılık gösterir. Efektif dielektrik sabitinin resonant frekansına etkisi bilindiğinden, FEKO simülatörü kullanılarak elde edilen durgun dalga grafiği aracılığı ile bağıl permitivite değeri 2.2 olan bir dielektriğin, efektif değeri hesaplanıp, literatür değerleri ile karşılaştırma yapılmıştır. Daha sonra, çok katmanlı dielektrik maddeler için de benzer çalışma yapılmıştır. Kare, daire ve üçgen yama antenler FEKO simülatörü kullanılarak resonat frekansı hesaplamaları yapılmış, litedatürdeki benzeri tasarım değerlerine uygumlu neticeler elde edilmiştir. Daire yama anten için resonant değerinde 1-3GHz gibi bir fark mevcutken, üçgen ve kare yama anten resonant değerleri eşit bulunmuştur.

Delik antenler, genişband elde etmek için kullanılmaktadır ancak, efektif permitivite değerinin hesaplanması gerekmektedir. FEKO simülatörü kullanılarak üçgen ve dikdörtgen delik antenlerin efektif permitivite değerleri hesaplanmış ve yayınlanmış değerlere çok yakın değerler elde edilmiştir.

Yama antenlede yarıklar sıkça uygulanmaktadır. FEKO simülatötü aracılığı ile değişik yüksekte üçgen yarıklar uygulanmış, yarıkların yükseklikleri arttıkça resonant frekansının azaldığı gözlemlenmiş ve geri dönüş kayıbı için en iyi tasarım hükseklik değeri tesbit edilmiştir. Ayrıca, daire yama antene uygulanan dairesel

yarıkların resonat frekansı ve geri dönüş yansıma katsayısı üzerindeki etkileri incelenmiştir.

Referans iletken üzerinde dikdörtgen, C ve + şeklinde boşluklar açarak anten kazancı artırılmıştır.

Dizi yama antenler kullanılarak anten performansını artırmak mümkündür. Bu tezde 2GHz frekansında dört elemanlı bir dizi anten tasarımı önerilmiş, 13.1 dB değerinde maximum kazanç elde edilmiştir.

Anahtar Kelimeler: Efektif dielektrik sabiti, Kazanç, geri dönüş kazancı, yama anten, dizi anten

ACKNOWLEDGMENTS

I would like to express my sincere thanks to my supervisor Assist. Prof. Dr. Rasime Uyguroğlu for supporting and guiding me throughout this thesis and for her valuable contributions in the implementation of this work.

I greatly thank all staff in my faculty, and specially to Prof. Dr. Aykut Hocanın, the Chair of Electrical and Electronic Engineering and Assoc. Prof. Dr. Hasan Demirel. They have greatly advised me and helped me make a lot of decisions during my study.

My warmest thanks and deepest appreciation to my family, I can not find enough words to express my gratitude towards them for their encourage and for standing by me, and supporting me to complete this work.

Last but not the least I am grateful to all my friends who participated directly or indirectly in finish this work.

TABLE OF CONTENTS

ABSTRACT iii

ACKNOWLEDGMENTS vii

LIST OF TABLES xi

LIST OF FIGURES xiii

LIST OF SYMBOLS /ABBREVIATIONS xvii

1 INTRODUCTION 1

1.1 Thesis Objectives 2

1.2 Thesis Overview 2

2 ANTENNAS 4

2.1 Antenna Definition 4

2.2 Antenna Parameters 5

2.2.1 Return Loss: 5

2.2.2 Bandwidth: 5

2.2.3 Gain and Directivity: 6

2.2.4 Voltage Standing Wave Ratio (VSWR): 7

2.2.5 Radiation Pattern: 7

2.3 Microstrip Patch Antenna 7

2.3.1 Advantages and Disadvantages of Microstrip Patch Antennas 9

2.3.2 Feeding Methods 10

2.3.3 Patch Array 13

2.3.4 Analysis Models of the Microstrip Patch Antennas 14

3 MICROSTRIP PATCH ANTENNA SIMULATIONS BY USING FEKO 5.5 SIMULATION SOFTWARE 20

3.1 Overview – FEKO Simulation 20

3.2 Introduction 21

3.3 Calculation of the ε_{reff} by using the Guiding Wavelength of a Microstrip Line 22

3.3.1 Effective Dielectric Constant Calculation by using SWP 24

3.4 Simulations of Patch Antennas Having Multi Substrate Layers 27

3.4.1 Circular Patch Antenna 27

3.4.2 Triangular Patch Antenna 35

3.4.3 Square Patch Antenna 38

3.5 Slot Antennas 42

3.5.1 FEKO Simulation Results of a Printed Isosceles Triangular Slot 43

3.5.2 FEKO Simulation Results for The Square Slot 46

3.6 Effects of Feed Techniques for The Patch Antennas 48

3.6.1 Probe Feed Varying in RMSA 48

3.6.2 Microstrip Line Feed Shifting in RMSA 55

4 PATCH ANTENNA SIMULATIONS BY USING FEKO AND IMPROVEMENTS IN THE RETURN LOSS, GAIN AND BANDWIDTH 59

4.1 Introduction 59

4.2 Effects of Triangular Slot Loading on Resonance Frequency of Patch Antennas 60

4.3 Improvement Return loss, VSWR and Bandwidth in Circular Patch Antenna 62

4.3.1 Case I: Annular Slot Patch Antenna 64

4.3.2 Case II: Inner Circular Slots Ring Shaped (cross shape within the ring) . 66

4.3.3 Case III: Inner Circular Slots in a Square Shape 67

4.4 Rectangular Aperture Coupled Antenna and Gain Improvement in Wireless Applications. 70

4.4.1 Effect of Rectangular Aperture Width (W_{ap}) in Microstrip Antenna..... 72

4.4.2 Effect of Rectangular Aperture Length (L_{ap}) in Microstrip Antenna 73

4.4.3 Effect of Length Stub (L_m) in Microstrip Antenna..... 74

4.4.4 Gain Improvement by using Different Shapes of Aperture Slot Antenna 75

5 PATCH ARRAY ANTENNA 84

5.1 Analysis and Design of a Single Microstrip Patch Antenna..... 85

5.2 Patch Array (2 X 1)..... 86

5.3 Patch Array (4X 1)..... 87

6 CONCLUSION AND FUTURE WORK 93

6.1 Conclusion 93

6.2 Future Work..... 94

REFERENCES 95

APPENDICES 100

Appendix A: Band designations (Approximate)..... 101

Appendix B: Roots Derivatives of Bessel functions..... 102

LIST OF TABLES

Table 3-1: Design parameters for $\varepsilon_r = 2.2$, $f_o = 12\,\text{GHz}$ 25

Table 3-2: Effective dielectric constant at different number of slots 26

Table 3-3: Experimental and theoretical values of the resonant frequencies of a circular patch antenna at $\varepsilon_{r2} = 1$ and $h_2 = 0$ 30

Table 3-4: Percentage errors of the resonant frequencies by theories compared with experimental results at $h_2 = 0$ 31

Table 3-5: Experimental and theoretical values of the resonant frequencies of a circular patch antenna at $\varepsilon_{r2} = 1$ and $h_2 = 0.5\text{mm}$ 32

Table 3-6: Percentage errors of the resonant frequencies by theories compared with experimental results at $h_2 = 0.5\text{mm}$ 32

Table 3-7: Experimental and theoretical values of the resonant frequencies of a circular patch antenna at $\varepsilon_{r2} = 1$ and $h_2 = 1\text{mm}$ 33

Table 3-8: Percentage errors of the resonant frequencies by theories compared with experimental results at $h_2 = 1\text{mm}$ 34

Table 3-9: Average % errors of resonant frequency in different theories 34

Table 3-10: Effective dielectric constant of substrates by FEKO software for $h_2 = 0$ 35

Table 3-11: Effective dielectric constant of substrates by FEKO software for $h_2 = 0.5\text{ mm}$ 35

Table 3-12: Effective dielectric constant of substrates by FEKO software for $h_2 = 1\text{ mm}$ 35

Table 3-13: Effective dielectric constant of substrates by FEKO for triangular patch antenna 38
Table 3-14: Return losses and resonant frequencies at different dielectric constants 42
Table 3-15: Design specifications of triangular slot antenna..... 44
Table 3-16: Results of triangular slot antenna 45
Table 3-17: Results at different feed point (single band frequency)..... 51
Table 3-18: Results at different feed point (dual band frequency) 53
Table 3-19: S11 and resonant frequency at some other feed positions..... 54
Table 3-20: Results at different feed line distance from the center of the patch 58
Table 4-1: Triangular slot loading effects on antenna parameters..... 62
Table 4-2: Improvement in the return loss, VSWR and bandwidth for different cases 70
Table 4-3: Design parameters of rectangular slot aperture coupled antenna..... 72
Table 4-4: Results at different values of w_{ap} 73
Table 4-5: Results at different values of L_{ap} 74
Table 4-6: Results at different values of L_m 75
Table 4-7: Gain at different shapes of ground aperture 83
Table 5-1: Literature results of a single patch, (2 X 1) array patch and (4 X 1) array patch at 2.4 GHz..... 84
Table 5-2: Single patch antenna design parameters..... 85
Table 5-3: Summary results of a single patch, (2 X 1) array patch and (4 X 1) array patch at 2 GHz..... 90

LIST OF FIGURES

Figure 2-1: BW for a particular design (produced by FEKO) 6

Figure 2-2: Regular shapes of microstrip patch antennas (commonly used) [6] 8

Figure 2-3: Radiating geometry of patch antenna [7] 9

Figure 2-4: Coaxial line feed [10] 10

Figure 2-5: Microstrip patch antenna with feed line [10] 11

Figure 2-6: Proximity coupling feed method [10] 12

Figure 2-7: Aperture coupling feed method [10] 13

Figure 2-8: Radiating slots in rectangular patch antenna [6] 14

Figure 2-9: E- field lines [11] 16

Figure 2-10: Effective length of a patch antenna [11] 17

Figure 2-11: Electric and magnetic walls of a cavity substrate [12] 19

Figure 3-1: Microstrip line design (a) Top view (b) Side view 23

Figure 3-2: SWP calculation 24

Figure 3-3: Standing wave pattern generated by FEKO 25

Figure 3-4: Microstrip line with different number of slots (a) 1 slot (b) 2 slots (c) 3 slots (d) 4 slots 26

Figure 3-5: Circular patch antenna (a) Side view (b) Top view [16] 29

Figure 3-6: S-parameter shows the resonant frequency for $h_2 = 0$ 30

Figure 3-7: S-parameter shows the resonant frequency at for $h_2 = 0.5\text{mm}$ 31

Figure 3-8: S-parameter shows the resonant frequency for $h_2 = 1\text{mm}$ 33

Figure 3-9: Triangular patch antenna (a) Side view (b) Top view [18] 37

Figure 3-10: Return losses of triangular patch antenna 37

Figure 3-11: (a) Substrate layers of proximity coupled antenna by FEKO (b) Proximity coupled feed by FEKO [14] 40
Figure 3-12: Return losses of square patch antenna by FEKO 41
Figure 3-13: Return losses at different dielectric constants by FEKO 42
Figure 3-14: Structures of triangular slot antenna (a) Side view (b) Top view by FEKO [15] 44
Figure 3-15: Return losses of triangular slot antenna 44
Figure 3-16: Return losses at different cell sizes 45
Figure 3-17: Structures of square slot antenna (a) Side view (b) Top view by FEKO 46
Figure 3-18: Return losses of square slot antenna 47
Figure 3-19: Geometry of RMSA (a) Top view (b) Side view [21] 48
Figure 3-20: S-parameters of RMSA at feed point (9, 18) mm from the edge of patch antenna 49
Figure 3-21: RMSA at different feed point (single band frequency) 50
Figure 3-22: S-parameters of RMSA at feed points (9, 18) mm, (10.245, 6.605) mm and (10, 18) mm 51
Figure 3-23: RMSA at different feed point (dual band frequency) 52
Figure 3-24: S-parameters of RMSA at feed points (10.245, 15.605) mm, (10.245, 14.605) mm and (9.245, 14.605) mm 53
Figure 3-25: Feed line shifting in Microstrip patch antenna 55
Figure 3-26: S-parameters of RMSA at D = (0, 1, 2, 3, 4, 5) mm 56
Figure 3-27: S-parameters of RMSA at D = (6, 7, 8, 9, 10) mm 56
Figure 3-28: S-parameters of RMSA at D = (-1,-2,-3,-4,-5) mm 57
Figure 3-29: S-parameters of RMSA at D = (-6,-7,-8,-9,-10) mm 57

Figure 4-1: (a) Antenna without slot (b) Antenna with triangular slot [23] 60

Figure 4-2: Return losses of antennas at different value of w_s 61

Figure 4-3: Proposed circular patch antenna..... 63

Figure 4-4: S-parameters of proposed circular patch antenna 63

Figure 4-5: VSWR of proposed circular patch antenna..... 64

Figure 4-6: Annular microstrip patch antenna [24] 64

Figure 4-7: S-parameters of annular patch antenna 65

Figure 4-8: VSWR of annular patch antenna..... 65

Figure 4-9: Inner circular slots a ring shape with cross shape within the ring 66

Figure 4-10: S-parameters of inner circular slots in a ring shape (with cross within the ring)..... 67

Figure 4-11: VSWR of inner circular slots in a ring shape (with cross within the ring) 67

Figure 4-12: Inner circular slots in a square shape 68

Figure 4-13: S-parameters of inner circular slots with a square shape 69

Figure 4-14: VSWR of inner circular slots with a square shape..... 69

Figure 4-15: Substrate parameters of rectangular aperture coupled antenna [25] 71

Figure 4-16: Rectangular slot aperture coupled antenna [25]..... 71

Figure 4-17: S-parameters at different values w_{ap} 73

Figure 4-18: S-parameters at different values of L_{ap} 74

Figure 4-19: S-parameters at different values of L_m 75

Figure 4-20: Gain values for rectangular slot shape in x-y plane 76

Figure 4-21: Phi-shape slot 77

Figure 4-22: 3-D Radiation pattern of Phi-shape slot in FEKO 78

Figure 4-23: Gain values for Phi-shape slot in x-y plane 78

Figure 4-24: C-shape slot 79
Figure 4-25: 3-D Radiation pattern of C-shaped slot in FEKO 80
Figure 4-26: Gain value for C-shaped slot in x-y plane 80
Figure 4-27: Plus-shaped slot 81
Figure 4-28: 3-D Radiation pattern of the plus-shaped slot in FEKO 82
Figure 4-29: Gain values for plus-shaped slot in x-y plane 82
Figure 5-1: Single patch antenna at 2 GHz in FEKO 86
Figure 5-2: Patch array (2 X 1) in FEKO 87
Figure 5-3: Patch array (4 x 1) in FEKO 87
Figure 5-4: S-parameters of a single patch, (2 X 1) patch array and (4 X 1) patch array 89
Figure 5-5: Antenna gain of single patch, (2 X 1) array patch and (4 X 1) array patch in x-y plane 90
Figure 5-6: 3-D Radiation pattern of a single patch antenna 91
Figure 5-7: 3-D Radiation pattern of (2 X 1) array patch antenna 91
Figure 5-8: 3-D Radiation pattern of (4 X 1) array patch antenna 92

LIST OF SYMBOLS /ABBREVIATIONS

D	Antenna Directivity
E_a	Electric Field Intensity
f_c	Center Frequency
f_H	Upper Frequency
f_L	Lower Frequency
f_o	Operating Frequency
G	Antenna Gain
h	Substrate Thickness
H_a	Magnetic Field Intensity
J_s	Current Density
L	Patch Length
L_g	Ground Length
L_{eff}	Effective Length of Patch
M_s	Magnetic Current Density
m	Number of half wavelength through a radius of waveguide
n	Number of half wavelength through a circumstance of waveguide
S11	Reflection coefficient
W	Patch Antenna Width
W_g	Ground Width
Z_L	Load Impedance
Z_o	Line Characteristic Impedance

ε_{reff}	Effective Dielectric Constant
ε_r	Dielectric Constant
λ_o	Wavelength in Free Space
λ_g	Guide Wavelength
η	Antenna Efficiency
ΔL	Extended Patch Length
π	PI
α_{mn}	n^{th} Zero Derivative in the Bessel Function
ADS	Advanced Design System
BW	Bandwidth
CAD	Computer Aided Design
DGS	Defected Ground Structure
ETPA	Equilateral Triangular Patch Antenna
ETPA	Equilateral Triangular Patch Antenna
GPS	Global Positioning System
HFSS	High Frequency Structural Simulator
IE3D	Integral Equation Three-Dimensional
MoM	Method of Moment
RMPA	Rectangular Microstrip Patch Antenna
SWP	Standing Wave Pattern
TMPA	Triangular Microstrip Patch Antenna
TM	Transverse Magnetic
TE	Transverse Electric
TEM	Transverse Electric and magnetic

VF	Velocity Factor
WIMAX	Worldwide Interoperability for Microwave Access

Chapter 1

INTRODUCTION

In recent years, there has been much attention given to patch antennas, due to their simple structures, low profiles, the compatibility to planar and non-planar circuits. Patch antennas can be defined as a kind of radio antenna; the patch is made of gold or copper placed on the dielectric substrate layer as a one part and the ground plane in another part [1]. There are many shapes used for microstrip patch antennas like rectangular, square and circular patches. The most widely used is a rectangular patch with radiation features and can be easily manufactured.

Munson and Howell implemented the first practical design in the beginning of 1970's [2] [3]. Then the patch antenna became commonly used for more applications, such as satellite and mobile communication applications, global positioning applications, WiMax, radar applications, rectenna applications, telemedicine applications and other applications.

Many mathematical models were used to develop this antenna, and they have been extended to applications in many other fields. The number of articles and papers published during the last years in journals, on microstrip antennas proves the importance placed of these antennas.

1.1 Thesis Objectives

This thesis aims to study and understand patch antennas in different structures, to show their effect on antenna performance, and simulate antennas for multi-band frequencies, high gain, wide bandwidth and minimum values for return loss and voltage standing wave ratio.

1.2 Thesis Overview

In Chapter 2, the concept of antennas and radiation parameters of the antennas are presented. The main advantages and disadvantages of patch antenna are clarified and the most important methods used in the analysis of microstrip patch antennas are explained. Different feed methods are considered such as coaxial feed, microstrip line feed, aperture coupled feed and proximity coupled feed.

In chapter 3, for patch antennas, some of the fields are in the substrate and some of them in air. Therefore the effective dielectric constant value of substrate layer was calculated. A simple method is used to calculate the value of effective dielectric constant of a substrate layer depending on the standing wave pattern generated by FEKO software. Antennas of single and multi-substrate layers are simulated by using FEKO software and the resonant frequencies are computed for different theories. Square, circular and triangular patches are applied and the value of effective dielectric constant of substrate is changed due to fringing fields. Due to the importance of slots in study and improve the antenna performance. Slot antennas are presented and simulated by FEKO. The effective permittivity of the substrate is compared for triangular and square slot antennas.

Both of the feed positions and types also affect the performance of antennas. Different feed positions are tested in the case of coaxial cable and microstrip line to obtain the best results of return loss, also dual band frequencies are achieved in this study.

In chapter 4, the effect of a triangular slot at one edge of the patch on the resonance frequency is studied. The bandwidth, return loss and voltage standing wave ratio (VSWR) are improved by applying different slot structures inside the circular patch.

Defected ground structure (DGS) is used as a technique to solve the surface wave problem by using different structures of ground aperture.

In chapter 5, Rectangular patch array is suggested at 2 GHz as a topology used for obtain high gain. The value of the gain is tested for single patch element, 2X1 and 4X1 arrays.

In Chapter 6, includes the conclusion and suggestions for future work.

Chapter 2

ANTENNAS

2.1 Antenna Definition

An antenna is a device that is used to transmit or/and receive the electromagnetic waves. Antennas are very significant elements of communication systems because they are used in transmitting and receiving signals. They possess same characteristics, whether in the case of transmitting or receiving signals. An antenna must be designed to a specific value of the frequency band of the system, or else the processes of sending and receiving signals will be of a low value. When an antenna is fed by a specific signal, the emitted radiation is distributed in the space in a particular way.

Antennas have been used over time for different purposes, including navigational and military applications. Many designers have worked to develop and improve the efficiency of antennas and today they are used in a wide range of fields such as GPS, military, cell phones, radar, satellite and other applications.

The main types of antennas are: Yagi-Uda Antenna which was discovered in 1920, Horn antennas in 1939, antenna Arrays in 1940 and Patch Antennas in 1970 [4].

2.2 Antenna Parameters

2.2.1 Return Loss

A return is shows the degree of mismatch. It is the ratio between the reflected power by the antenna and the power that feeds the antenna via the transmission line measured in dB. The following formula is used to compute the return loss:

$$RL = 20\log|\Gamma| \tag{2.1}$$

Where $|\Gamma|$ represents the magnitude of the reflection coefficient and this value is always below 1. The mathematical expression is:

$$\Gamma = \frac{Z_L - Z_o}{Z_L + Z_o} \tag{2.2}$$

Where Z_L is the load impedance and Z_o is the line characteristic impedance of the transmission line.

2.2.2 Bandwidth

Bandwidth (BW) refers to the difference between the higher frequency (f_H) and lower frequency (f_L) for a particular band, as shown in Equation 2.3:

$$BW = f_H - f_L \tag{2.3}$$

The bandwidth is also described as a percentage of frequency:

$$BW = 100 \times \frac{f_H - f_L}{f_c} \tag{2.4}$$

Where f_c is the center frequency in the band = $(f_H + f_L)/2$

Figure 2.1 shows the bandwidth of a rectangular patch antenna obtained by using the FEKO software.

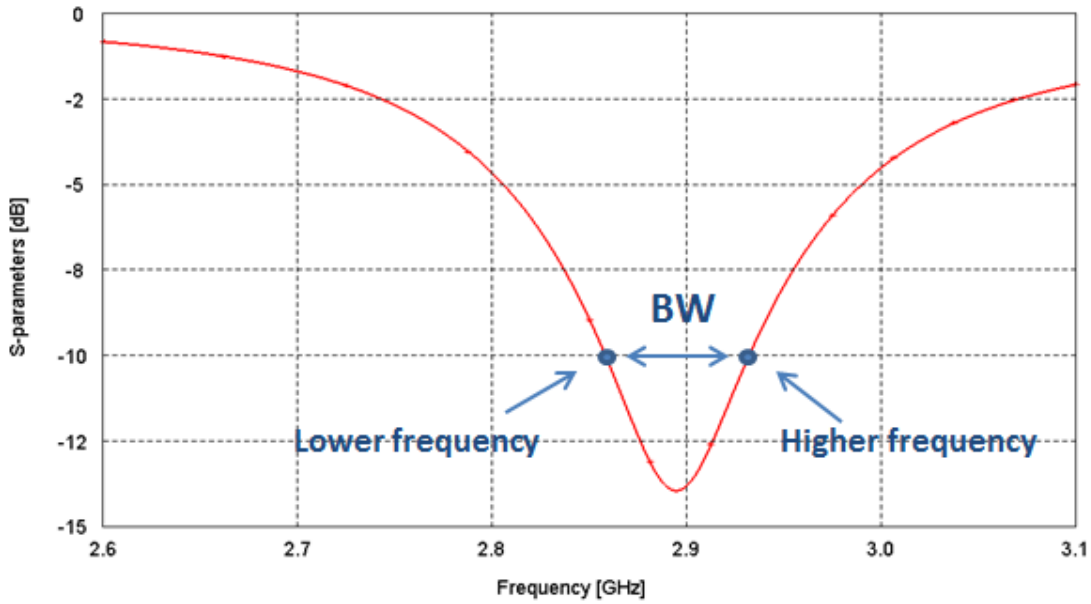

Figure 2-1: BW for a particular design (produced by FEKO)

2.2.3 Gain and Directivity

Antenna gain is defined as "the ratio of intensity, in a given direction, to the radiation intensity that would be obtained if the power accepted by the antenna were dedicated isotropically" [5]. The gain of an antenna takes into account the losses that occur, so it is more commonly used in the study of antenna specifications. Directivity is the ratio of power received (or transmitted) by the antenna in a certain direction to the power received (or transmitted) in that direction by an isotropic source.

The relationship between the antenna gain and directivity can be expressed by Equation 2.5:

$$G = \eta D \tag{2.5}$$

Where, G is the gain of the antenna, η is the antenna efficiency and D is the directivity of the antenna.

2.2.4 Voltage Standing Wave Ratio (VSWR)

VSWR is a "function of reflection coefficient" which is a measure of the reflected power from the antenna. When the reflection coefficient Γ is given, the value of VSWR is calculated using Equation 2.6:

$$VSWR = \frac{1+|\Gamma|}{1-|\Gamma|} \tag{2.6}$$

Always the VSWR is a positive number for antennas. The minimum value of VSWR is 1. In that situation, the power is not reflected from the antenna, which is ideal.

2.2.5 Radiation Pattern

The radiation pattern is expressed as the relative power of a radiated field in different directions of an antenna. It also describes the receiving characteristics of an antenna. Radiation pattern is represented in three-dimensions, but may be computed in two-dimensions, in the vertical or horizontal planes, in either polar or rectangular format.

2.3 Microstrip Patch Antenna

A microstrip patch antenna is a type of radio antenna, which can be installed on a planar surface, generally comprises from four parts (patch, substrate, ground and a part of feeding). The patch part is very thin ($t << \lambda_o$), where λ_o is the wavelength in free space. A patch is placed on one substrate, while the ground plane is placed on the other side. The patches may have different shapes according to the desired design. Due to their ease of fabrication and design , square, dipole, triangular,

rectangular, circular and circular ring are most commonly used patch antenna shapes as we demonstrate by Figure 2.2.

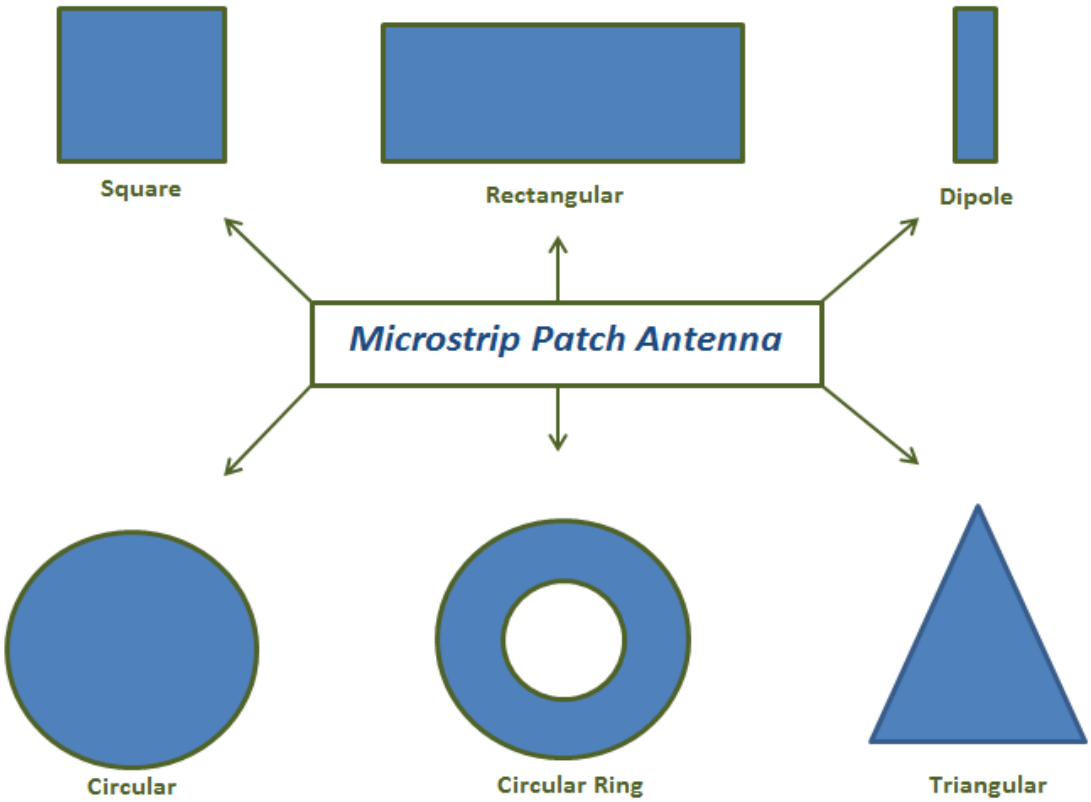

Figure 2-2: Regular shapes of microstrip patch antennas (commonly used) [6]

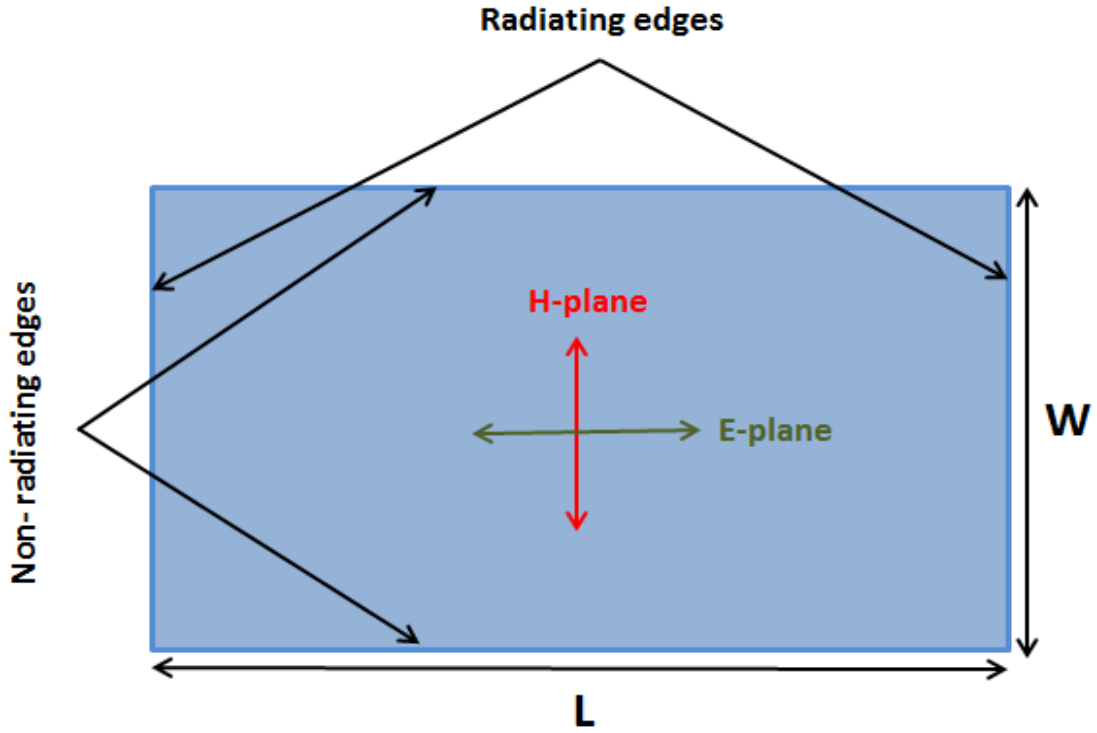

Figure 2-3: Radiating geometry of patch antenna [7]

2.3.1 Advantages and Disadvantages of Microstrip Patch Antennas

The demand of patch antennas has increased because they are used in many wireless applications, like cellular phones. Another field of application of patch antennas is in the satellite communication; this increased the popularity of patch antenna over time.

Patch antennas are very popular due to their small sizes, low manufacturing cost, multi-band properties and compatibility to microwave circuits [8].

On the other hand they have some drawbacks such as limited bandwidth, poor radiation efficiency, low gain and losses produced by the excitation of surface waves [9].

2.3.2 Feeding Methods

There are many methods used for feeding a microstrip antenna. The most commonly used ones are [10]:

1. Coaxial Feed,
2. Microstrip Line,
3. Proximity Coupling,
4. Aperture Coupling.

2.3.2.1 Coaxial Feed

Coupling power to a patch antenna through a coaxial connector is very cheap, simple and an effective way. The coaxial connector is connected to the ground plane of the microstrip antenna and it is passed across the substrate at the center and soldered to the patch, as shown in the Figure 2.4:

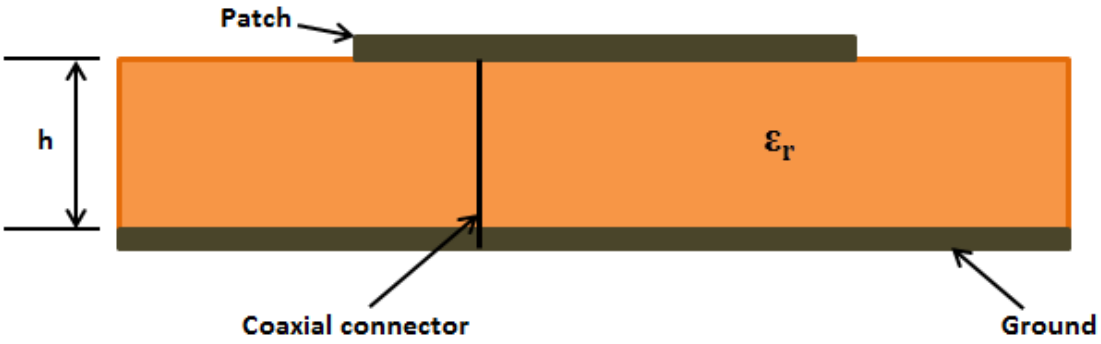

Figure 2-4: Coaxial line feed [10]

2.3.2.2 Microstrip Line

This method of feeding is more commonly used because it is very simple to design and analyze, and very easy to manufacture. The Figure 2.5 shows a patch with microstrip line feed. Also, this type of feeding is mostly used in the case of multi-patches (patch array).

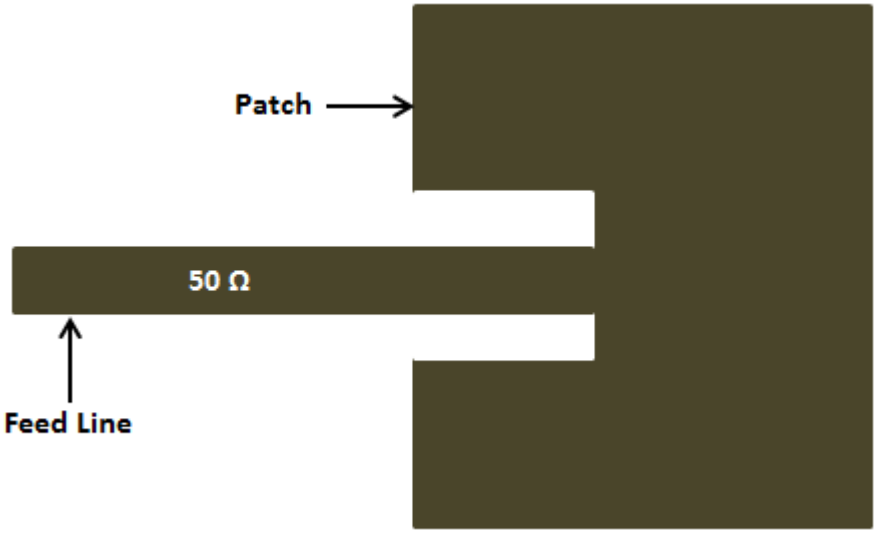

Figure 2-5: Microstrip patch antenna with feed line [10]

2.3.2.3 Proximity Coupling

Two substrates are used in a proximity coupling feeding method with permittivities ε_{r1} and ε_{r2}. The patch is placed on the top, the ground plane in the bottom and a feed line is connected to the source with a placing between the two substrates as shown in the figure 2.6:

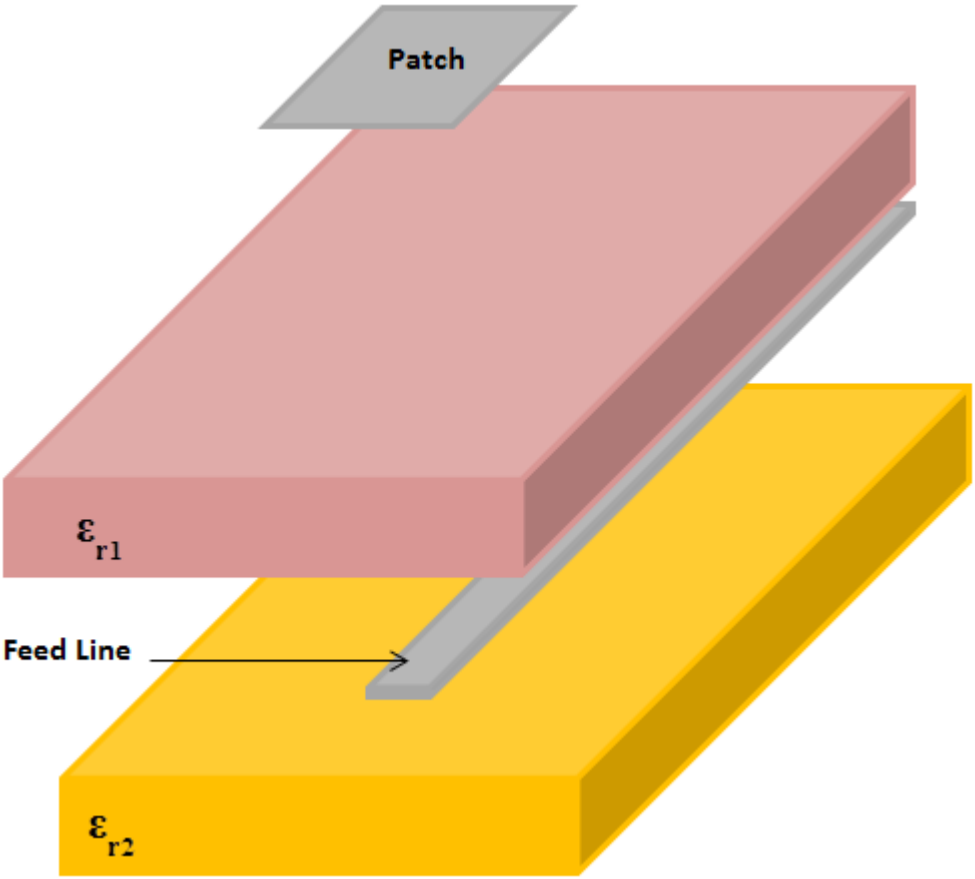

Figure 2-6: Proximity coupling feed method [10]

2.3.2.4 Aperture Coupling

The microstrip patch antenna uses the aperture mechanism in the type of feeding as shown in Figure 2.7. The ground plane has an aperture in different shapes, and it placed between two substrates: the upper substrate ε_{r1} with the patch over it, and the lower substrate ε_{r2} with the microstrip feed line below it. This type of feeding gives wider bandwidth.

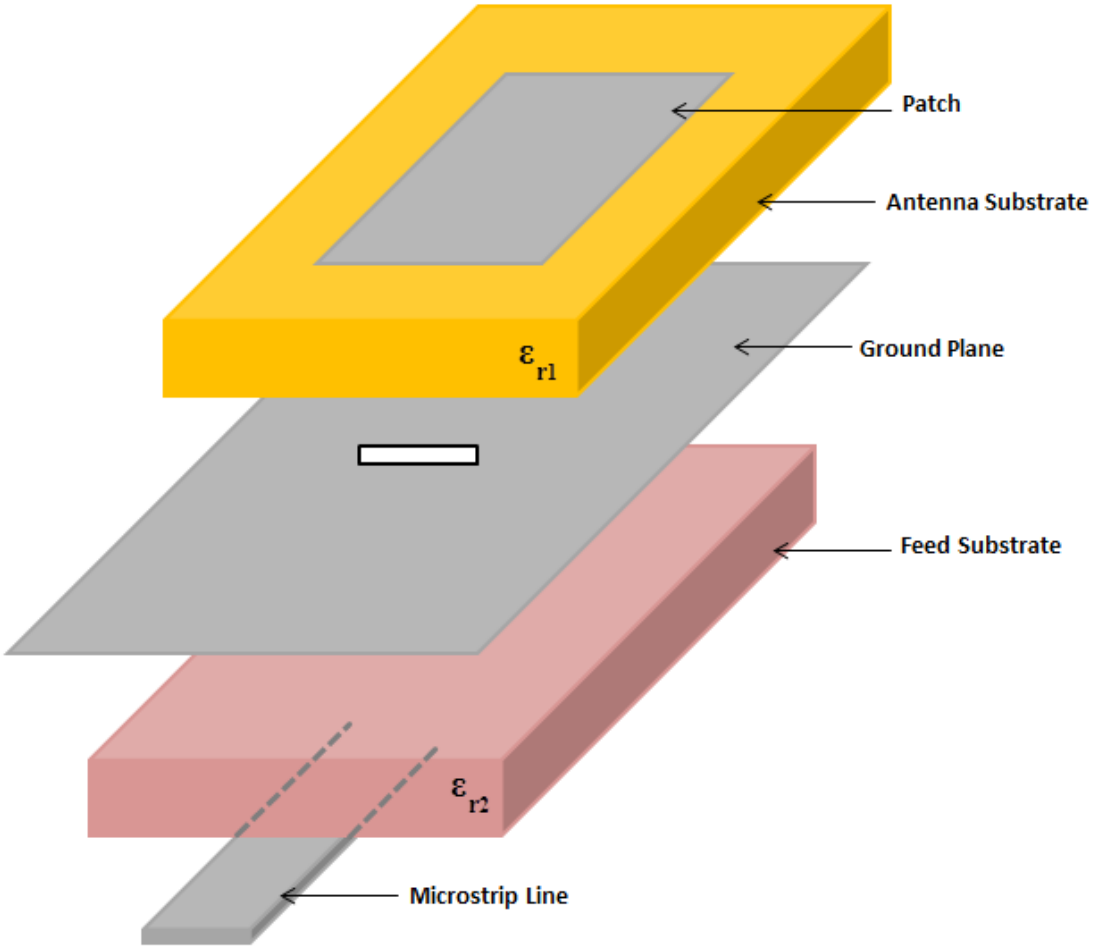

Figure 2-7: Aperture coupling feed method [10]

2.3.3 Patch Array

The radiation pattern of a single element is relatively wide, and each element gives low values of directivity and gain. In most applications, it is necessary to design antennas with high gain for long distance communications. This can only be achieved by increasing the electrical size of the antenna. This new antenna, is formed by multi-elements, which is referred to as an array.

2.3.4 Analysis Models of the Microstrip Patch Antennas

There are different methods used in the analysis of the patch antennas. The method of the transmission line is the most popular way to analyze patch antennas since they look like a transmission line or part of it.

The second popular way is the cavity model which assumes that the patch is similar to a loaded cavity [5].

2.3.4.1 Transmission Line Model

The transmission line model is the simplest way to illustrate and understand the microstrip antenna through representing the patch antenna by two slots. The results are less accurate, however, it is sufficiently good for designing the antenna.

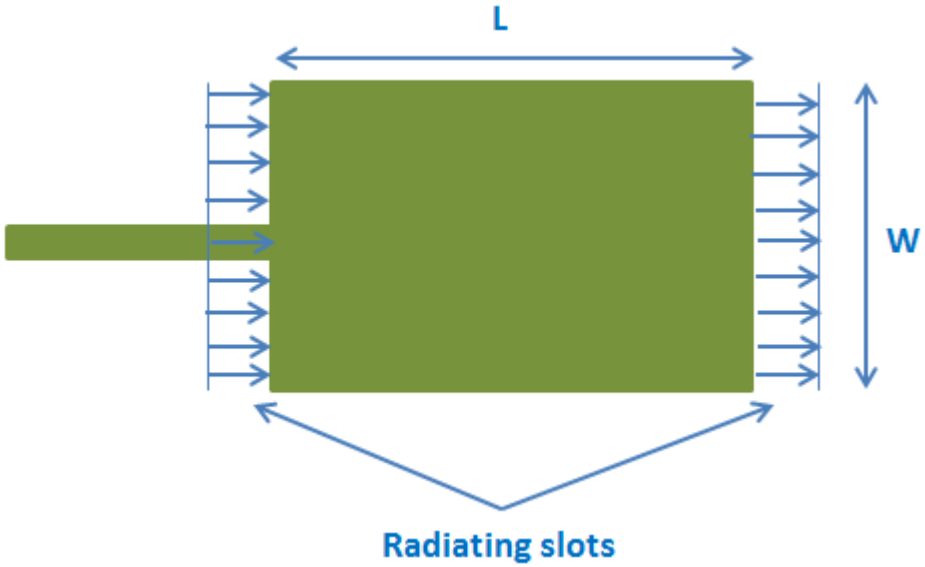

Figure 2-8: Radiating slots in rectangular patch antenna [6]

Design Parameters of Patch Antennas:

A. The Patch Width (W):

It is given by the following formula:

$$W = \frac{c}{2f_o}\sqrt{\frac{2}{\varepsilon_r + 1}} \tag{2.7}$$

Where c is the speed of light, ε_r is the relative permittivity of substrate and f_o is the operating frequency.

Equation 2.7 shows that the width is approximately equal to a half wavelength. Thus, the patch can be seen as a "continuous planar source" consisting of an infinite number of infinitesimally dipoles.

B. The Effective Length (L_{eff}):

The length of the patch looks electrically slightly larger than the usual length of design, because of the fringing field along the patch width, and this parameter can be calculated by using Equation 2.8 given below:

$$L_{eff} = \frac{c}{2f_o\sqrt{\varepsilon_{reff}}} \tag{2.8}$$

Here, ε_{reff} is the effective permittivity of the dielectric.

C. The Effective Dielectric Constant (ε_{reff}):

The dielectric constant of the substrate differs due to the fringing effects.

It is appropriate to define another parameter called the effective dielectric constant of substrate which is less than the real permittivity i.e. $1 < \varepsilon_{reff} < \varepsilon_r$.

For larger values of ε_r, ε_{reff} approaches ε_r, since larger amounts of electric field intensity will be absorbed by the dielectric material.

Fringing depends on the ratio of the patch length (L) to the height of the substrate (h). i.e. L/h. The value of effective dielectric constant is computed as in the following formula:

$$\varepsilon_{reff} = \frac{\varepsilon_r + 1}{2} + \frac{\varepsilon_r - 1}{2}\left(1 + 12\frac{h}{W}\right)^{-\frac{1}{2}} \qquad (2.9)$$

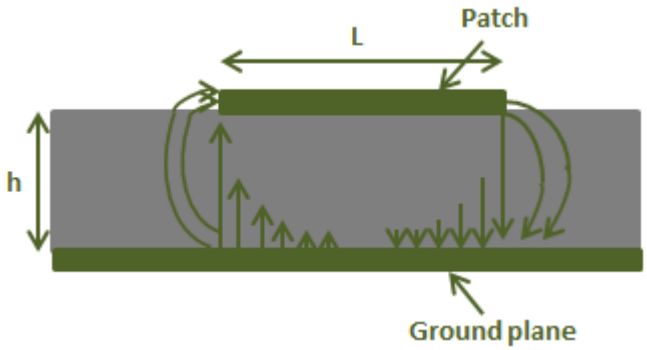

Figure 2-9: E- field lines [11]

D. The Extended Length (ΔL):

Due to the fringing fields along the antenna it is appropriate to use extended length for a better performance. The length is extended by (ΔL) given by the Equation 2.10 below:

$$\Delta L = \frac{(\varepsilon_{reff} + 0.3)\left(\frac{W}{h} + 0.264\right)}{(\varepsilon_{reff} + 0.258)\left(\frac{W}{h} + 0.8\right)} \tag{2.10}$$

After the calculation of each of effective and extended lengths of the patch, the actual value of the patch length (L) is calculated by using Equation 2.11:

$$L = L_{eff} - 2\Delta L \tag{2.11}$$

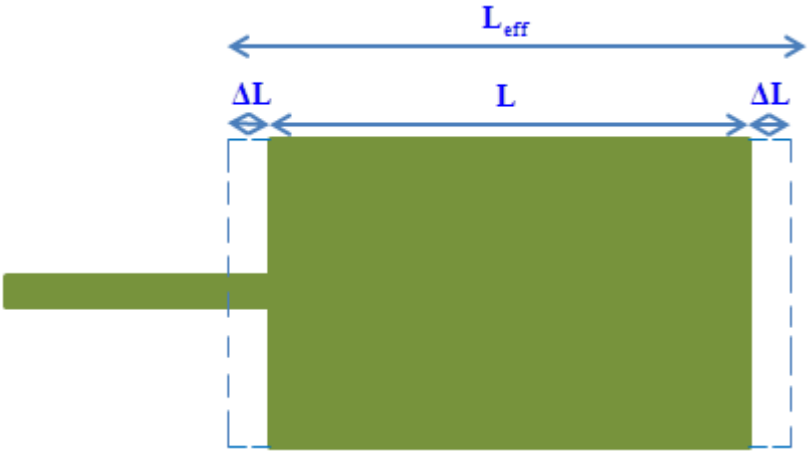

Figure 2-10: Effective length of a patch antenna [11]

E. The Dimensions of Ground Plane (W_g and L_g):

The transmission line model is applied to the ground only. For practical purposes, it is necessary to have a finite ground plane. It has been proven that identical results for infinite and finite ground plane can be obtained if the size of the ground plane is larger than the dimensions of the patch by about six times the thickness of substrate all over the periphery. The dimensions of the ground are explained by the Equations 2.12 and 2.13 below:

$$L_g = L + 6h \qquad (2.12)$$

$$W_g = W + 6h \qquad (2.13)$$

2.3.4.2 Cavity Model

The patch performance is affected by higher order modes. Microstrip antennas similar to cavities of dielectric-loaded waveguide, show the higher order resonances. The fields inside the substrate (between the ground plane and the patch) can be observed more accurately by dealing with that region as a cavity which is bounded by:

- Electrical conductive walls (top and bottom).
- Magnetic walls (along the surrounding of the patch).

Each magnetic wall is represented by:

$$J_s = \hat{n} \times H_a \qquad (2.14)$$

$$M_s = -\hat{n} \times E_a \tag{3.15}$$

Where J_s and M_s are the electric current and magnetic current densities respectively, E_a and H_a are intensity of electric and magnetic fields respectively and $\hat{n}$ is the unit vector normal to the walls. Both electric and magnetic walls are shown in Figure 2.11.

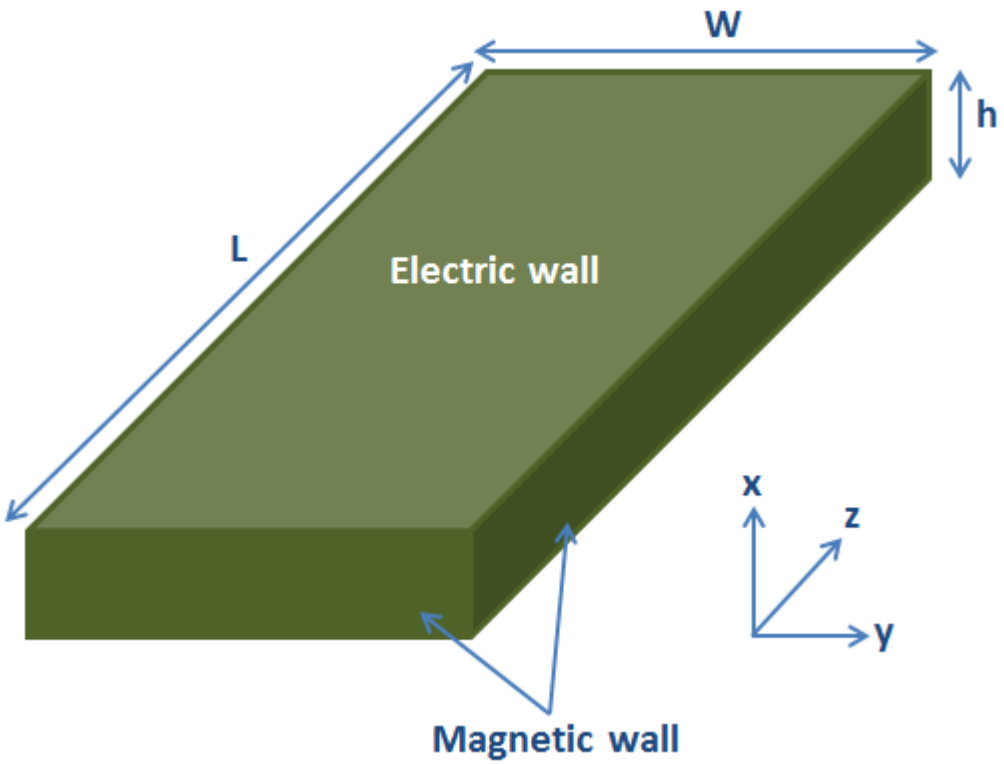

Figure 2-11: Electric and magnetic walls of a cavity substrate [12]

The thickness (h) of the antenna's substrate is too small. Generated waves are propagated below the patch. Only a small percentage of them are radiated. The field configurations are similar to the TM^x field configurations, i.e., modes without H_x component based on the coordinates in Figure 2.11.

Chapter 3

MICROSTRIP PATCH ANTENNA SIMULATIONS BY USING FEKO 5.5 SIMULATION SOFTWARE

3.1 Overview – FEKO Simulation

FEKO is a software tool used for electromagnetic simulation and it is suitable for various kinds of problems. Typical broad applications that deal with FEKO include analysis of microstrip patches, scattering problems, reflector antennas, wire antennas, arrays and analysis of antenna radiation [13].

FEKO is the first Method of Moment (MOM) package released in June 2004. Subsequently MOM hybrids with others techniques follow:

- Geometrical Optics (GO).
- Uniform Theory of Diffraction (UTD).
- Physical Optics (PO).
- Finite Element Method (FEM).

These techniques make this software suitable to solve many of the problems relevant to electromagnetics.

3.2 Introduction

This chapter covers simulations of patch antennas using FEKO 5.5 full wave simulation software, which is based on the Method of Moments (MoM).

For patch antennas, some of the fields are in the substrate and some of them are in air, i.e. fringing occurs. Due to this phenomenon the value of the relative permittivity will be lower than its effective permittivity, which will affect the velocity of the wave in the substrate. For this reason, it is necessary to calculate the effective dielectric constant.

There are some empirical formulas available for the conventional stiplines [5], but some simulation tools or techniques, like FEKO are required, under the conditions that we apply some irregularities like slots.

A simple method is used in this chapter to calculate the value of the effective dielectric constant of substrate by using the standing wave pattern, which is the magnitude of the electric field beneath the metal. The standing wave pattern was obtained by using the FEKO software.

On the one hand, multi-substrate layers were considered. Square, circular and triangular patches were applied and the value of effective dielectric constants were calculated. Shubham Gupta and Shilpa Singh (2012) presented [14] a formula to determine ε_{reff} for multi substrate layers.

Slots are used to increase the antenna performance. The effective permittivity of triangular [reference] and square slot antennas are examined. Wen-Shan Chen and

Fu-Mao Hsieh (2005) presented [15] a formula to calculate the guide wavelength in order to compute the value of ε_{reff} .

The effective dielectric constant is a function of the resonant frequency [5]. For this reason, some of the above studies focused on the calculation of the resonant frequency by making use of antenna simulations by different softwares. The values of resonant frequencies generated by FEKO software were compared with the results of previous studies.

3.3 Calculation of the ε_{reff} by using the Guiding Wavelength of a Microstrip Line

The wavelength of the microstrip line in the substrate is different from its value in the ordinary unbounded substrate. This difference is due to the fringing fields between the conducting plates, and the effective value of the relative permittivity also differs. The determination of the guiding wavelength by using FEKO software will help us to find the effective value of the permittivity. It is known that, the standing wave pattern (SWP) can be obtained by short circuiting the two parallel plates. The difference between two successive minima (or maxima) gives ($\lambda_g/2$). By making use of the Equation 3.1 ε_{reff} can be calculated by using the following formula:

$$\lambda_g = \frac{\lambda_o}{\sqrt{\varepsilon_{reff}}} \tag{3.1}$$

Where λ_o is wavelength in free space and λ_g is the guide wavelength. The results can be calculated by the available approximations and compare with the FEKO results for validation.

The design geometry consists of two parallel planes, the lower plane as a ground with the dimensions L_g X W_g and the upper plane as a microstrip line with the dimensions L_f X W_f, the substrate layer between the planes with the dielectric constant ε_r and thickness h. Figure 3.1 shows the geometry of the design.

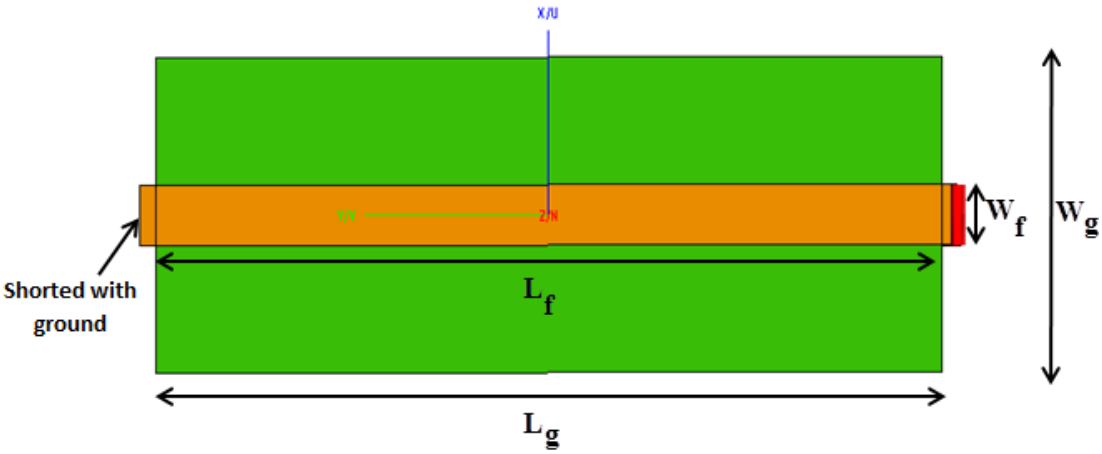

(a)

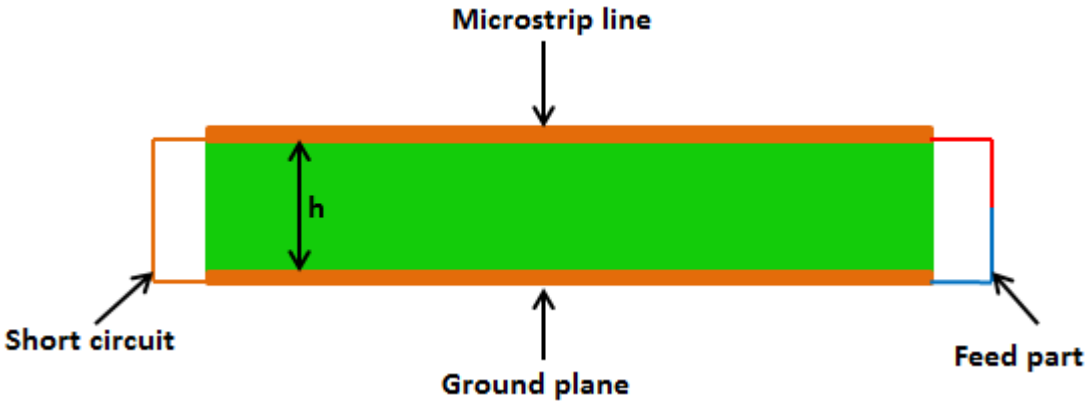

(b)

Figure 3-1: Microstrip line design (a) Top view (b) Side view

Microstrip line is fed in one edge and short circuited to the ground at the second edge. Because of the short circuit, standing waves are formed and the reflection coefficient becomes 1. By using FEKO software and requesting near field along the y-direction below the microstrip line, the standing wave pattern, similar to the one in Figure 3.2 will be obtained.

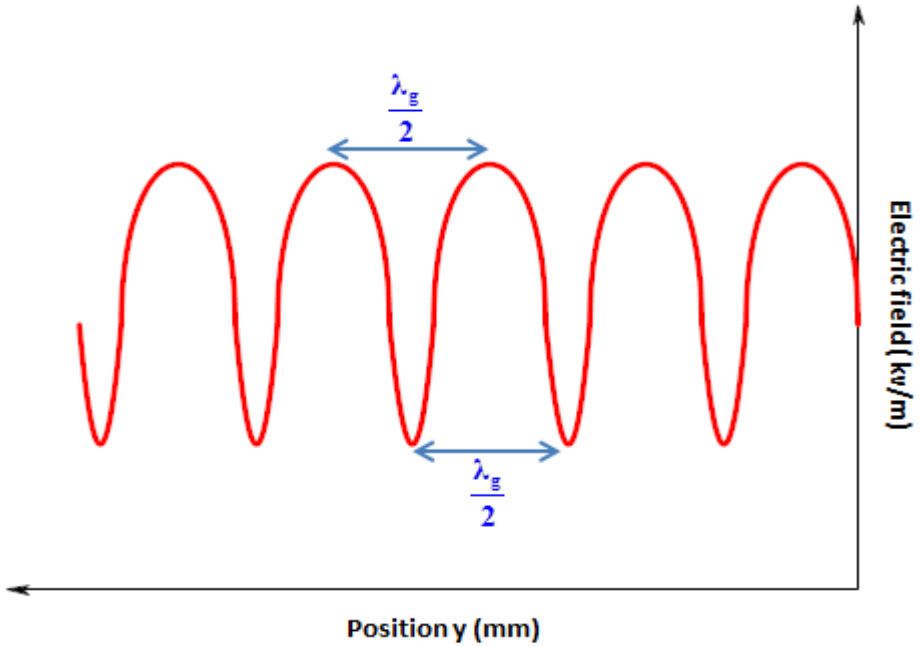

Figure 3-2: SWP calculation

3.3.1 Effective Dielectric Constant Calculation by using SWP

A microstrip line having the dimensions given by Table 3.1 was simulated by FEKO, having a substrate relative permittivity of 2.2. The microstrip line was excited by using an edge feed at the operating frequency of $f_0 = 12$ GHz. The SWP simulation result obtained is shown by Figure 3.3. λ_g was extracted from this pattern and the ε_{reff} was calculated in the way that explained above.

Table 3-1: Design parameters for $\varepsilon_r = 2.2$, $f_o = 12\,\text{GHz}$

Parameter	Value (mm)
Length of microstrip line (L_f)	50
Width of microstrip line (W_f)	3.88
Thickness of substrate (h)	1.35
Length of ground (L_g)	50
Width of ground (W_g)	20

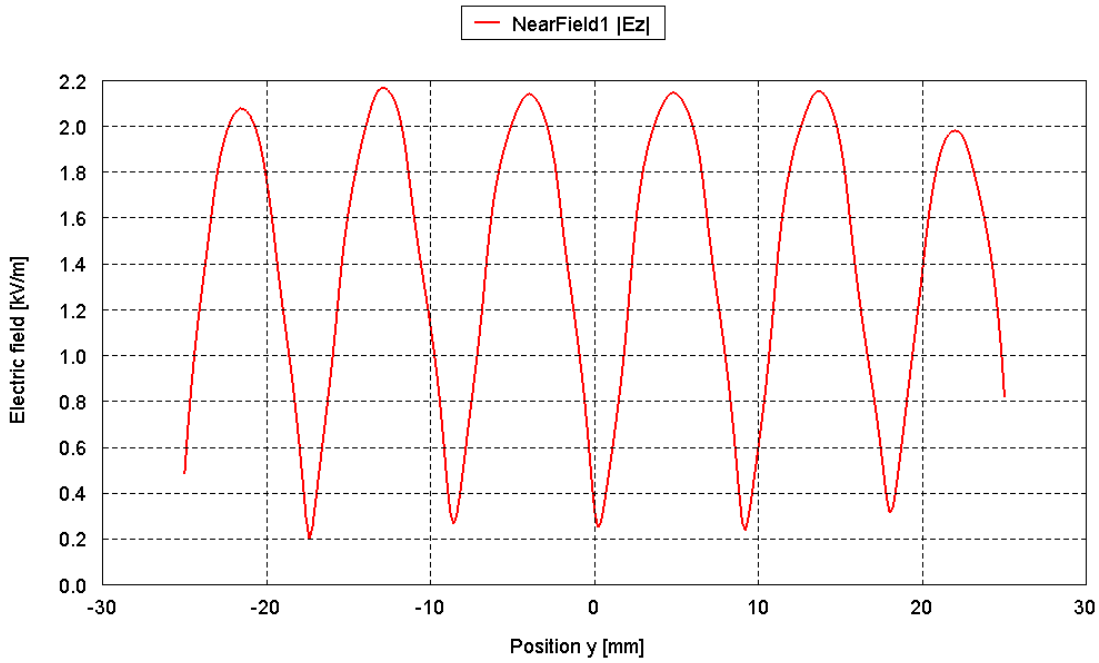

Figure 3-3: Standing wave pattern generated by FEKO

The effective dielectric constant of the substrate obtained from the above SWP 1.975. The value of the same parameter calculated by using the approximate formula given by Equation 2.9 is 1.863. These two values are in agreement.

In the next study, a small rectangular slot (0.5 X 2) mm is applied on the microstrip line as shown in Figure 3.4.a the value of ε_{reff} is calculated. The same work has been carried out to calculate the ε_{reff} for 2, 3 and 4 slots line. The results are in Table 3.2.

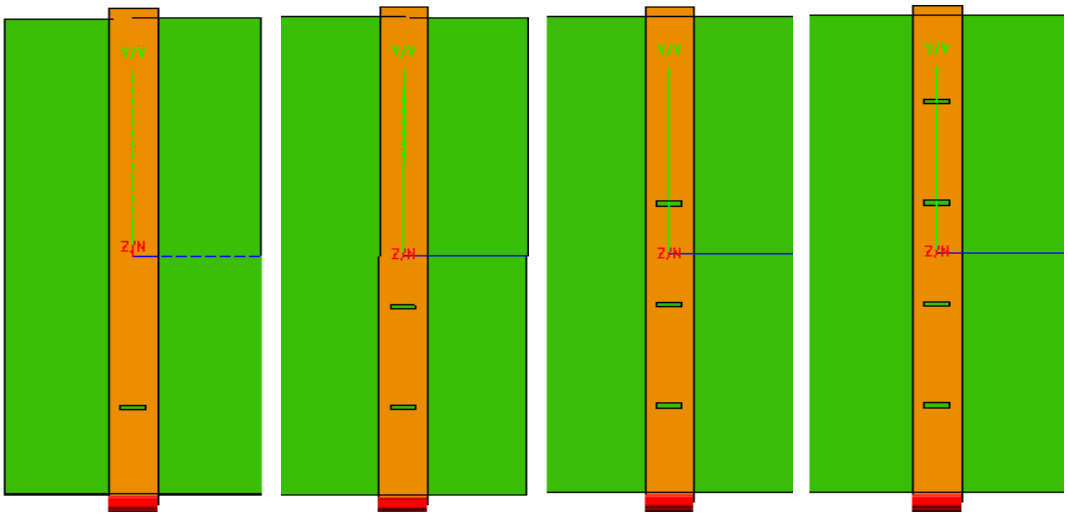

(a) (b) (c) (d)

Figure 3-4: Microstrip line with different number of slots (a) 1 slot (b) 2 slots (c) 3 slots (d) 4 slots

Table 3-2: Effective dielectric constant at different number of slots

Number of slot	**λ_g (mm)**	**ε_{reff}**
Without slot	17.786	1.975
1 –slot	17.916	1.947
2 –slot	18.042	1.920
3 –slot	18.152	1.896
4 –slot	18.178	1.891

From the above table, it can be observed that the value of effective dielectric constant of the substrate in the case of microstrip line without slot is equal to 1.975, the value computed by using Equation 2.9 is 1.863. Also the decrease in the effective permittivity can be observed from the figures when the number of slots increases.

3.4 Simulations of Patch Antennas Having Multi Substrate Layers

In this section, patch antennas with multi-substrate layers are analyzed instead of a single layer.

Resonant frequency generated by FEKO would be compared with other results obtained from the theories and results of the commercial available software then, the effective permittivity will be computed by making use of the resonant frequency.

Various shapes of patches will be treated as a perfect conductors used for radiation which are circular, triangular and square.

3.4.1 Circular Patch Antenna

For the first case a circular patch was considered [16]. A simple general expression of the resonant frequency for the circular patch antenna can be written as Equation 3.2 by using the cavity model analysis. The fields of the patch antenna are similar to the fields of a cavity. In this case, the fields are equivalent to TM_x [17].

In this study, the resonant frequency was produced by the FEKO software and the ε_{reff} was calculated by making use the following equation:

$$\varepsilon_{reff} = \left(\frac{\alpha_{mn} c}{2\pi a_e f_{r,mn}} \right)^2 \tag{3.2}$$

Where α_{mn} is the n^{th} zero derivative in the Bessel function of order *m* and the Bessel function was defined by mathematician Daniel Bernoulli which are the canonical solutions of Bessel's differential equation used in applications of electromagnetic

waves in a waveguide, a_e is the effective radius of the circular microstrip antenna as given by Equation 3.3:

$$a_e = a\left[1 + p\gamma_1\right]^{\frac{1}{2}} \tag{3.3}$$

p and γ_1 are expressed by Equations 3.4 and 3.5:

$$p = \left\{\frac{2h}{\pi\varepsilon_{re}a}\left[\log\left(\frac{a}{2h}\right) + \left(1.41\varepsilon_{re} + 1.77\right) + \frac{h}{a}\left(0.268\varepsilon_{re} + 1.65\right)\right]\right\}^{1/2} \tag{3.4}$$

$$\gamma_1 = \frac{0.79^n 0.51^m}{0.54^m} \tag{3.5}$$

ε_{re} is the relative permittivity of the medium under the patch and it is expressed by Equation 3.6:

$$\varepsilon_{re} = \frac{\varepsilon_{r1}\varepsilon_{r2}h}{\varepsilon_{r1}h_2 + \varepsilon_{r2}h_1} \tag{3.6}$$

Where ε_{reff} is calculated by using Equation 3.7:

$$\varepsilon_{reff} = \frac{\varepsilon_{re} + 1}{2} + \frac{\varepsilon_{re} - 1}{2}\left[1 + \frac{10h\gamma_2}{3^{0.3}a}\right]^{-\frac{1}{2}} \tag{3.7}$$

Here, γ_2 is the dependent correction factor which is given by Equation 3.8:

$$\gamma_2 = \frac{1.37^m 0.25^n}{\left(m+n\right)^{0.4}} \tag{3.8}$$

3.4.1.1 Simulation Results of the Circular Patch Antenna by using FEKO

The circular patch antenna is simulated with radius a =50 mm centered on the two substrate layers with dielectric constants and thicknesses ε_{r1}, ε_{r2}, h_1 and h_2 respectively. The ground plane is below them with dimensions 120 X 120 mm. The FEKO simulation structure is shown by Figure 3.5. A coaxial cable feed is at (-20.86mm, 0) between the ground and the patch.

The resonant frequency obtained by FEKO shown in Figures 3.6, 3.7 and 3.8 is compared by analytical and experimental results for different substrate thicknesses [16] as shown in Tables 3.3, 3.4, 3.5, 3,6, 3.7 and 3.8. Figure 3.6 refers to a single substrate layer. i.e. $h_2 = 0$. The comparison of experimental results, HFSS results and FEKO results for the resonant frequencies are shown for TM_{11}, TM_{21} and TM_{31} cases. Table 3.4 shows the percentage errors of the resonant frequencies among the modes and solution tecniques.

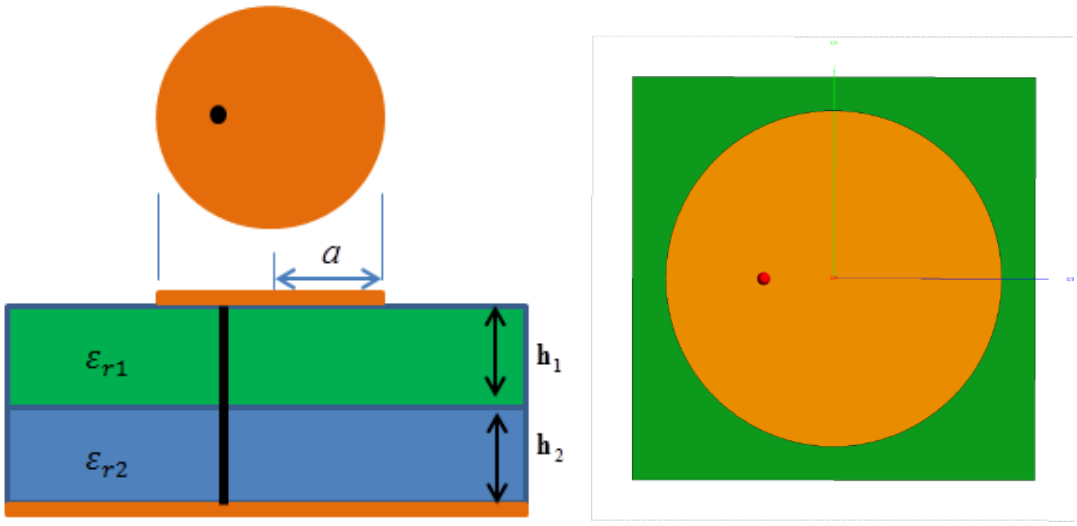

(a) (b)

Figure 3-5: Circular patch antenna (a) Side view (b) Top view [16]

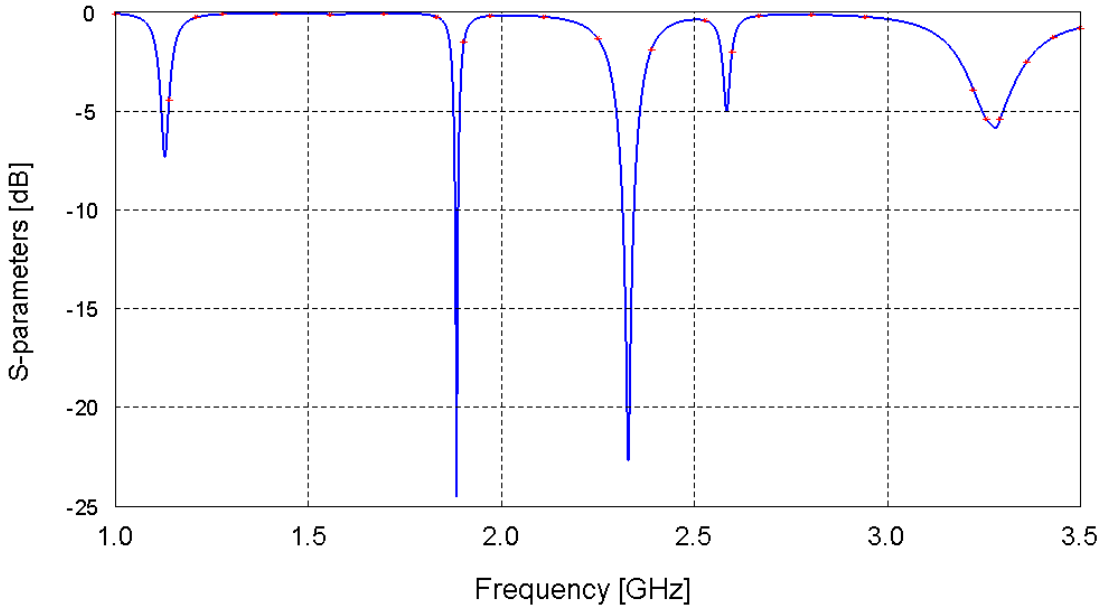

Figure 3-6: S-parameter shows the resonant frequency for $h_2 = 0$

Table 3-3: Experimental and theoretical values of the resonant frequencies of a circular patch antenna at $\varepsilon_{r2} = 1$ and $h_2 = 0$

a mm	mode	ε_{r1}	h_1 mm	h_2 mm	a/h	Experiment (GHz)	HFSS (GHz)	Comput-ed [16] (GHz)	FEKO (GHz)
50	TM_{11}	2.32	1.59	0	31.44	1.128	1.162	1.13	1.147
50	TM_{21}	2.32	1.59	0	31.44	1.879	1.934	1.879	1.914
50	TM_{31}	2.32	1.59	0	31.44	2.596	2.356	2.590	2.364

Table 3-4: Percentage errors of the resonant frequencies by theories compared with experimental results at $h_2 = 0$

Mode	HFSS	Computed [16]	FEKO
TM_{11}	-3.014	-0.177	-1.684
TM_{21}	-2.927	0.0	-1.862
TM_{31}	9.245	0.231	8.936

Figure 3.7 shows the resonant frequencies of two layer structure, when $h_2 = 0.5\text{mm}$. A table similar to Table 3-3 is prepared and shown by Table 3-5. The comparison of the results are in Table 3-5.

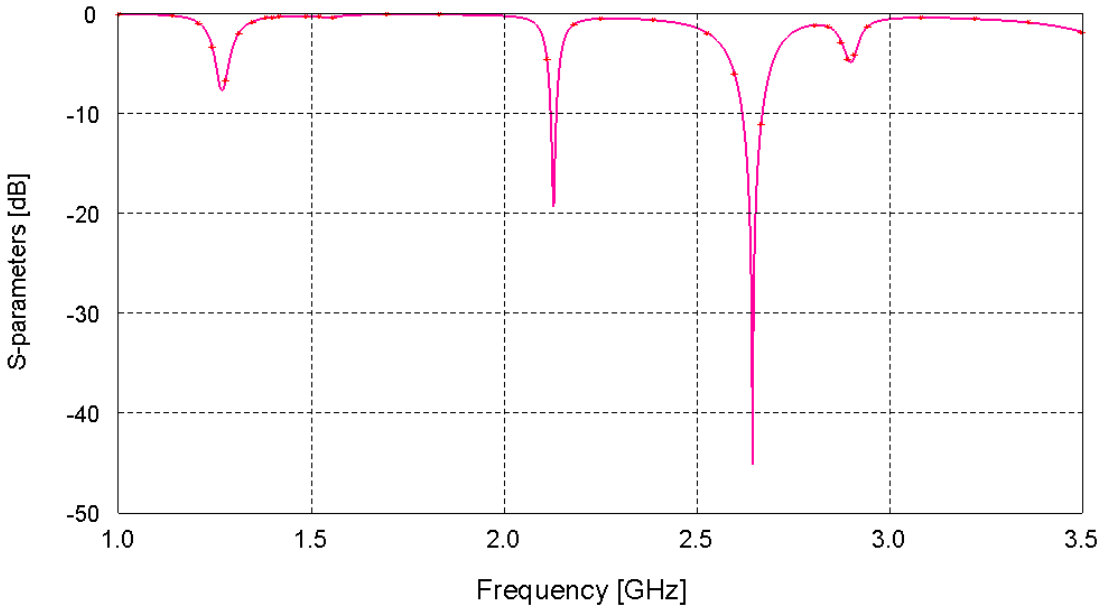

Figure 3-7: S-parameter shows the resonant frequency at for $h_2 = 0.5\text{mm}$

Table 3-5: Experimental and theoretical values of the resonant frequencies of a circular patch antenna at $\varepsilon_{r2}=1$ and $h_2=0.5\text{mm}$

a mm	mode	ε_{r1}	h_1 mm	h_2 mm	a/h	Experiment (GHz)	HFSS (GHz)	Comput-ed [16] (GHz)	FEKO (GHz)
50	TM_{11}	2.32	1.59	0.5	23.92	1.286	1.334	1.281	1.268
50	TM_{21}	2.32	1.59	0.5	23.92	2.136	2.203	2.13	2.127
50	TM_{31}	2.32	1.59	0.5	23.92	2.951	2.645	2.939	2.646

Table 3-6: Percentage errors of the resonant frequencies by theories compared with experimental results at $h_2=0.5\text{mm}$

mode	HFSS	Computed [16]	FEKO
TM_{11}	-3.732	0.389	1.339
TM_{21}	-3.137	0.281	0.421
TM_{31}	10.369	0.407	10.335

The same calculations were repeated for $h_2=1\text{mm}$. Figure 3.8 shows the resonant frequencies and Tables 3-7 and 3-8 are prepared for this design.

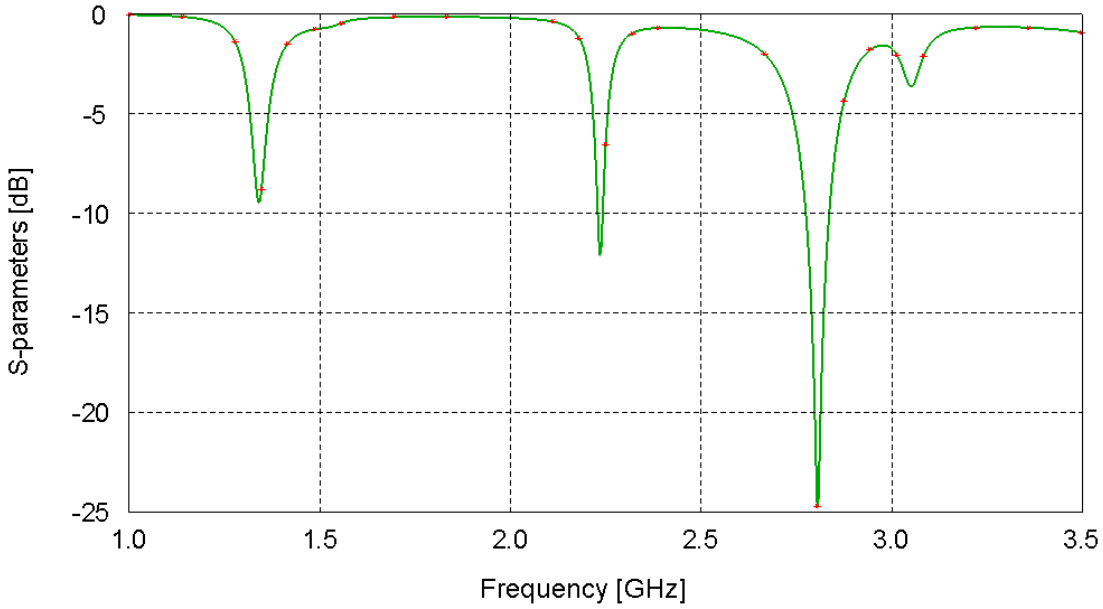

Figure 3-8: S-parameter shows the resonant frequency for $h_2 = 1\text{mm}$

Table 3-7: Experimental and theoretical values of the resonant frequencies of a circular patch antenna at $\varepsilon_{r2} = 1$ and $h_2 = 1\text{mm}$

a mm	mode	ε_{r1}	h_1 mm	h_2 mm	a/h	Experiment (GHz)	HFSS (GHz)	Comput-ed [16] (GHz)	FEKO (GHz)
50	TM_{11}	2.32	1.59	1	19.30	1.350	1.435	1.357	1.339
50	TM_{21}	2.32	1.59	1	19.30	2.256	2.353	2.259	2.235
50	TM_{31}	2.32	1.59	1	19.30	3.106	2.829	3.116	2.806

Table 3-8: Percentage errors of the resonant frequencies by theories compared with experimental results at $h_2 = 1\text{mm}$

mode	HFSS	Computed [16]	FEKO
TM_{11}	-6.296	-0.518	0.814
TM_{21}	-4.3	-0.133	0.93
TM_{31}	8.918	-0.322	9.658

The average error in the upper tables is shown in Table 3.9.

Table 3-9: Average % errors of resonant frequency in different theories

Table	**Average % error [HFSS]**	**Average % error [Computed** [16]**]**	**Average % error [FEKO]**
Table (3-4)	5.062	0.136	4.16
Table (3-6)	5.746	0.359	4.051
Table (3-8)	6.505	0.324	3.8

Effective dielectric constant can be computed by using the values of the resonant frequencies obtained by FEKO and after the substitution of these values in Equation 3.3 the values in Tables 3.10, 3.11 and 3.12 are obtained.

Table 3-10: Effective dielectric constant of substrates by FEKO software for $h_2 = 0$

Mode	Frequency (GHz)	ε_{reff} (FEKO)
TM_{11}	1.147	2.016
TM_{21}	1.914	2.068
TM_{31}	2.364	2.565

Table 3-11: Effective dielectric constant of substrates by FEKO software for $h_2 = 0.5$ mm

Mode	Frequency (GHz)	ε_{reff} (FEKO)
TM_{11}	1.268	1.59
TM_{21}	2.127	1.613
TM_{31}	2.646	1.97

Table 3-12: Effective dielectric constant of substrates by FEKO software for $h_2 = 1$ mm

Mode	Frequency (GHz)	ε_{reff} (FEKO)
TM_{11}	1.339	1.426
TM_{21}	2.235	1.408
TM_{31}	2.806	1.691

3.4.2 Triangular Patch Antenna

In this section, the circular radiating patch is replaced by a triangular patch. The multi substrate layer is placed between the conductors. A simple and general formula for the resonant frequency of an equilateral triangular patch antenna (ETPA) is

expressed in Equation 3.9 using the cavity model analysis [18], where the side length is the essential parameter in this formula.

The resonant frequency of a triangular patch antenna is computed by FEKO simulation. Equation 3.9 is used to find the effective permittivity of the substrates.

$$\varepsilon_{reff} = \left(\frac{2c}{3a_e f_{r,nm}} \left(n^2 + nm + m^2 \right)^{1/2} \right)^2 \tag{3.9}$$

Where *m*=1 and *n*=0.

$$\varepsilon_{r,effc} = \frac{\varepsilon_{re}+1}{2} + \frac{\varepsilon_{re}-1}{2} \left(1 + \frac{12d}{3^{0.3}\, a/2} \right)^{-\frac{1}{2}} \tag{3.10}$$

$$a_e = a + d \left(0.01 + \frac{3.84}{\sqrt{\varepsilon_{r,effc}}} \right) \tag{3.11}$$

Here a_e is side length affected in triangular patch antenna.

$$\varepsilon_{re} = \frac{\varepsilon_{r1}\varepsilon_{r2}d}{\varepsilon_{r1}d_2 + \varepsilon_{r2}d_1} \tag{3.12}$$

3.4.2.1 Simulation of the Triangular Patch Antenna by using FEKO

An equilateral triangular patch antenna (ETPA) having a side length of $a = 30$ mm and two triangular substrates with side length of r =32 mm was used. The dielectric constant of the first substrate below the patch is $\varepsilon_{r1} = 2.4$ with thickness $d_1 = 1$ mm. The second substrate is air gap with $\varepsilon_{r2} = 1$ with thickness $d_2 = 1$ mm as shown in Figure 3.9. ETPA is simulated by using FEKO software.

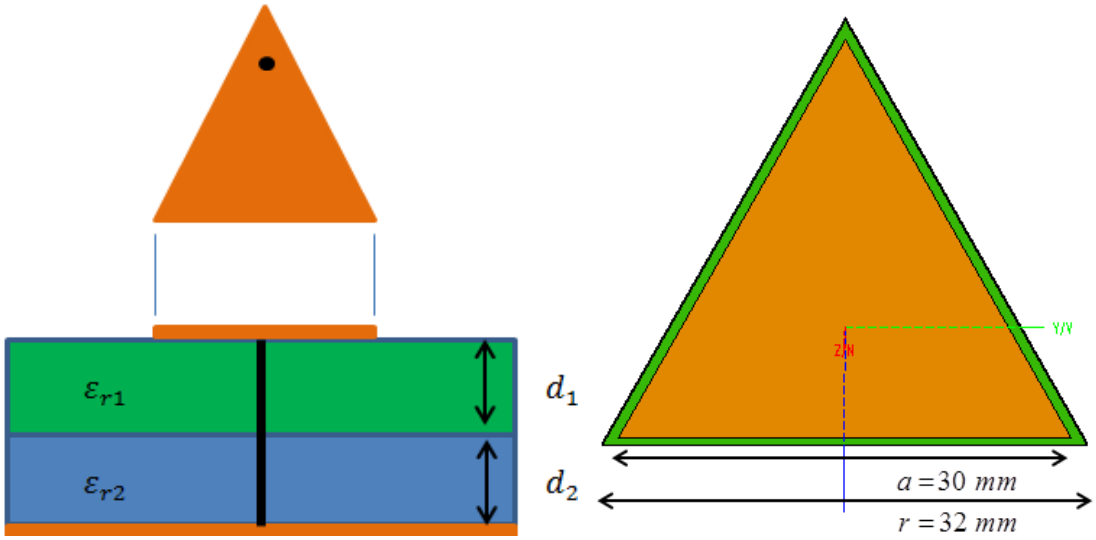

(a) (b)

Figure 3-9: Triangular patch antenna (a) Side view (b) Top view [18]

A coaxial cable feed is at (14.25mm, 0) from the ground to the patch.

The return loss of the triangular patch antenna can be seen in Figure 3.10 produced by FEKO software when the resonant frequency is equal to 4.02 GHz, while the resonant frequency according to the CAD model is about 3.95 GHz.

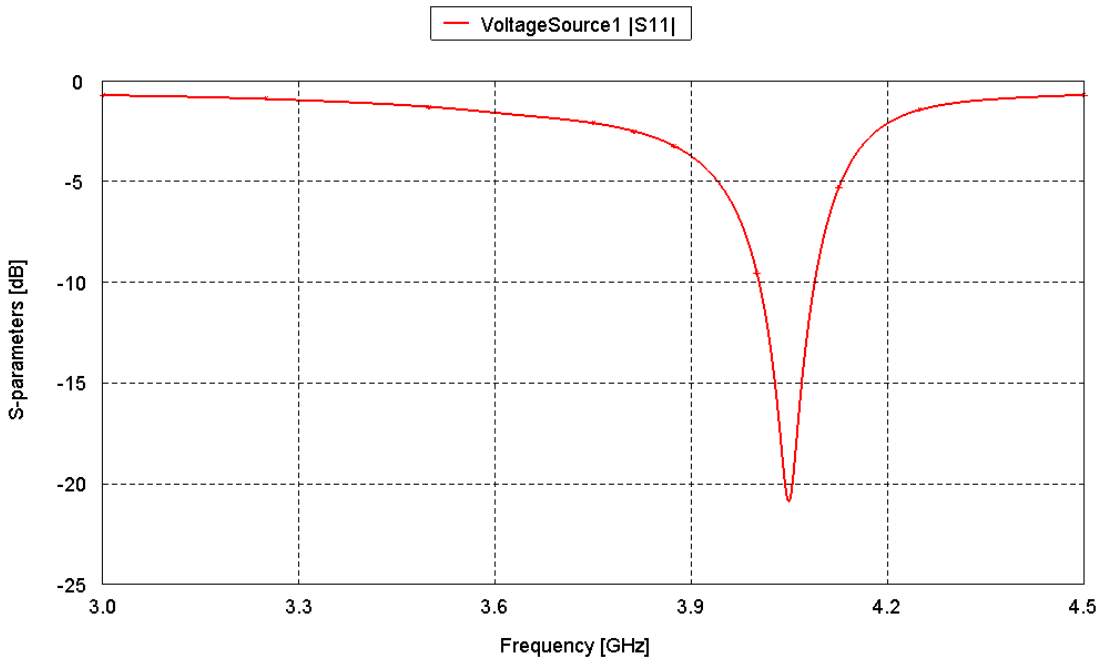

Figure 3-10: Return losses of triangular patch antenna

The value of the resonant frequency obtained by FEKO was used to compute ε_{reff} by using Equation 3.10. The results are in Table 3.13.

Table 3-13: Effective dielectric constant of substrates by FEKO for triangular patch antenna

Antenna	ε_{reff} **FEKO**
Triangular patch antenna	1.964

3.4.3 Square Patch Antenna

The effective dielectric constant of the substrates can be determined by using the formula in Equation 3.13, which takes the multilayer property into consideration. FEKO will model the square patch antenna in this section to compute the resonant frequency which is substituted in Equation 3.14 to calculate quasi-static permittivity.

The dispersive behavior of the permittivity is determined by Equation 3.13 [19].

$$\varepsilon_{reff} = \varepsilon_r^{'} - \frac{\varepsilon_r^{'} - \varepsilon_e}{1 + p(f)} \tag{3.13}$$

Where ε_e is the quasi static permittivity which is computed by Equation 3.14:

$$f_r = \frac{c}{2(L + 2\Delta L)\sqrt{\varepsilon_e}} \tag{3.14}$$

$\varepsilon_r^{'}$ and ε_{reff} are the permittivities which take the effect of the multilayer on a microstrip line into consideration.

$$\varepsilon_r^{'} = \frac{(\varepsilon_e * 2) - 1 + A}{1 + A} \tag{3.15}$$

$$A = \left(1 + \frac{12h_{12}}{w}\right)^{-1/2} \tag{3.16}$$

Here the parameter A is used to simplify the Equation in 3.15 and h_{12} is the height of the substrates.

$p(f)$ is the normalized frequency and can be determined as the equations [20] below:

$$p(f) = p_1 p_2 [(0.1844 + p_3 p_4) 10fh]^{1.5763} \tag{3.17}$$

With

$$p_1 = 0.27488 + [0.6315 + 0.525/(1 + 0.157fh)^{20}]u - 0.065683\exp(-8.7513u) \tag{3.18}$$

Where $u = w/h$.

$$p_2 = 0.33622[1 - \exp(-0.03442\varepsilon_r)] \tag{3.19}$$

$$p_3 = 0.0363\exp(-4.6u)\,x\{1 - \exp[-(fh/3.87)^{4.97}]\} \tag{3.20}$$

$$p_4 = 1 + 2.751\{1 - \exp[-(\varepsilon_r/15.916)^8]\} \tag{3.21}$$

3.4.3.1 Simulation Results of the Square Patch Antenna by using FEKO

The square patch antenna with multilayer proximity coupled microstrip antenna is simulated by using FEKO software as shown in Figure 3.11. The operating frequency is 7 GHz having equal side lengths L=W=13 mm. The feeding is proximity stripline having length 6 mm and width 5 mm. Feed substrate has a dielectric constant of 3.2 and thickness of 0.55 mm. For the antenna substrate, the dielectric constant is 2.33 and thickness 0.35 mm. The two air gaps have heights of

2.2 mm and each with the dielectric constant of 1.10 [14]. Ground plate is placed below them with dimensions 26 X 23 mm.

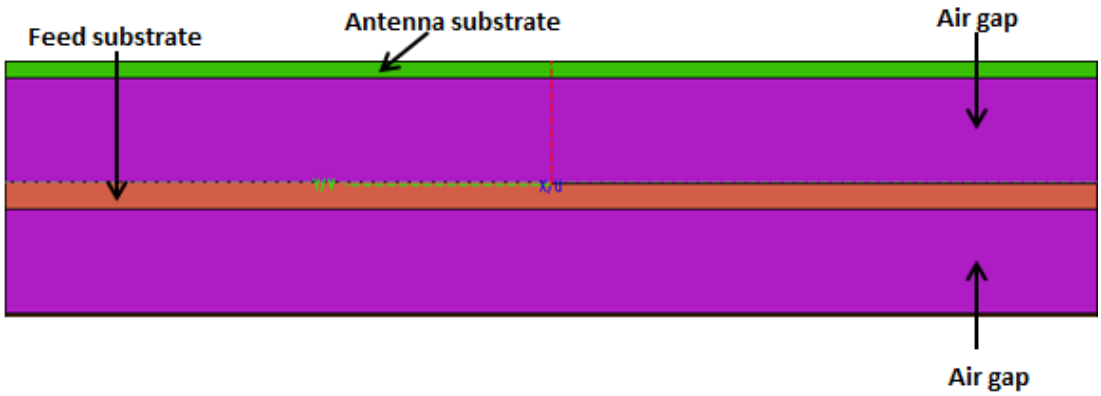

(a)

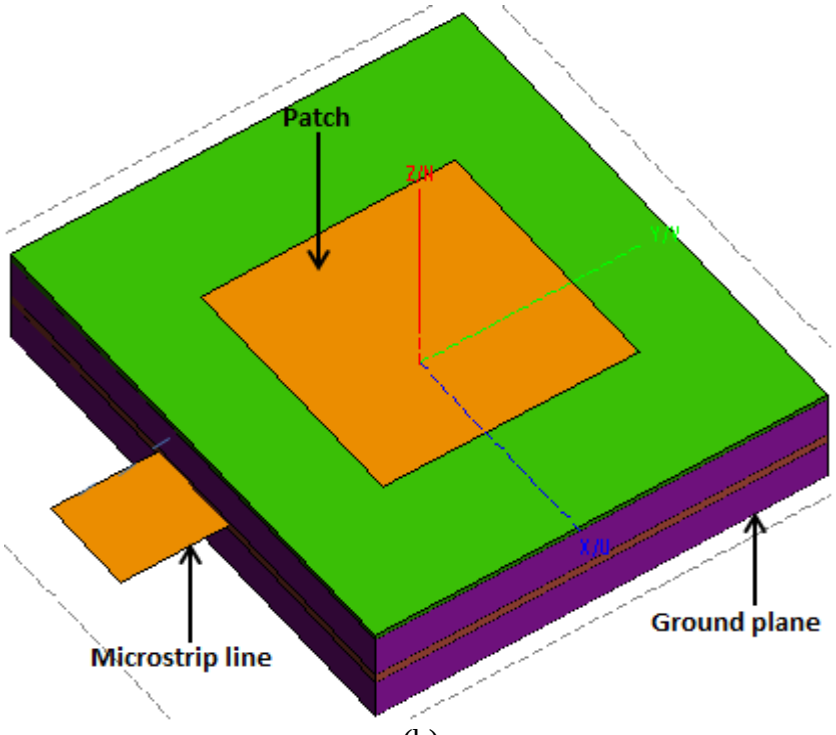

(b)

Figure 3-11: (a) Substrate layers of proximity coupled antenna by FEKO (b) Proximity coupled feed by FEKO [14]

The value of the effective permittivity for substrates was calculated as 3.94 by using the result of the resonant frequency obtained by FEKO which was equal to 7.03 GHz. The return loss of the square patch is shown in Figure 3.12.

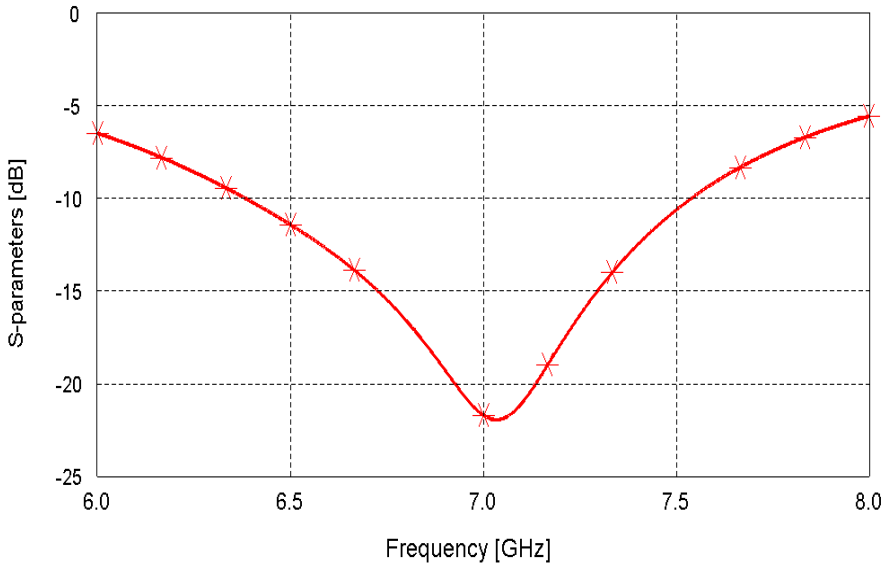

Figure 3-12: Return losses of square patch antenna by FEKO

By replacing the air gap layer with dielectrics having 1.2, 1.3, 1.4 and 1.5 the resonant frequency will be decreased and return losses will be increased gradually as shown in Figure 3.13 and Table 3.14.

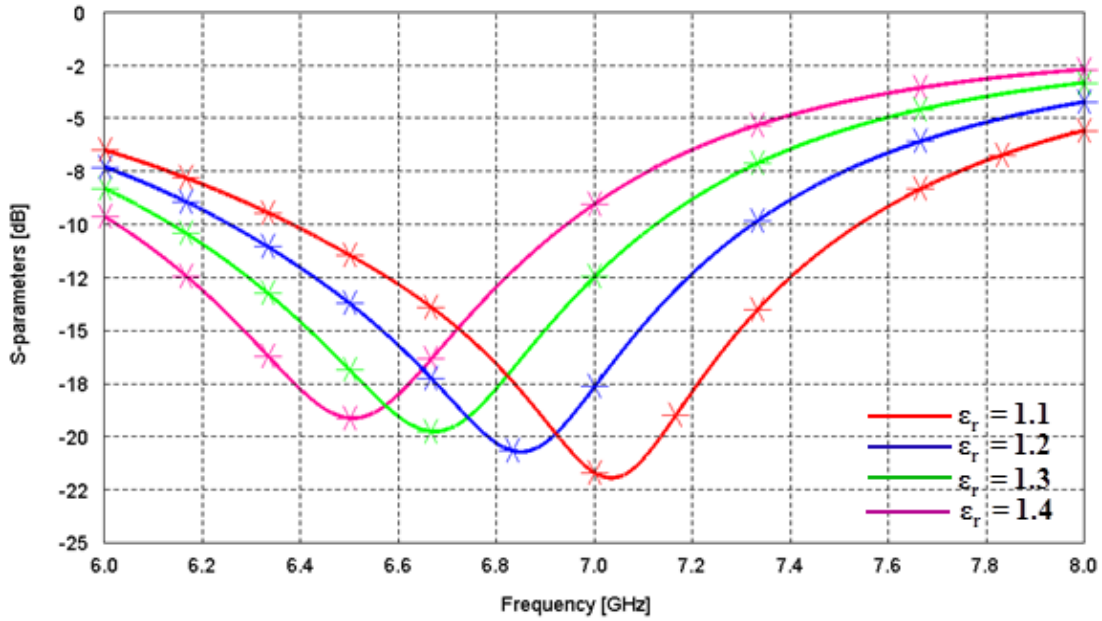

Figure 3-13: Return losses at different dielectric constants by FEKO

Table 3-14: Return losses and resonant frequencies at different dielectric constants

Dielectric constant	**Resonant frequency (GHz)**	**S11 (dB)**	**BW (MHz)**
1.1	7.03	-22.07	1150
1.2	6.84	-20.84	1070
1.3	6.66	-20.09	990
1.4	6.50	-19.39	920

Also, we can observed from the above table that, the bandwidth value was reduced gradually by increasing the value of dielectric constant.

3.5 Slot Antennas

Slot antennas are used to enhance the antenna performance like bandwidth, [15]. But on the other hand due to fringing fields the study of the effective dielectric constant is required. In this section, the following procedure will be used to calculate ε_{reff} .

The guide wavelength λ_g will be calculated by using the numerical experiment formula as in Equation 3.22 [15], depending on the essential parameters w_f, ε_r, h and λ_o. By calculating the lowest frequency and using it to compute the wavelength value, it is easy to calculate λ_g in order to find the value of ε_{reff} using the same formula in Equation 3.1:

$$\lambda_g = \lambda_o\{0.9217 - 0.277\ln\varepsilon_r + 0.0322\left(\frac{w_f}{h}\right)\bullet\left[\frac{\varepsilon_r}{\left(\frac{w_f}{h}\right)} + 0.435\right]^{0.5} - 0.01\ln\left(\frac{h}{\lambda_o}\right)$$

$$\bullet\left[4.6 - \frac{3.65}{\varepsilon_r^2\sqrt{\frac{w_f}{\lambda_o}\left(9.06 - \frac{100w_f}{\lambda_o}\right)}}\right]\} \qquad (3.22)$$

3.5.1 FEKO Simulation Results of a Printed Isosceles Triangular Slot

Triangular slot antenna is simulated in this section by using FEKO software. The configuration of the antenna is shown in Figure 3.14. The geometry of antenna consists of a triangular slot with a small rectangular slot with dimensions (L X W) and the thickness of substrate is h=1.6 mm with dimensions 123 X 145 mm. A microstrip feed line having a width w_f =3 mm is used to feed aperture coupled patch antenna. Table 3.15 demonstrates the design specifications of the antenna.

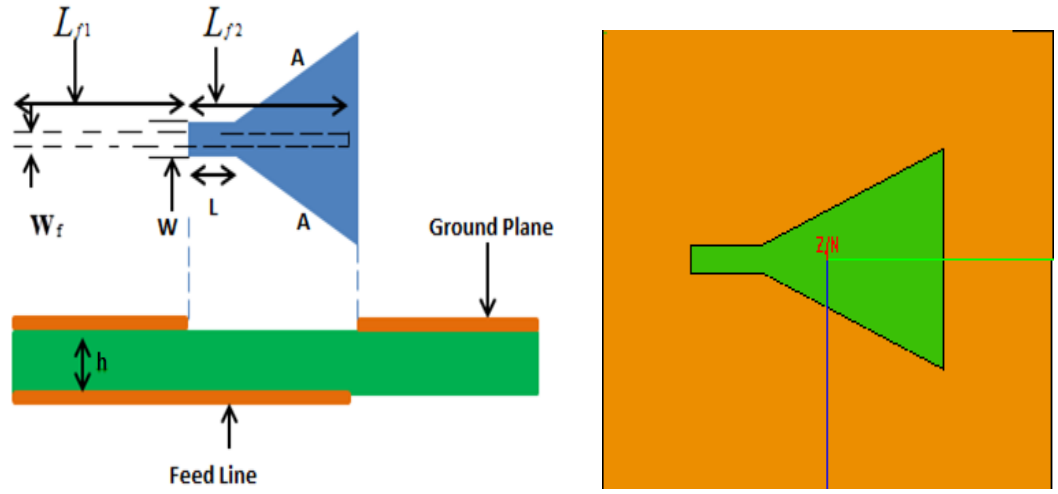

(a) (b)

Figure 3-14: Structures of triangular slot antenna (a) Side view (b) Top view by FEKO [15]

Table 3-15: Design specifications of triangular slot antenna

W	L	L_{f1}	L_{f2}	A	L_b
7.6 mm	23.0 mm	28.5 mm	67.4 mm	63.9 mm	59.0 mm

Figure 3.15 shows the simulation result of the triangular slot antenna by using FEKO software.

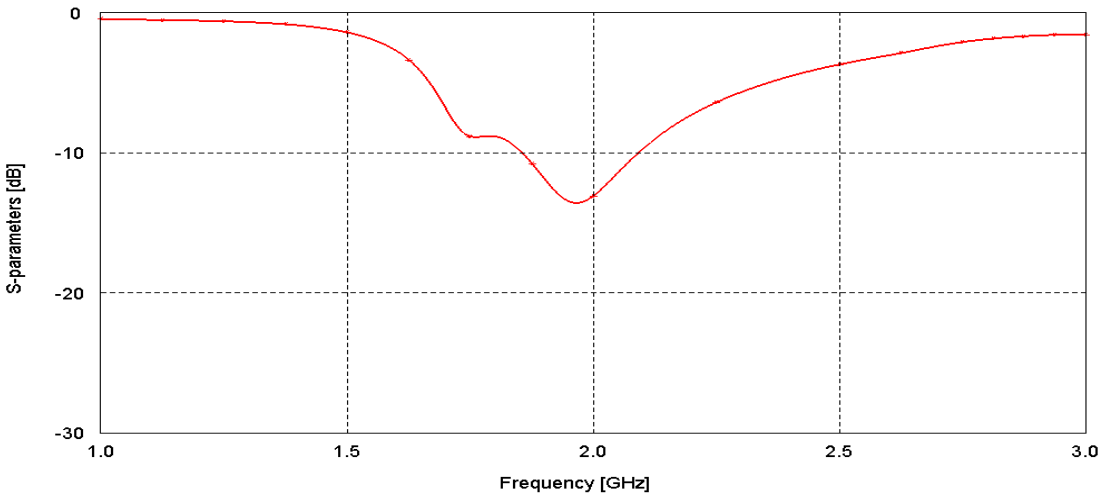

Figure 3-15: Return losses of triangular slot antenna

At the lowest frequency, all the results obtained by FEKO are compared with results obtained by HFSS as shown in Table 3.16.

Table 3-16: Results of triangular slot antenna

Simulation software	f_{Lo} **(GHz)**	λ_o **mm**	λ_g **mm**	ε_{reff}	$\varepsilon_{reff} / \varepsilon_r$
HFSS	1.82	164.84	131.68	1.567	35.6%
FEKO	1.85	162.162	129.435	1.5696	35.67%

The cell size (mesh) is important in each design, which affects the accuracy of the results. Different cell sizes show the effect on the return losses and resonant frequency on results in FEKO in Figure 3.16.

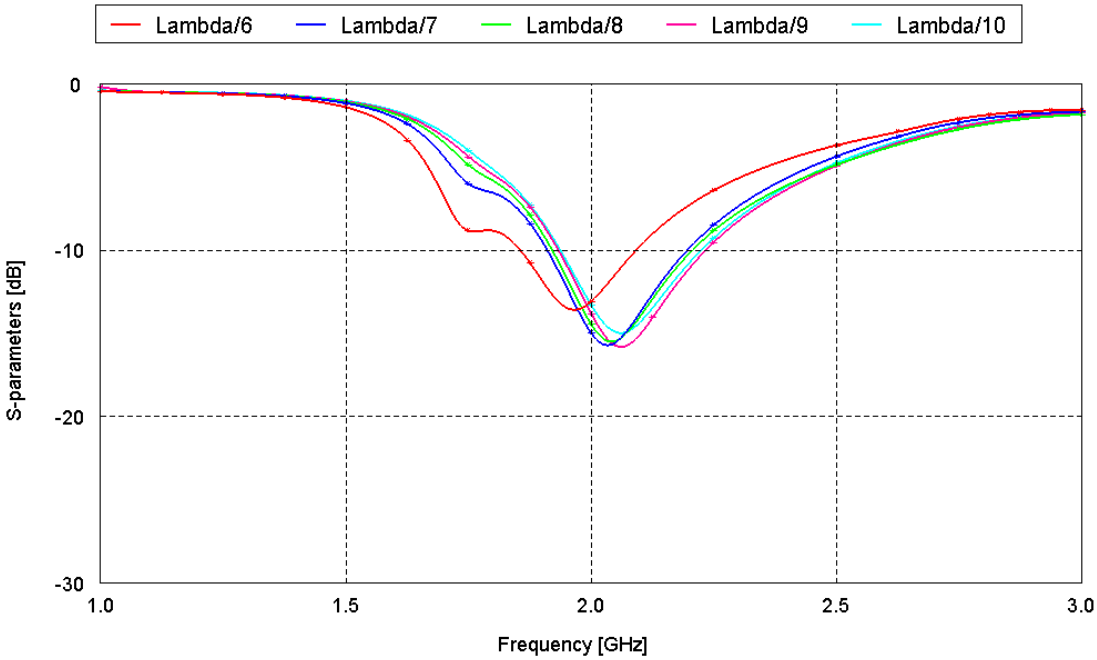

Figure 3-16: Return losses at different cell sizes

3.5.2 FEKO Simulation Results for The Square Slot

After discussing the simplified formula in section 3.5, the same procedure will be used, but in this case the square slot antenna is suggested instead of a triangular.

The primary goal is to increase the slot area, and see its effect on the effective dielectric constant value of substrate.

A square slot antenna with dimensions $L_A = W_A$ =63.9 mm as shown in Figure 3.17 is simulated instead of a triangular slot, which has the same dimensions of a small rectangular slot and feed line in section (3.5.1). Substrate thickness is 1.6 mm.

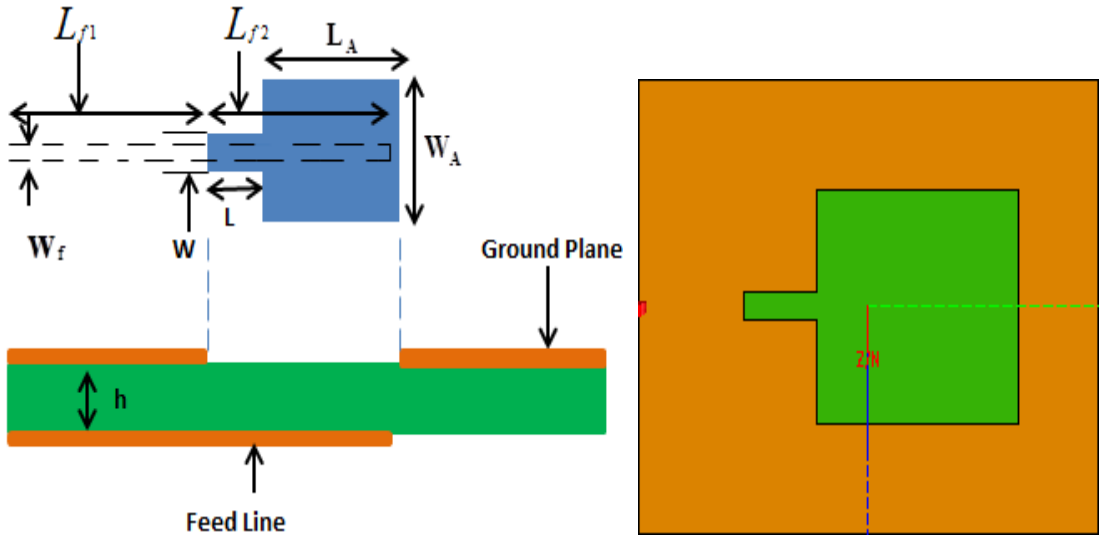

(a) (b)

Figure 3-17: Structures of square slot antenna (a) Side view (b) Top view by FEKO

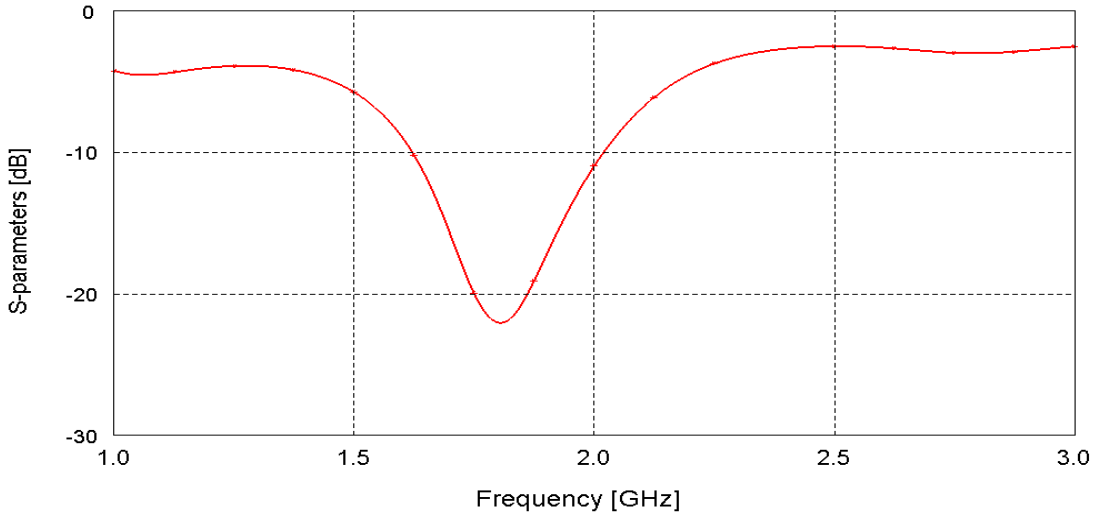

Figure 3-18: Return losses of square slot antenna

By appling the same formula in Equation 3.22, it can be seen that the value of ε_{reff} at 1.62 GHz will be reduced to 1.54 as a result of an increase in the slot area of the antenna.

3.6 Effects of Feed Techniques for The Patch Antennas

The feeding techniques and feed points may change the antenna performance. In this study, different feed point positions and different feed techniques are discussed.

3.6.1 Probe Feed Varying in RMSA

First of all, different feed point positions are studied in rectangular patch antenna which has dimensions (L X W) mm with substrate thickness (h) mm and dielectric constant ε_r as shown in Figure 3.19. The S-parameter at resonant frequency 2.49 GHz is -14.35 dB [21] as shown in Figure 3.20.

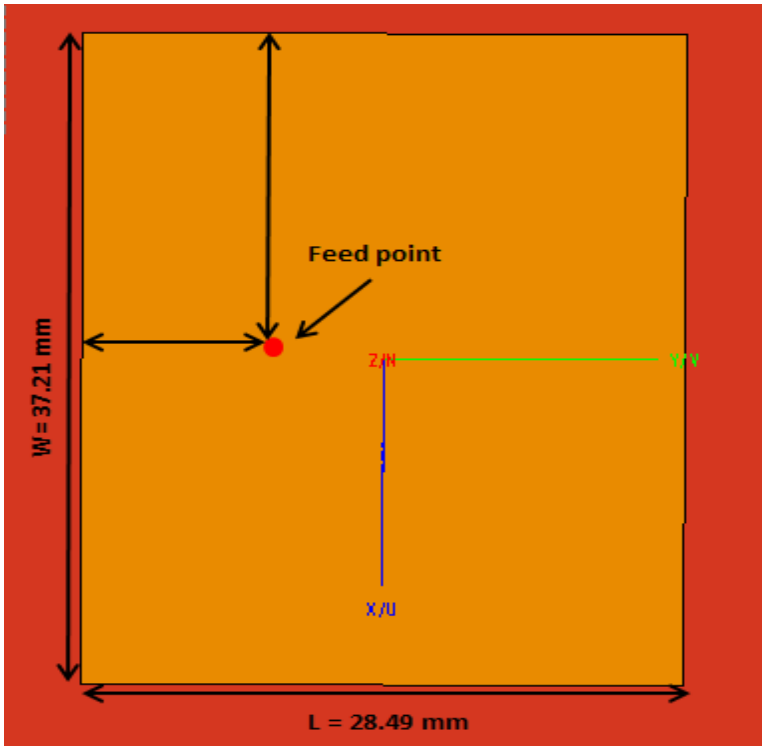

(a)

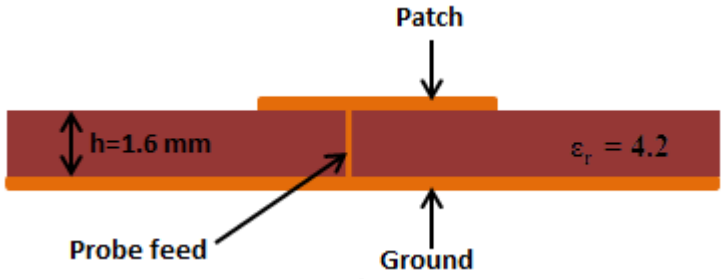

(b)

Figure 3-19: Geometry of RMSA (a) Top view (b) Side view [21]

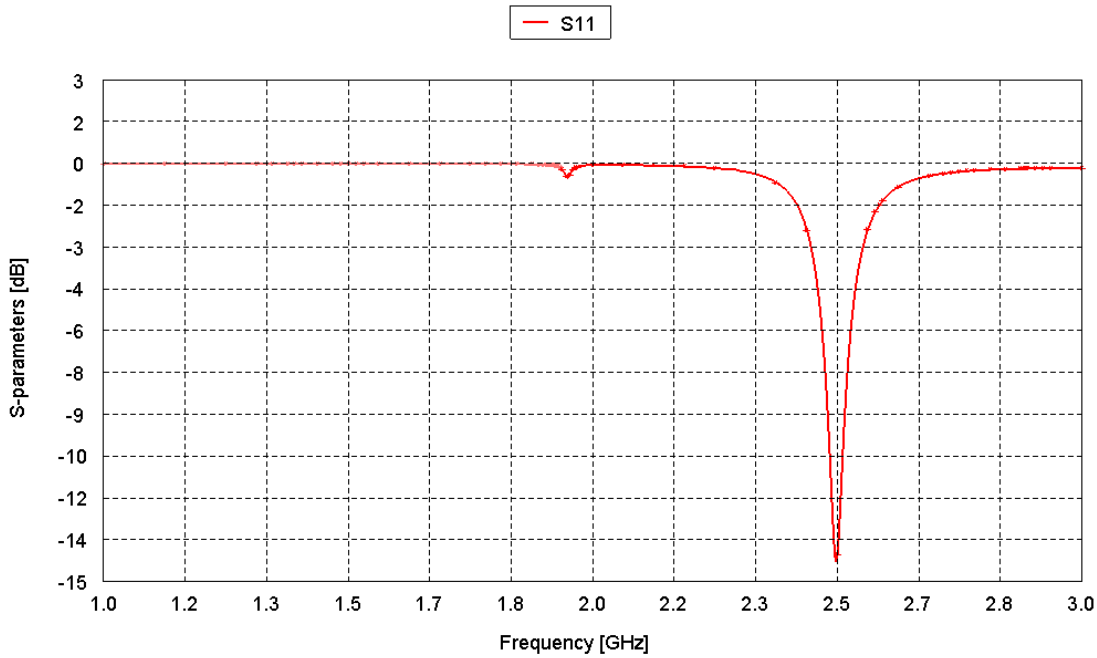

Figure 3-20: S-parameters of RMSA at feed point (9, 18) mm from the edge of patch antenna

Two cases are proposed to reduce return losses of antenna above. In the first case the value of return loss reduced at the same resonant frequency by selecting different feed points, while in the second case, dual bands was obtained and return losses improved in the same time by selecting other feed points.

3.6.1.1 Case I: Single Band Frequency

The value of return loss increased in new feed point positions as shown in Figure 3.22. That is when the value of return loss at the feed point (10.245, 6.605) mm is (-24.93 dB) while it is (-47.02 dB) at the feed point (10, 18) mm. Table 3.17 shows all the results of S-parameter at the same resonant frequency.

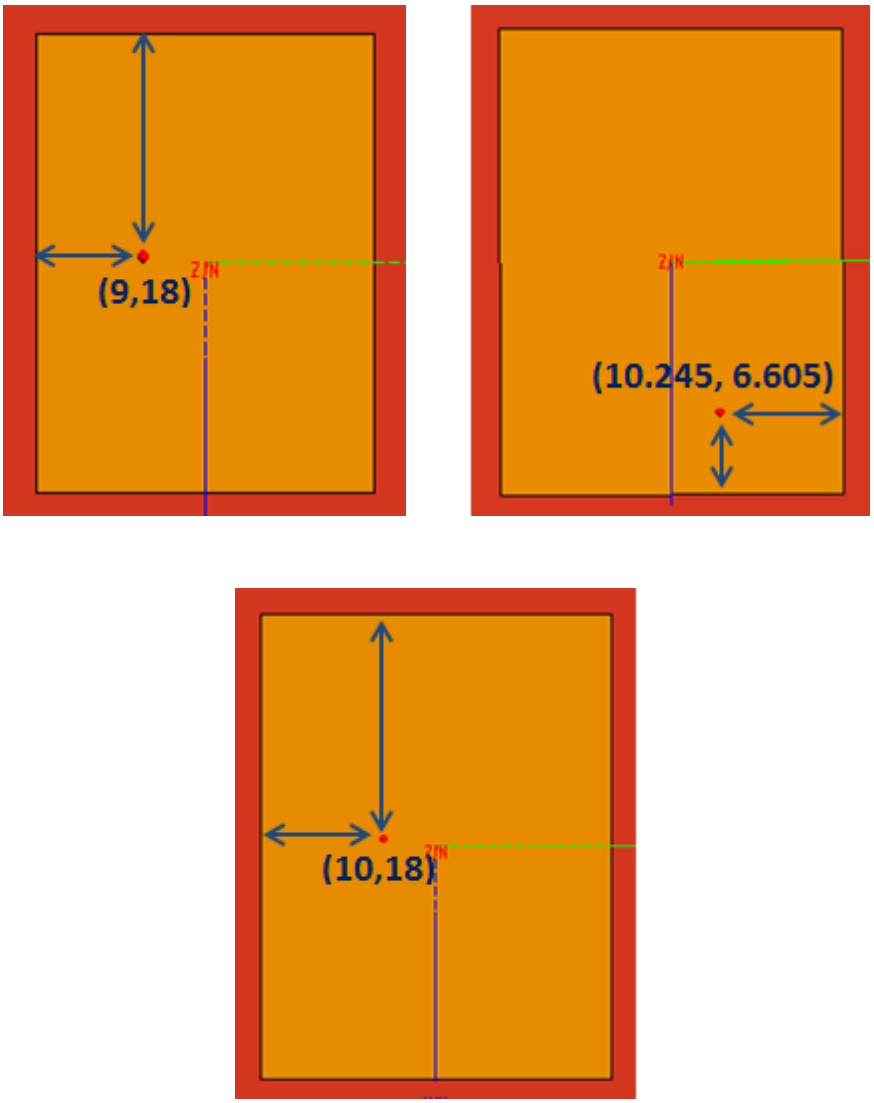

Figure 3-21: RMSA at different feed point (single band frequency)

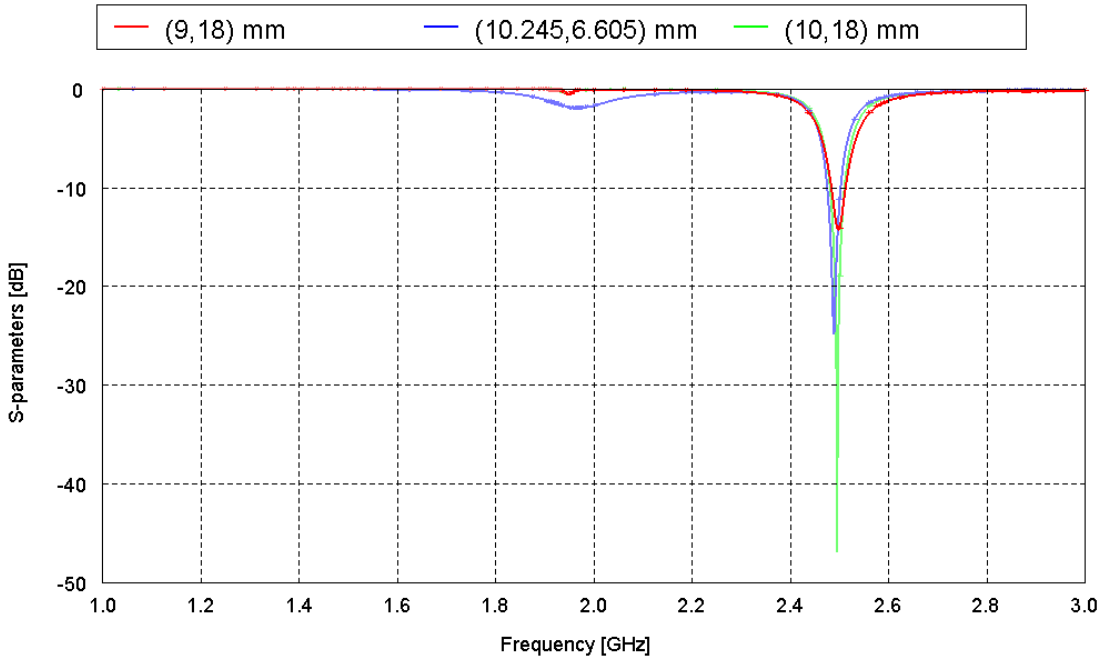

Figure 3-22: S-parameters of RMSA at feed points (9, 18) mm, (10.245, 6.605) mm and (10, 18) mm

Table 3-17: Results at different feed point (single band frequency)

Feed point (mm)	**Resonant frequency (GHz)**	**S11 (dB)**	**BW MHz**
(9, 18)	2.49	-14.35	30
(10.245, 6.605)	2.49	-24.93	30
(10, 18)	2.49	-47.02	30

3.6.1.2 Case II: Dual Band Frequency

The other study of feed position gives dual band frequency in (L-band) and (S-band) as show in Figure 3.24 and this allows the antenna to be used in wide fields of applications. Table 3.18 shows the S-parameter for the new position of feed.

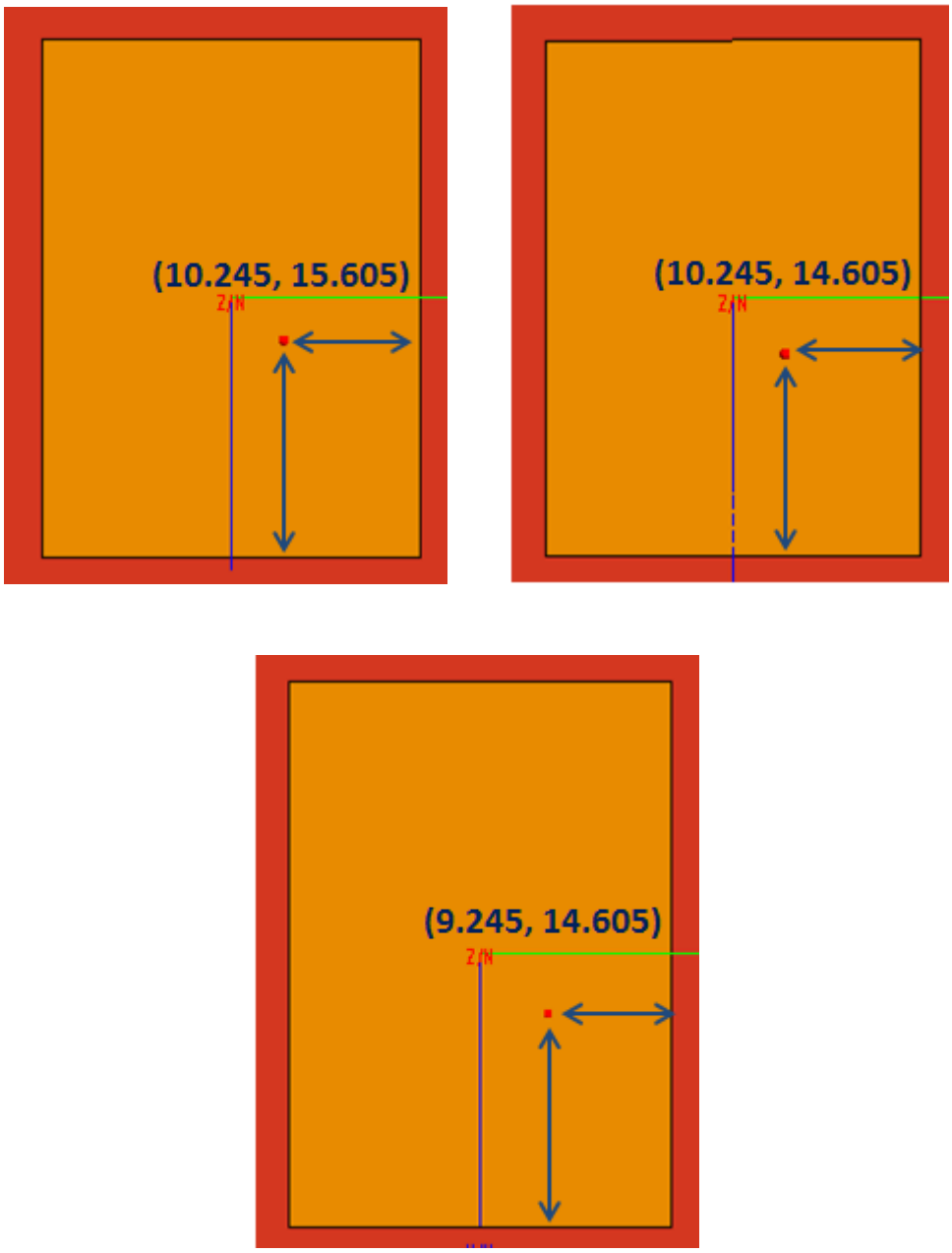

Figure 3-23: RMSA at different feed point (dual band frequency)

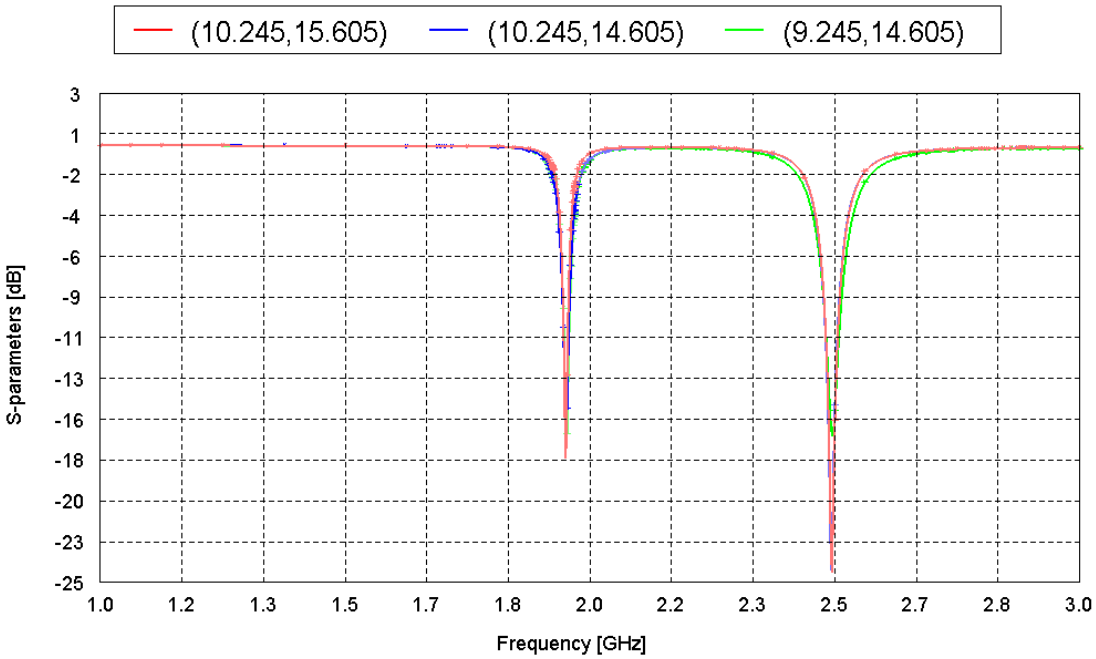

Figure 3-24: S-parameters of RMSA at feed points (10.245, 15.605) mm, (10.245, 14.605) mm and (9.245, 14.605) mm

Table 3-18: Results at different feed point (dual band frequency)

Feed point (mm)	**Band**	**Resonant frequency (GHz)**	**S11 (dB)**	**BW MHz**
(10.245, 15.605)	L-band	1.95	-18	10
	S-band	2.49	-24.92	20
(10.245, 14.605)	L-band	1.95	-16.95	10
	S-band	2.49	-24.52	20
(9.245, 14.605)	L-band	1.95	-17.13	10
	S-band	2.49	-16.73	30

Table 3.19 shows the return loss and the resonant frequency for different feed positions.

Table 3-19: S11 and resonant frequency at some other feed positions

Feed point (mm)	Resonant frequency (GHz)	S11 (dB)	BW MHz
10, 18	2.49	-47.02	30
9, 18	2.49	-14.35	30
8, 18	2.49	-9.48	---------
7, 18	2.50	-7.25	---------
6, 18	2.50	-5.87	---------
5, 18	2.51	-5.06	---------
10.245, 6.605	2.49	-24.93	30
9.245, 6.605	2.48	-16.53	20
8.245, 6.605	2.49	-10.52	10
7.245, 6.605	2.49	-7.71	---------
6.245, 6.605	2.49	-6.20	---------
10.245, 15.605	1.95	-18	10
	2.49	-24.92	20
9.245, 15.605	1.94	-17.25	10
	2.94	-17.22	40
8.245, 15.605	1.94	-17	10
	2.49	-10.61	10
7.245, 15.605	1.94	-16.82	10
	2.49	-7.89	---------
10.245, 14,605	1.59	-17.01	10
	2.49	-24.52	20
9.245, 14.605	1.95	-16.96	10
	2.49	-16.71	30
8.245, 14.605	1.95	-17.54	10
	2.49	-10.65	10
7.245, 14.605	1.95	-18.24	10
	2.50	-7.88	---------
11.245, 13.605	1.95	-9.13	---------
	2.48	-10.24	10
10.245, 13.605	1.95	-9.25	---------
	2.49	-24.92	30
9.245, 13.605	1.95	-9.42	---------
	2.49	-16.60	40
8.245, 13.605	1.95	-9.54	---------
	2.49	-10.51	10

3.6.2 Microstrip Line Feed Shifting in RMSA

The second type of RMSA feeding in this section is the microstrip feed line, which demonstrates the affect of shifting the position of feed line along the x-axis of the patch. The basic parameters of rectangular microstrip patch are shown in Figure 3.25 [22] with patch dimensions length (L) = 35.2535 mm and width (W) = 45.63 mm, cut width = 5 mm and cut length = 10 mm, the length of feed line is L_f = 32.815 mm and width W_f = 3.009 mm. The dielectric constant and thickness of substrate layer are 4.4 and 1.6 mm respectively. D is the value of the shift from the center of the patch and it was varied as shown in Table 3.20.

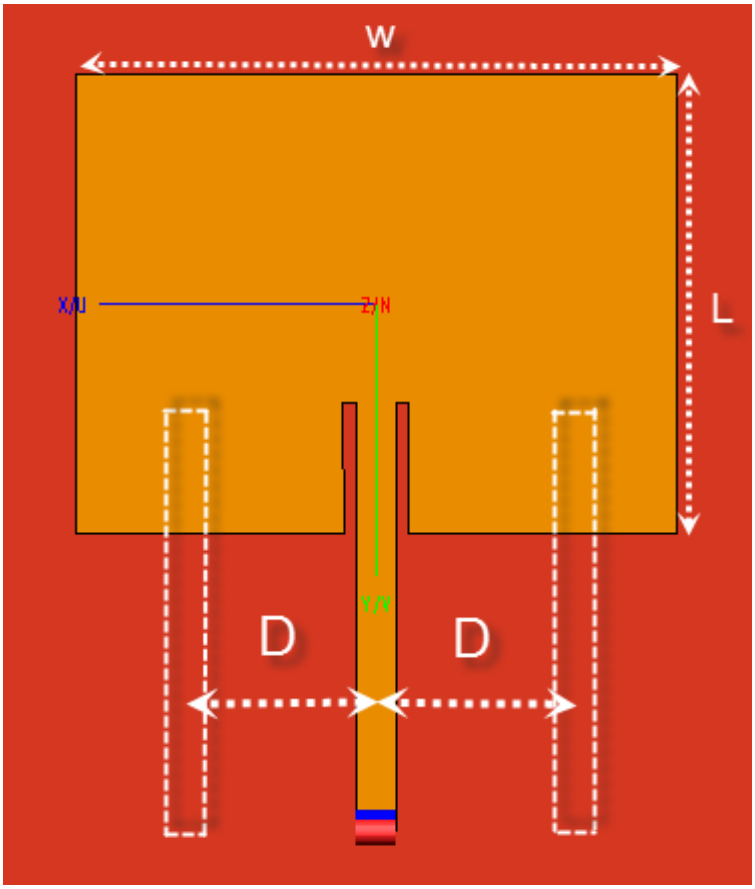

Figure 3-25: Feed line shifting in Microstrip patch antenna

The return loss is varied by changing the position of the feed line as shown in Figures 3.26, 3.27, 3.28 and 3.29.

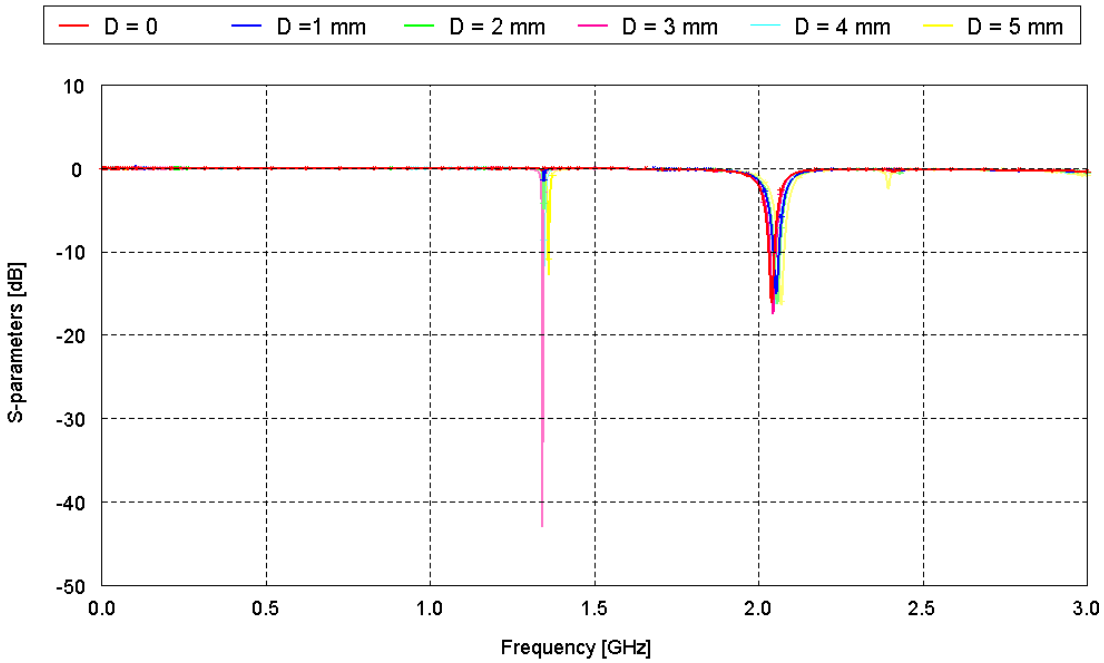

Figure 3-26: S-parameters of RMSA at D = (0, 1, 2, 3, 4, 5) mm

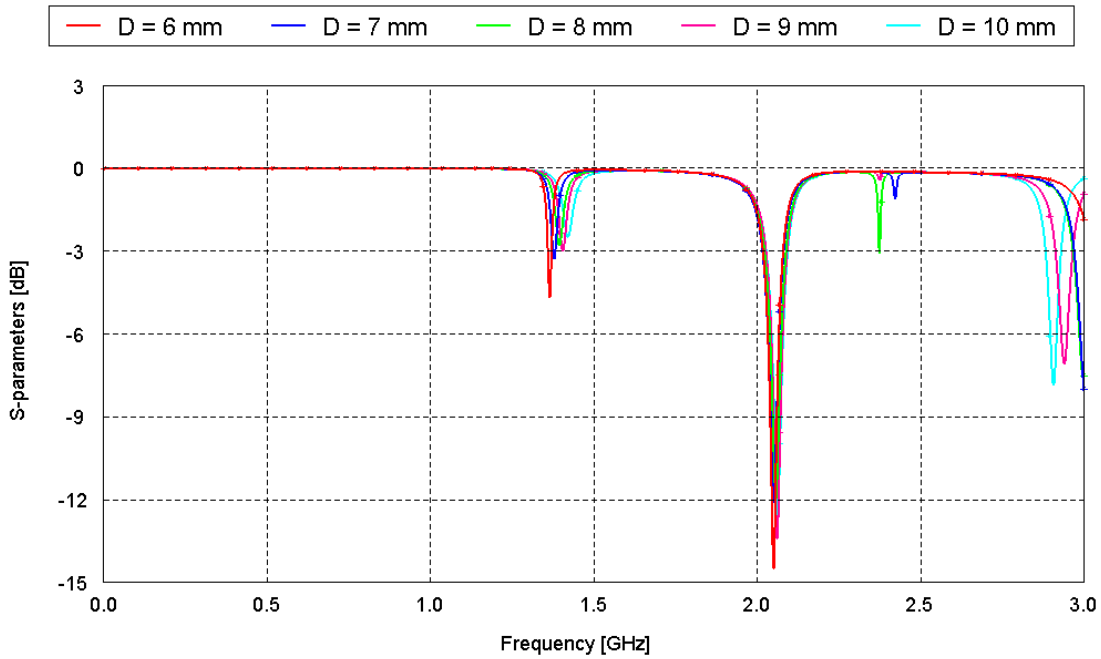

Figure 3-27: S-parameters of RMSA at D = (6, 7, 8, 9, 10) mm

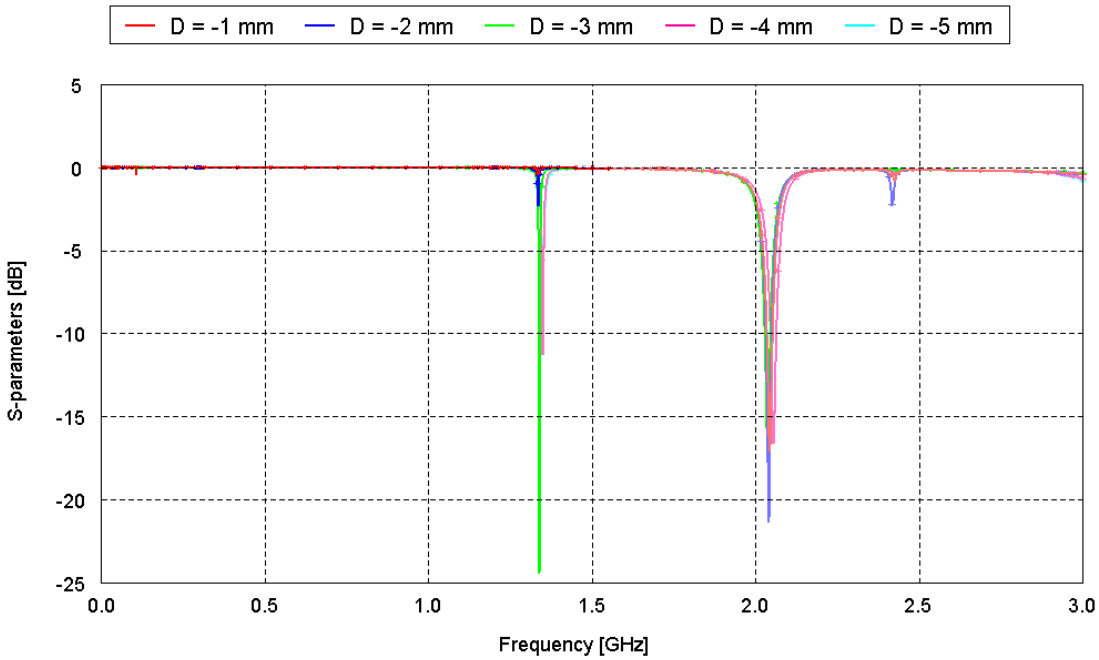

Figure 3-28: S-parameters of RMSA at D = (-1,-2,-3,-4,-5) mm

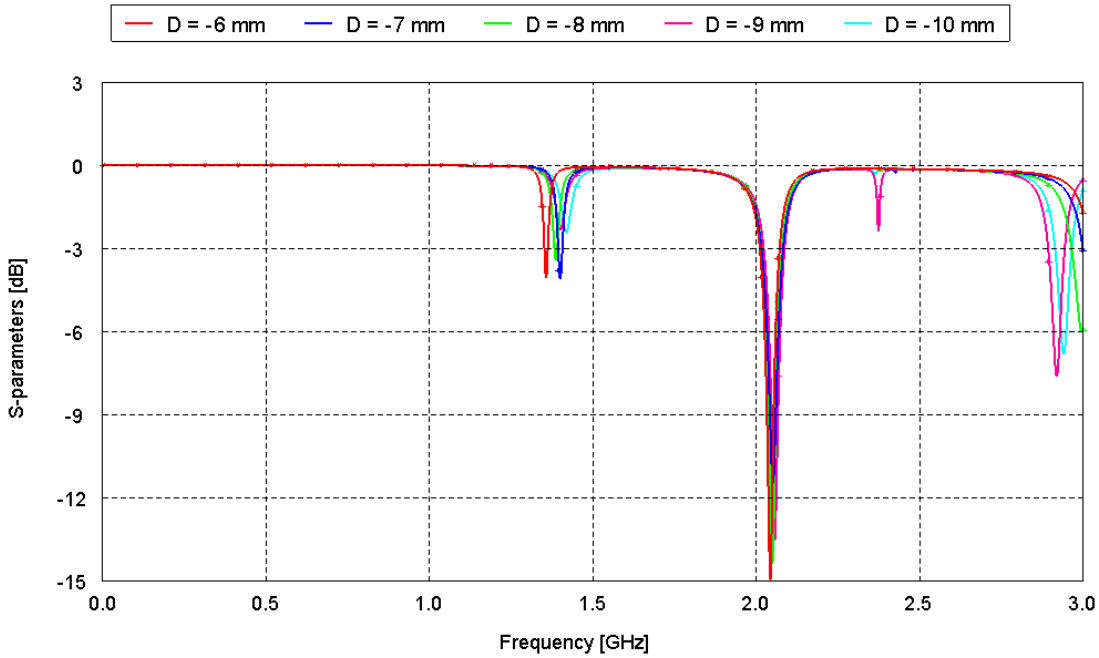

Figure 3-29: S-parameters of RMSA at D = (-6,-7,-8,-9,-10) mm

Table 3-20: Results at different feed line distance from the center of the patch

D (mm)	Resonant frequency (GHz)	S11 (dB)
0	2.03	-16.24
1	2.05	-15.07
2	2.05	-16.41
3	1.34	-43.17
	2.04	-17.65
4	1.34	-11.81
	2.05	-16.33
5	1.35	-12.82
	2.06	-16.45
6	2.05	-14.58
7	2.05	-12.18
8	2.05	-11.98
9	2.06	-13.50
10	2.06	-12.69
-1	2.04	-17.17
-2	2.04	-21.4
-3	1.33	-24.55
	2.03	-17.35
-4	1.34	-11.41
	2.05	-16.65
-5	2.04	-15.84
-6	2.04	-14.98
-7	2.05	-11.50
-8	2.05	-14.44
-9	2.05	-13.59
-10	2.05	-12.95

The optimum position is 3mm in +x direction from the center of the patch.

Chapter 4

PATCH ANTENNA SIMULATIONS BY USING FEKO AND IMPROVEMENTS IN THE RETURN LOSS, GAIN AND BANDWIDTH

4.1 Introduction

The slot in antennas affects the antenna performance. S. Bhunia (2012) examined the effect of rectangular slot loading on microstrip patch antennas [23]. The impact of the slot on a resonant frequency, bandwidths and the return loss was investigated by using a small slot load at one edge of the radiating patch antenna.

Also different slot shapes were applied on the circular patch to get an improvement in the values of return loss, bandwidth and voltage standing wave ratio. Sachin S. Khade and S.L.Badjate (2012) studied modeling and design of annular ring microstrip antenna [24].

Surface waves are the drawback for patch antennas, this chapter focuses on solving this problem by using defected ground structure (DGS) with different shapes of ground apertures to improve the antenna gain.

4.2 Effects of Triangular Slot Loading on Resonance Frequency of Patch Antennas

The study of cutting a triangular slot from the one edge of the patch antenna is proposed. It is compared with the traditional rectangular patch antenna as shown in Figure 4.1. The resonance frequency value will be changed gradually by increasing the area of the triangular slot.

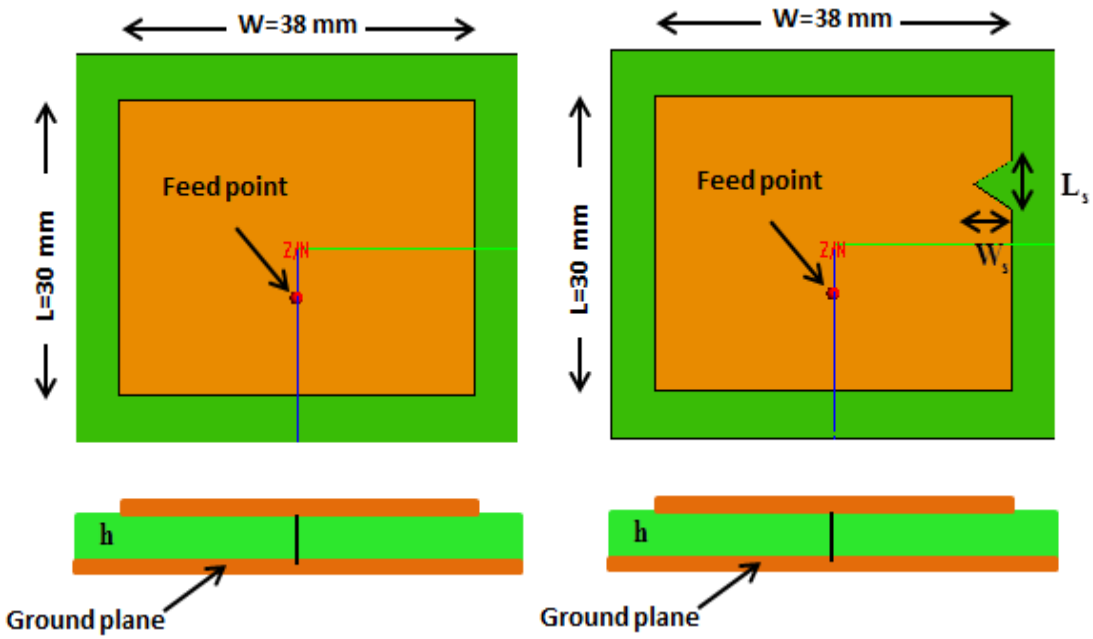

(a) (b)

Figure 4-1: (a) Antenna without slot (b) Antenna with triangular slot [23]

Patch antenna simulated by using the FEKO software has dimensions W=38 mm and L=30 mm, the thickness of substrate layer is 1.5875 mm with dielectric constant $\varepsilon_r = 2.4$. The antenna is fed by a coaxial cable, which is located at 5 mm from the center of the patch and having 0.5 mm as radius [23]. The patch and substrate are placed over a ground plane with dimensions 47.525 X 39.525 mm.

By cutting a triangular slot antenna at the edge of patch radiation with $L_s = 5\,\text{mm}$ and w_s is varied in the range 4 to 10 mm which increases the load on the patch antenna and also the radiation at the edge of the antenna. The current length obviously will be lengthened as you force the current lines to bend, which results in an increase of the half wavelength resulting and by reducing the frequency as shown in Figure 4.2. Table 4.1. The figure shows all the results of antenna for different values of w_s.

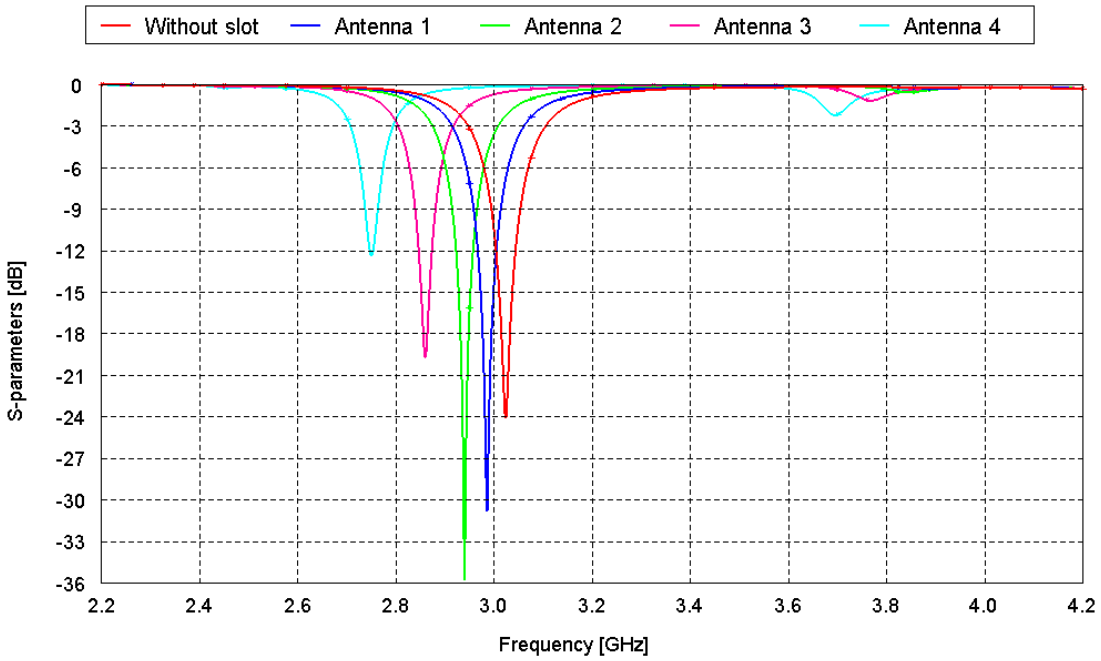

Figure 4-2: Return losses of antennas at different value of w_s

We can observed that, resonant frequency changes by the height of the triangular and the optimum return loss is at $W_s = 6\text{mm}$ for this particular design with the same bandwidth.

Table 4-1: Triangular slot loading effects on antenna parameters

Antenna	**W_s mm**	**Resonant frequency(GHz)**	**S11 (dB)**	**BW (MHz) at 10 dB**
Without slot	0	3.022	-24.26	50
Antenna 1	4	2.98	-30.89	50
Antenna 2	6	2.93	-36.31	50
Antenna 3	8	2.86	-19.81	30
Antenna 4	10	2.74	-12.44	20

4.3 Improvement Return loss, VSWR and Bandwidth in Circular Patch Antenna

In this study, three cases will be considered to reduce the return loss and VSWR and to improve the bandwidth of the proposed circular patch antenna by using FEKO software. The patch is placed on a substrate of thickness h=2.87 mm and permittivity $\varepsilon_r = 5.8$. The size of the ground plane is considered infinity, as shown in Figure 4.3. The radius of the proposed patch is kept at 11.8 mm. VSWR and return loss values are presented in Figures 4.4 and 4.5 respectively. This design is fed by a coaxial cable at the point (1.5, 8.282) mm from the ground to the patch and this point was keep constant in the same position in all cases.

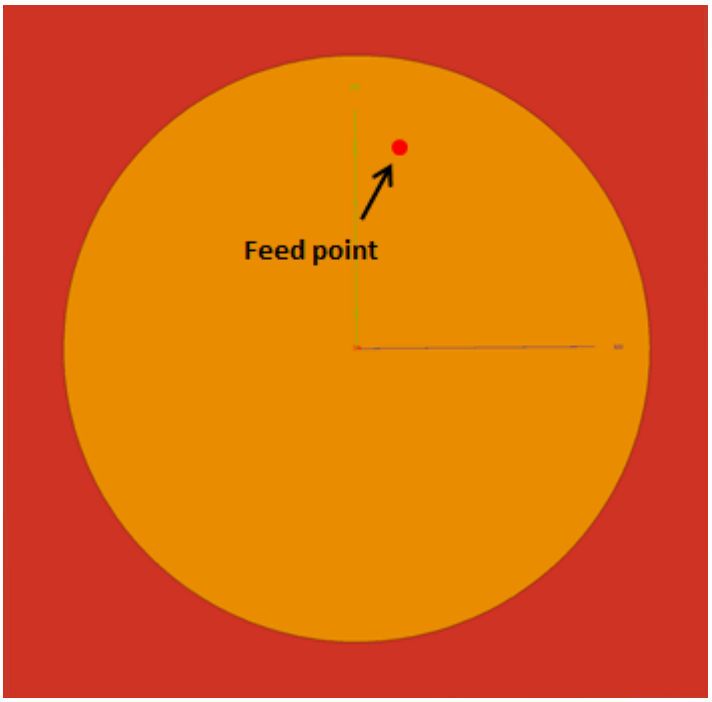

Figure 4-3: Proposed circular patch antenna

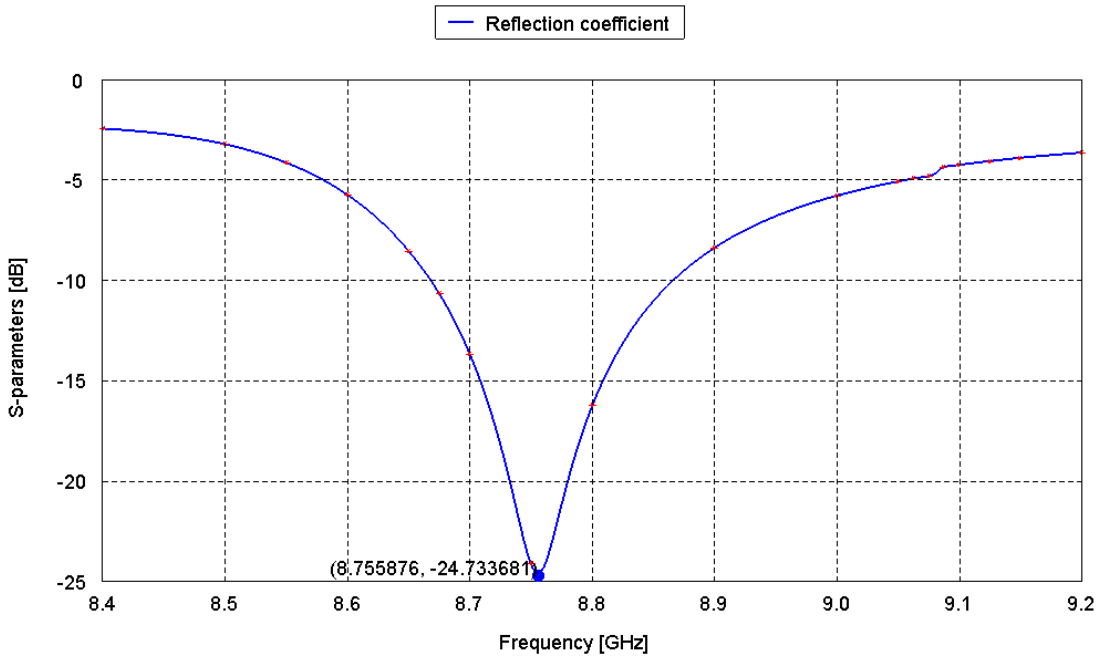

Figure 4-4: S-parameters of proposed circular patch antenna

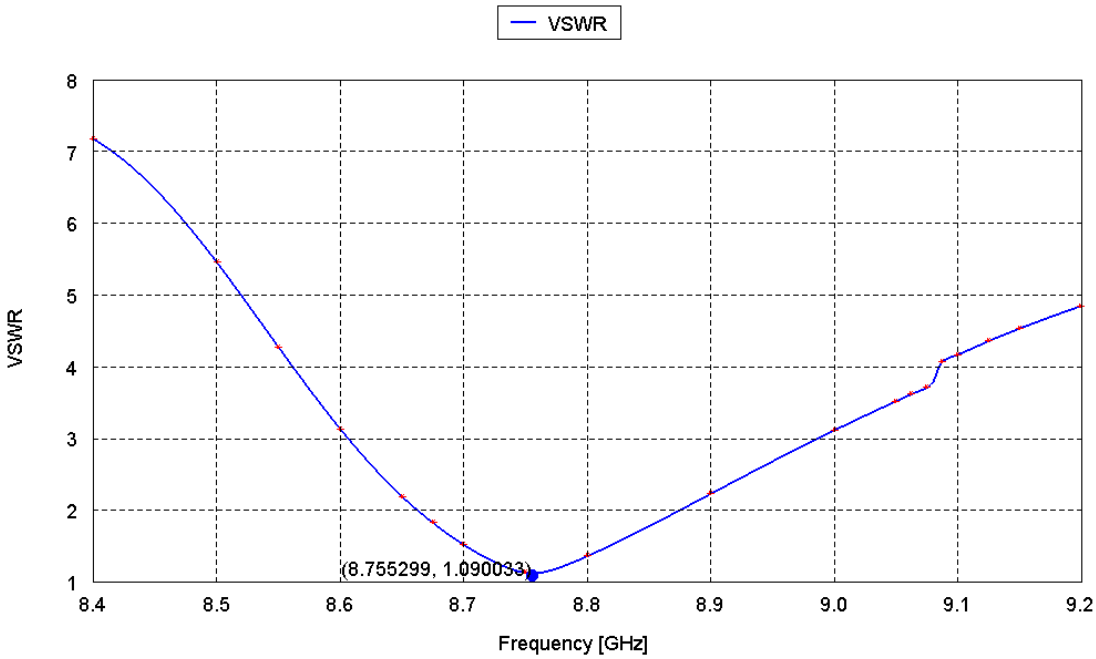

Figure 4-5: VSWR of proposed circular patch antenna

4.3.1 Case I: Annular Slot Patch Antenna

Considering the antenna in the previous section, the effect of the inner radius of the microstrip antenna will be investigated in this case at the radius 5 mm [24]. Figure 4.6 shows the geometry of the antenna.

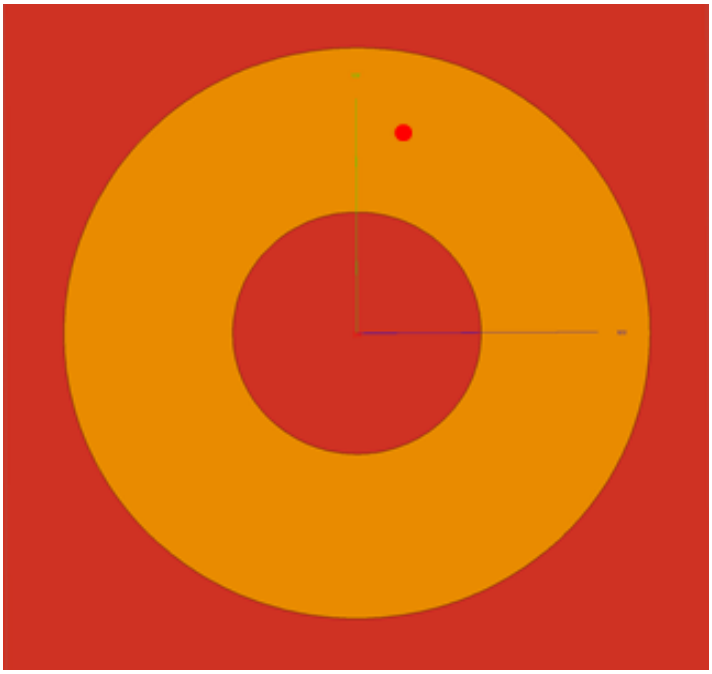

Figure 4-6: Annular microstrip patch antenna [24]

The value of the return loss will be reduced in this part up to 27.16 dB, as shown in Figure 4.7.

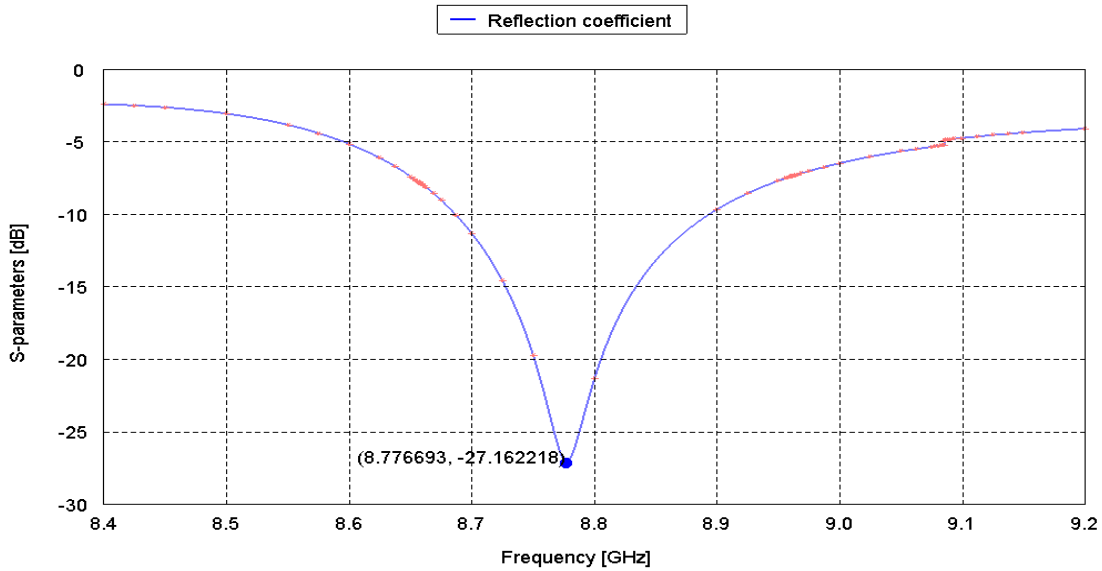

Figure 4-7: S-parameters of annular patch antenna

In addition, the value of VSWR will be improved to (1.05) as shown in Figure 4.8.

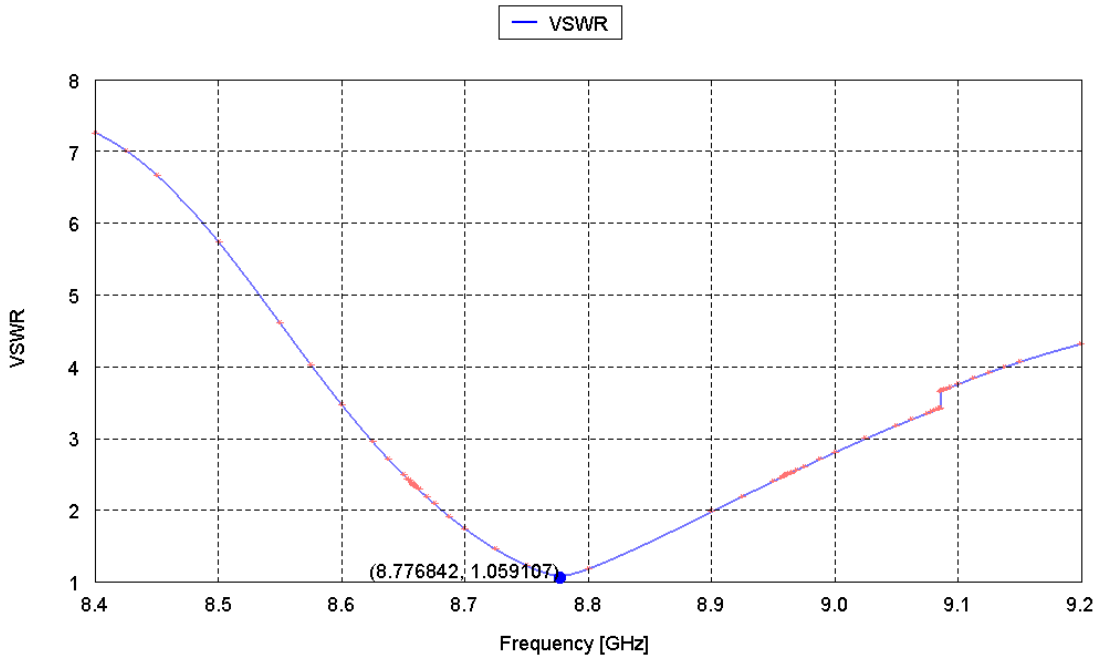

Figure 4-8: VSWR of annular patch antenna

4.3.2 Case II: Inner Circular Slots Ring Shaped (cross shape within the ring)

In this section a multi circular slot had been cut from the patch as shown in Figure 4.9. Each slot has a radius of 1 mm, where the slots are arranged as a ring with cross shape inside the patch.

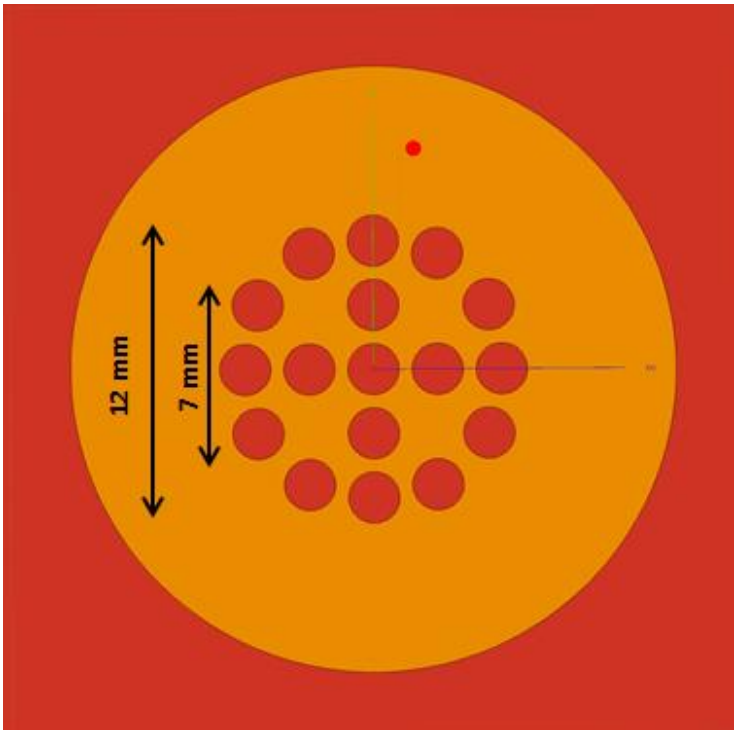

Figure 4-9: Inner circular slots a ring shape with cross shape within the ring

Figures 4.10 and 4.11 shows the return loss and VSWR, which they have values of 27.29 dB and 1.06 respectively.

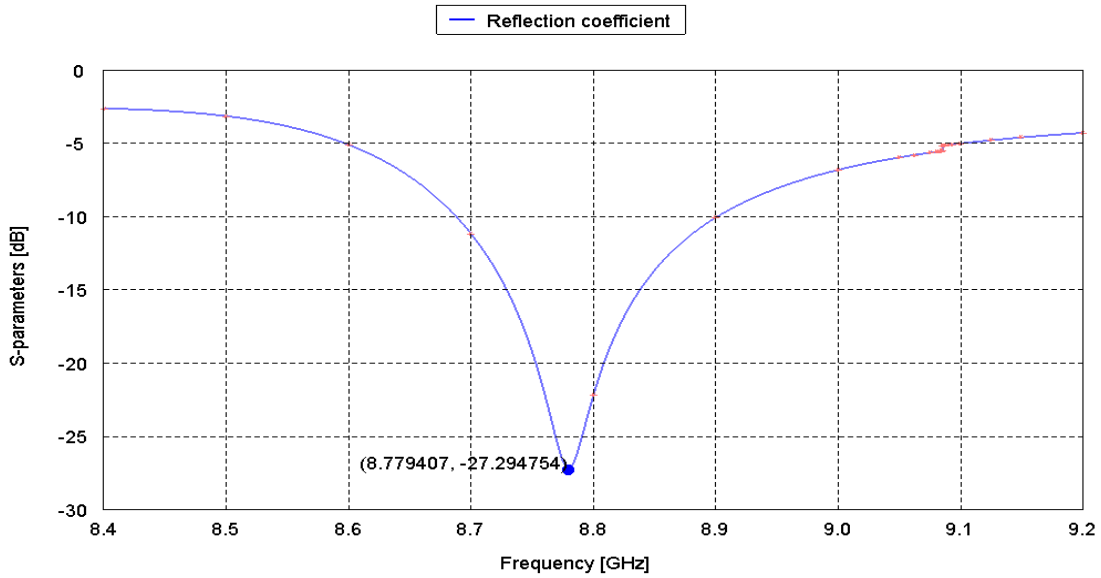

Figure 4-10: S-parameters of inner circular slots in a ring shape (with cross within the ring)

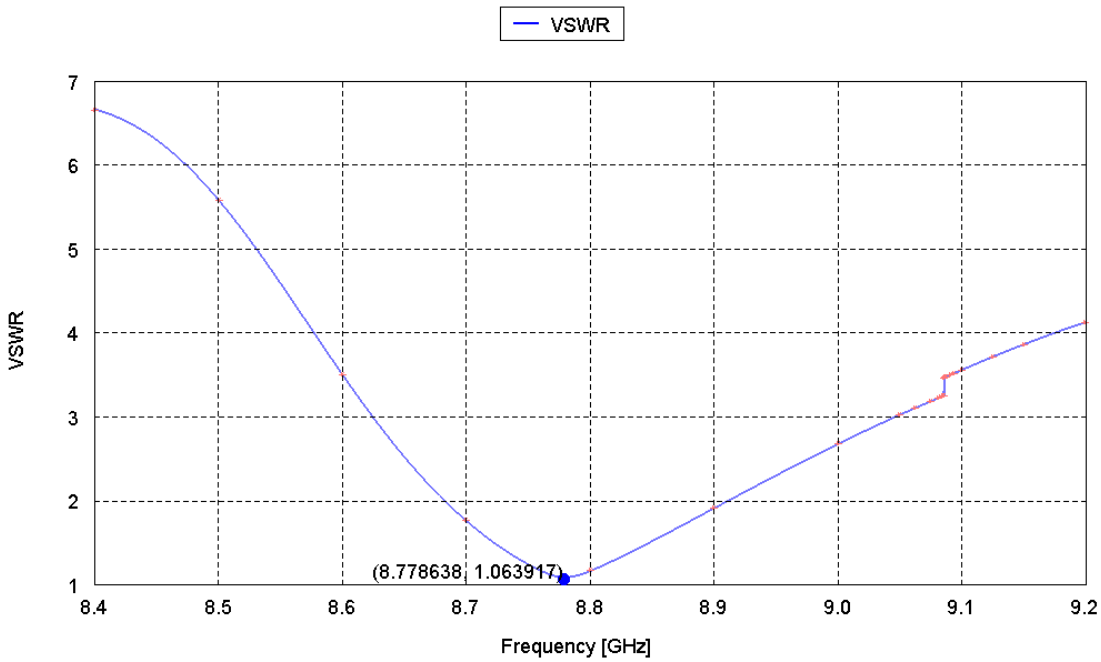

Figure 4-11: VSWR of inner circular slots in a ring shape (with cross within the ring)

4.3.3 Case III: Inner Circular Slots in a Square Shape

The same design in Figure 4.9 will be repeated, but in this case, the circular slots will be represented as a square shape inside the circular patch as shown in Figure 4.12.

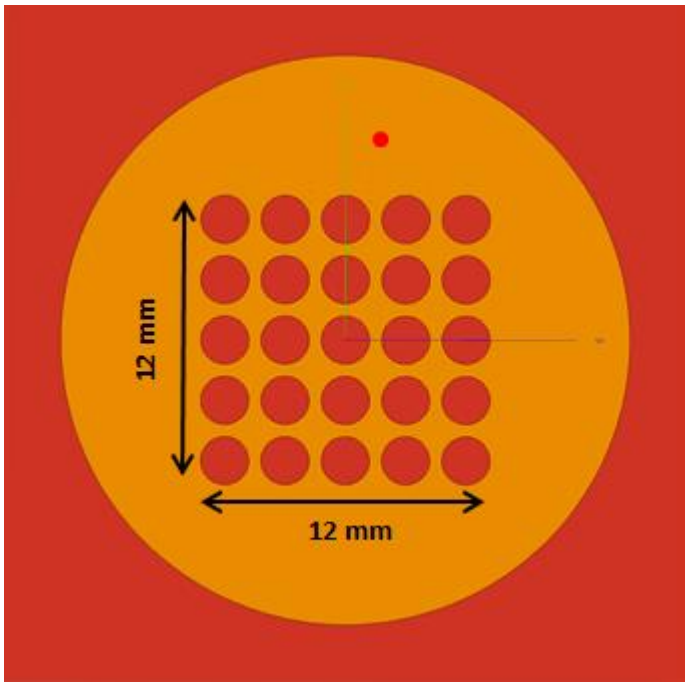

Figure 4-12: Inner circular slots in a square shape

Return loss and VSWR are reduced when compared to the results of proposed antenna as shown in Figures 4.13 and 4.14 respectively.

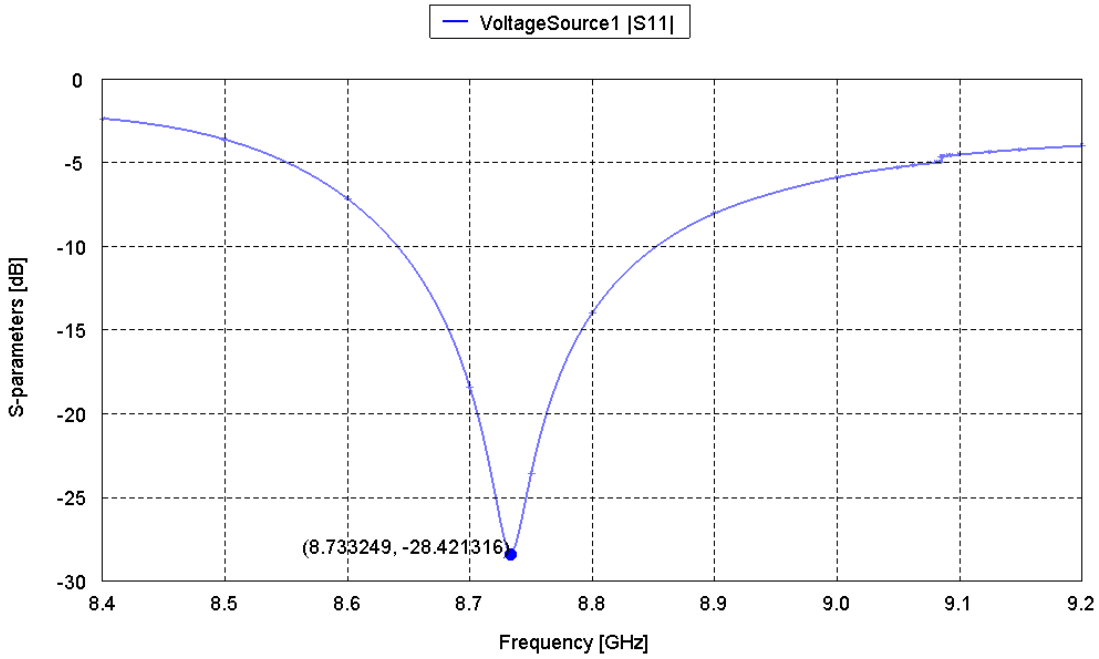

Figure 4-13: S-parameters of inner circular slots with a square shape

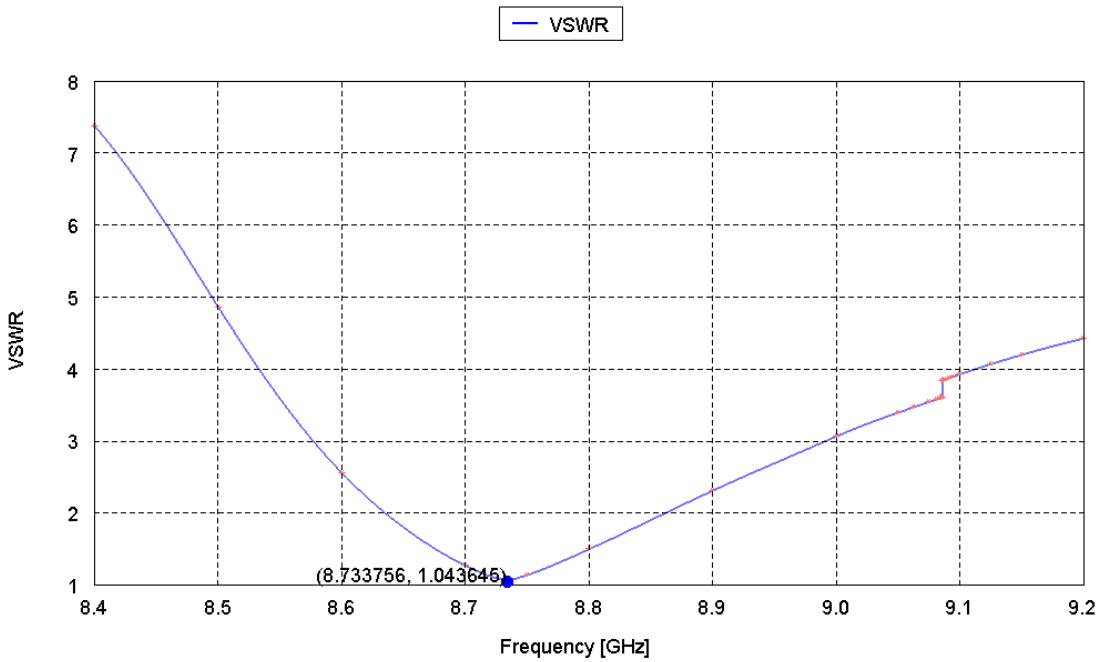

Figure 4-14: VSWR of inner circular slots with a square shape

At resonant frequency of 8.73 GHz, return loss is 28.42 dB, while the VSWR value at the same resonant frequency is 1.04.

All the results for the cases above are shown in Table 4.2.

Table 4-2: Improvement in the return loss, VSWR and bandwidth for different cases

Case	Resonant frequency (GHz)	S-parameter (dB)	VSWR	BW (MHz)
Proposed antenna	8.75	-24.73	1.09	200
Case I	8.77	-27.16	1.05	210
Case II	8.77	-27.29	1.06	220
Case III	8.73	-28.42	1.04	210

It is observed that from the above table, the maximum bandwidth was achieved in case II, which is equal to 220 MHz and both the return loss and voltage standing wave ratio were improved in case III which are equal to 28.42 dB and 1.04 respectively.

4.4 Rectangular Aperture Coupled Antenna and Gain Improvement in Wireless Applications.

Rectangular aperture coupled antenna is investigated as shown in the Figures 4.15 and 4.16 with resonant frequency at 2.21 GHz. The parametric analysis is done for each variable, antenna was simulated by FEKO software, with the evaluation of various parameters' effects on the optimization of design. The parameters are analyzed one by one, with the particular effect on antenna performance

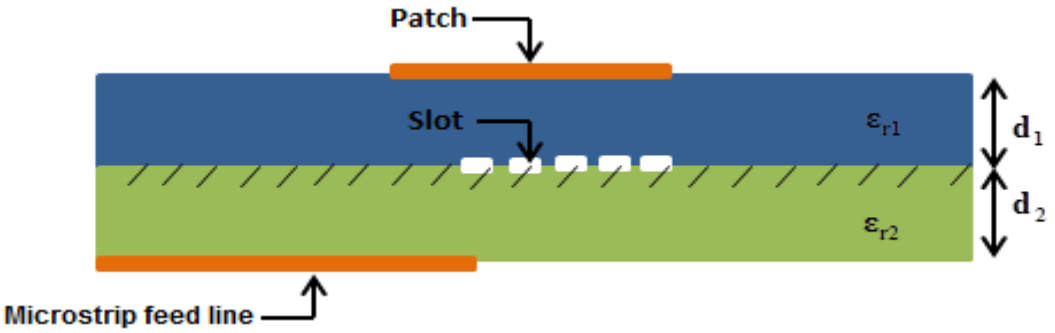

Figure 4-15: Substrate parameters of rectangular aperture coupled antenna [25]

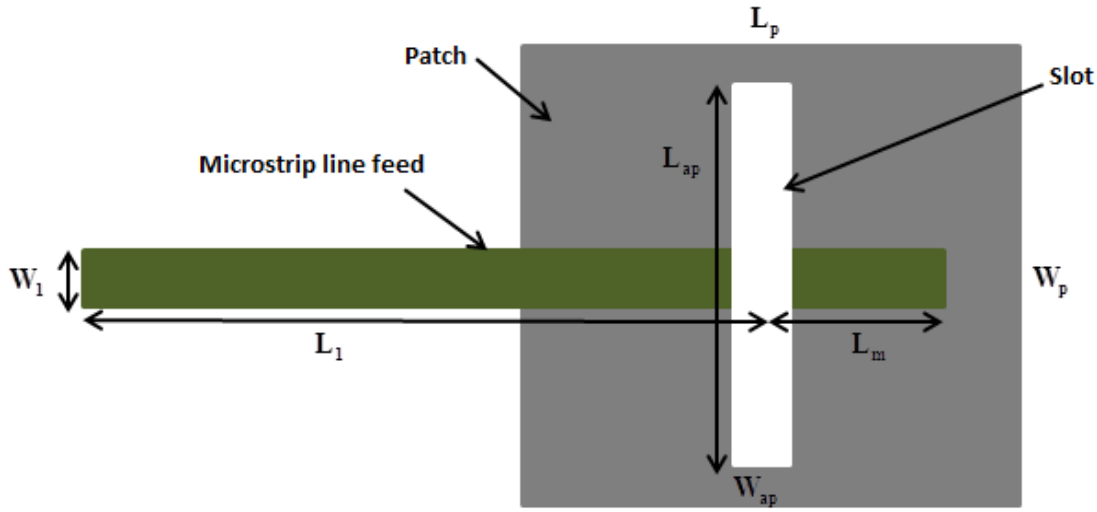

Figure 4-16: Rectangular slot aperture coupled antenna [25]

All the dimensions are explored in Table 4.3 [25].

Table 4-3: Design parameters of rectangular slot aperture coupled antenna

Design parameter	**value**
L_p = Length of the patch	30 mm
W_p = Width of the patch	40 mm
w_{ap} = Rectangular aperture width	1.55 mm
L_{ap} = Rectangular aperture length	12 mm
L_1 = Length of the feed line	50 mm
W_1 = Width of the feed line	4.42 mm
L_m = distance between the center of slot and the edge of feed line	16 mm
ε_{r1} = Dielectric constant of the first substrate	3.38
d_1 = Thickness of the first substrate	2.5 mm
ε_{r2} = Dielectric constant of the second substrate	2.54
d_2 = Thickness of the second substrate	1.6 mm
Ground width	68 mm
Ground length	68 mm

4.4.1 Effect of Rectangular Aperture Width (w_{ap}) in Microstrip Antenna

The effect of the rectangular aperture is tested in this section by taking three different values of w_{ap} as shown in Figure 4.17.

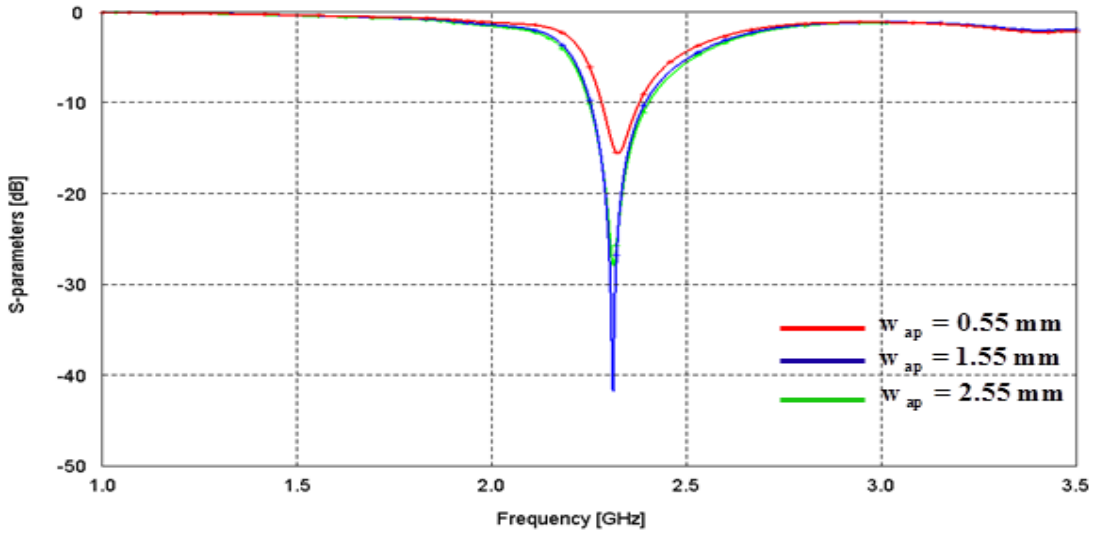

Figure 4-17: S-parameters at different values w_{ap}

Return losses for each rectangular aperture width is listed as show in Table 4.4.

Table 4-4: Results at different values of w_{ap}

w_{ap} mm	Resonant frequency (GHz)	S11 (dB)
0.55	2.32	-15.68
1.55	2.31	-42.17
2.55	2.31	-28.02

4.4.2 Effect of Rectangular Aperture Length (L_{ap}) in Microstrip Antenna

The second important parameter in rectangular aperture antenna is the length which is studied by selecting three different values and keeping the value of width fixed at 1.55 mm. Figure 4.18 and Table 4.5 shows all the results computed for this case.

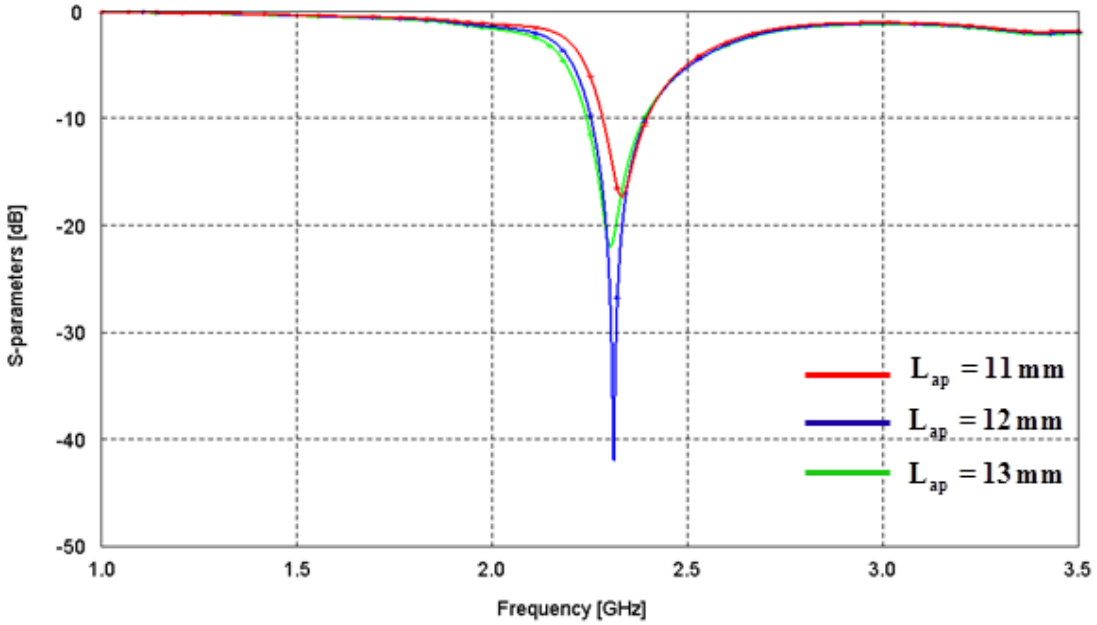

Figure 4-18: S-parameters at different values of L_{ap}

Table 4-5: Results at different values of L_{ap}

L_{ap} mm	Resonant frequency (GHz)	S11 (dB)
11	2.33	-17.73
12	2.31	-42.17
13	2.30	-22.13

It can be concluded from the results obtained in the above table that, by increasing the length of rectangular aperture, the resonant frequency will be decreased [26].

4.4.3 Effect of Length Stub (L_m) in Microstrip Antenna

L_m, represents the distance between the center of slot and the edge of feed line. By keeping the length and the width of the slot constant at 12 mm, 1.55 mm respectively and varying L_m value of the rectangular slot, S11 is obtained and resonant frequency values are shown in Table 4.6.

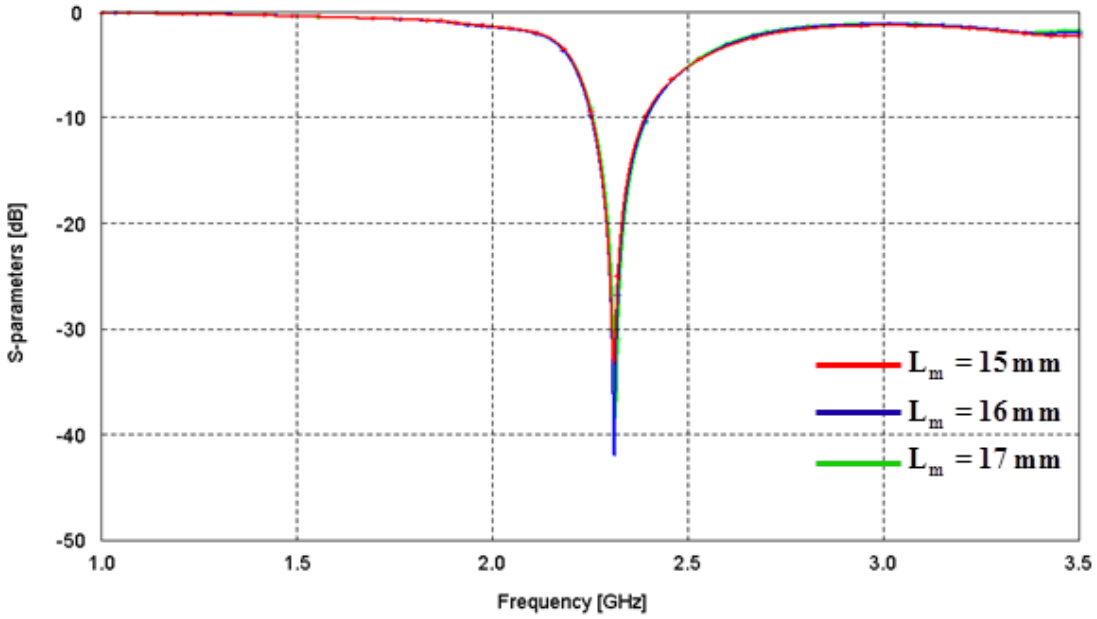

Figure 4-19: S-parameters at different values of L_m

Table 4-6: Results at different values of L_m

L_m mm	Resonant frequency (GHz)	S11 (dB)
15	2.31	-33.46
16	2.30	-42.17
17	2.31	-38.60

4.4.4 Gain Improvement by using Different Shapes of Aperture Slot Antenna

In this section, new loads of aperture slots have been proposed to improve the performance of the antenna. i.e. the gain. One of the disadvantages of the patch antenna is surface waves which are undesirable. During the radiation from the radiating patch antenna, part of the total available radiated power becomes trapped on the surface of the substrate.

An increase in the side lobe level, limitations in gain and efficiency, increase in cross polarization and limited bandwidth are the main disadvantages of surface waves. Defected ground structures with different shapes are used to increase the value of the gain. The gain of a rectangular aperture at four values of frequencies are shown in Figure 4.20.

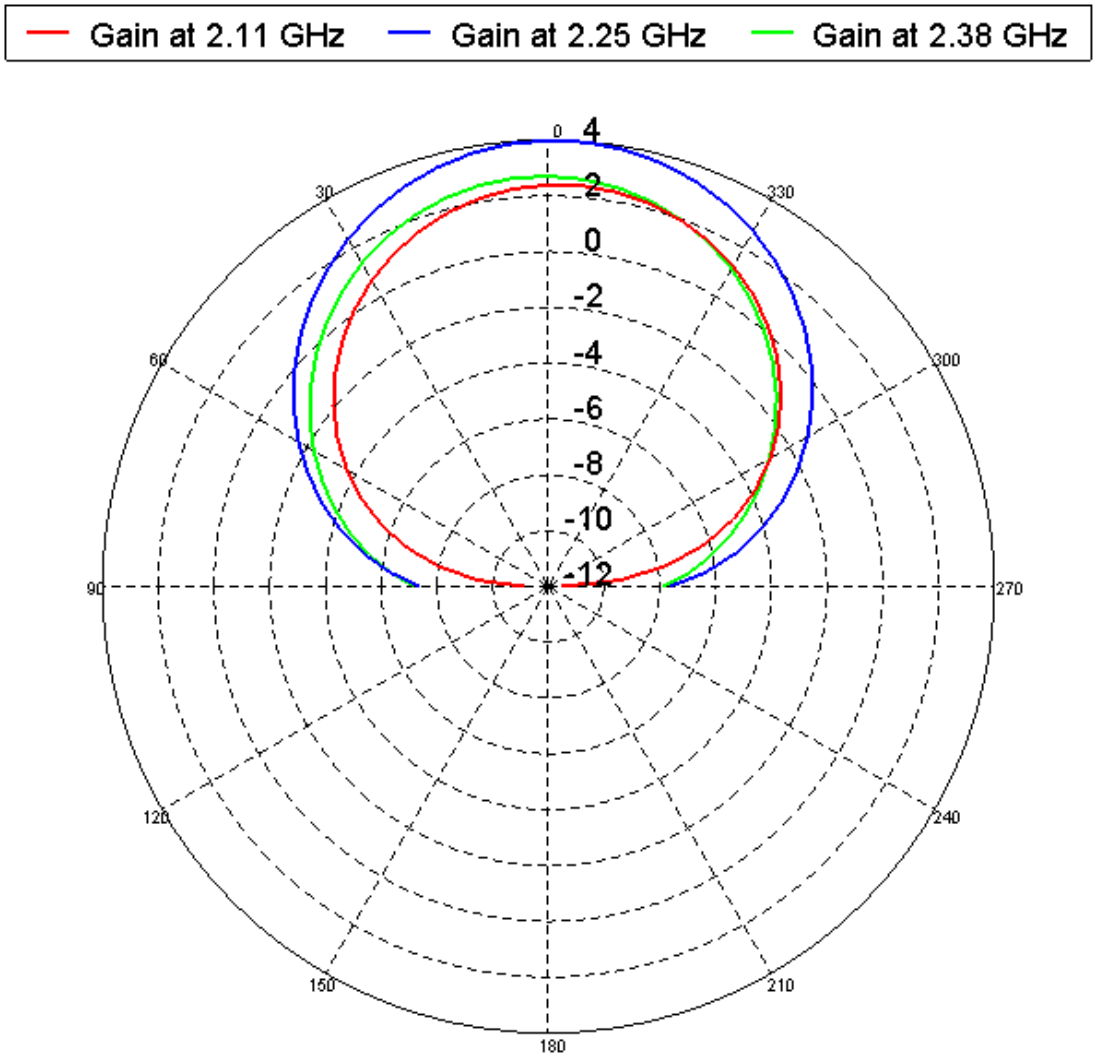

Figure 4-20: Gain values for rectangular slot shape in x-y plane

4.4.4.1 Phi-Shape Slot

In this section Phi-Shape cut will be considered from the ground plane as shown in Figure 4.21. Gain was studied at frequencies 2.11 GHz, 2.25 GHz and 2.38 GHz as shown in Figure 4.23.

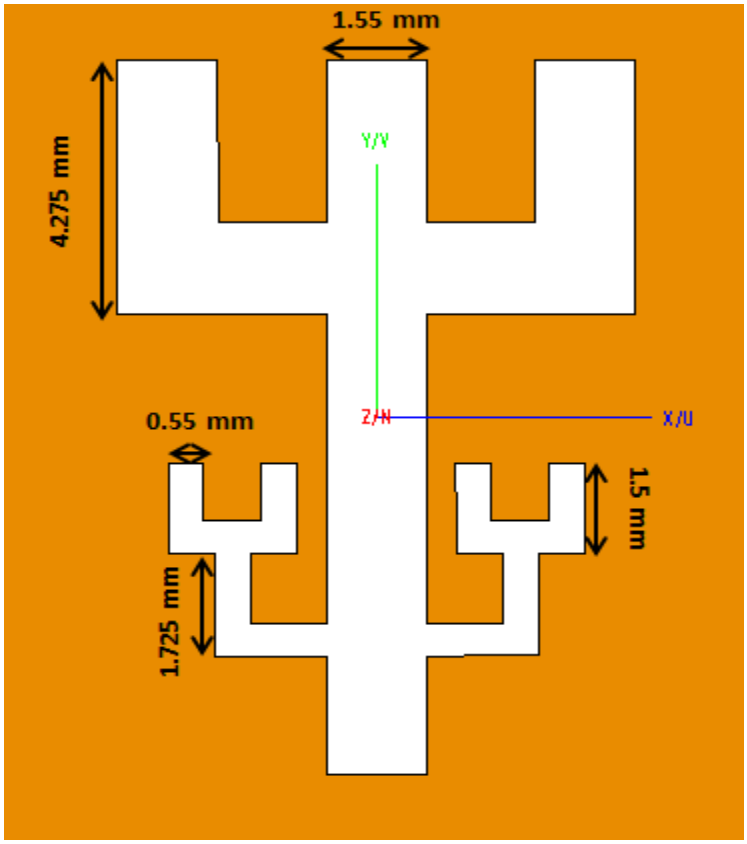

Figure 4-21: Phi-shape slot

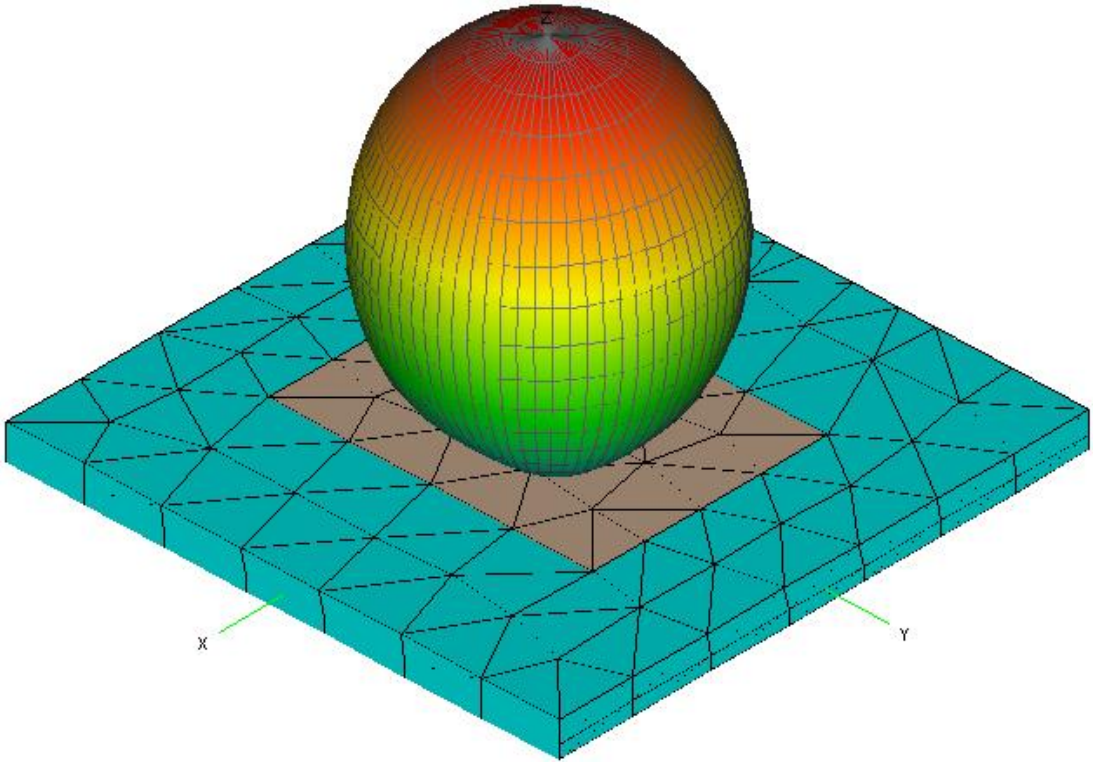

Figure 4-22: 3-D Radiation pattern of Phi-shape slot in FEKO

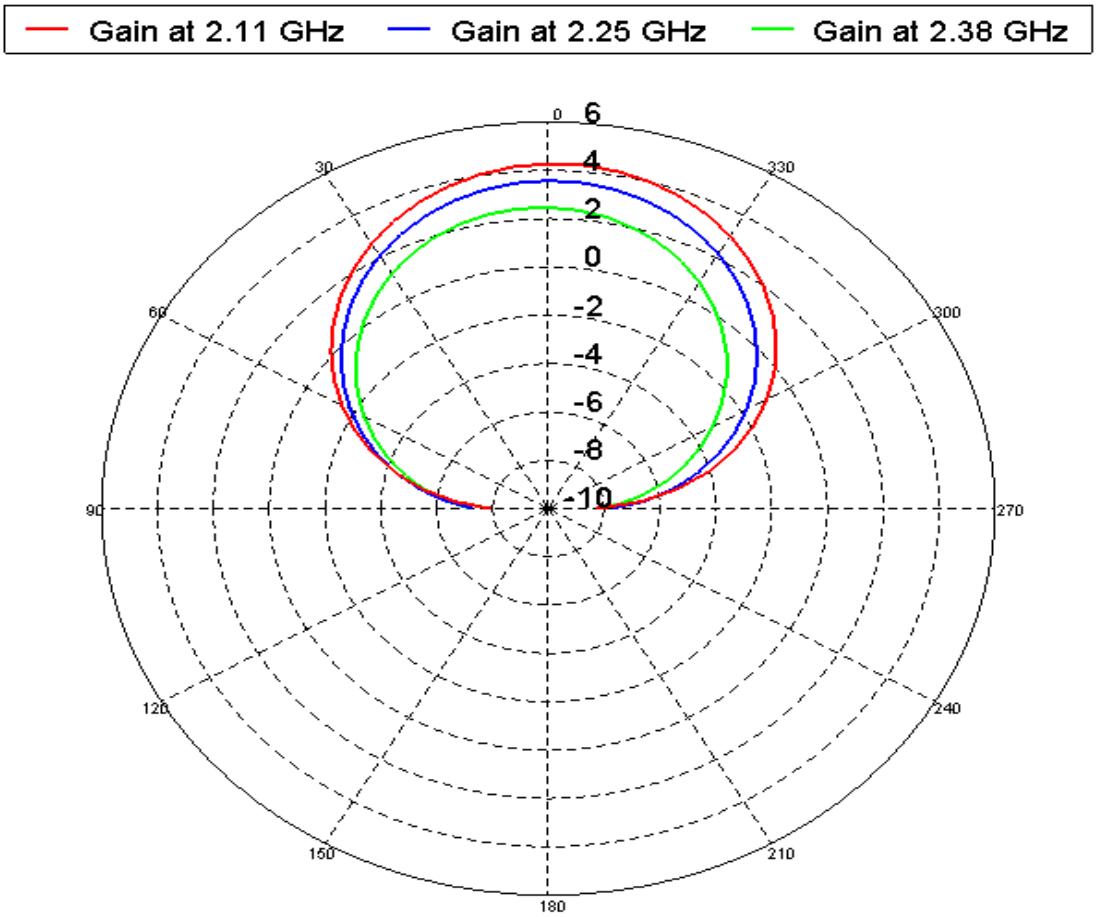

Figure 4-23: Gain values for Phi-shape slot in x-y plane

4.4.4.2 C-Shape Slot

The second shape cut from the ground plane is C-Shape, which consists of two opposite C-shaped halves having a length equal to 12.275 mm and width equal to 2.275 mm as shown in Figure 4.24.

The gain was calculated as shown in Figure 4.26.

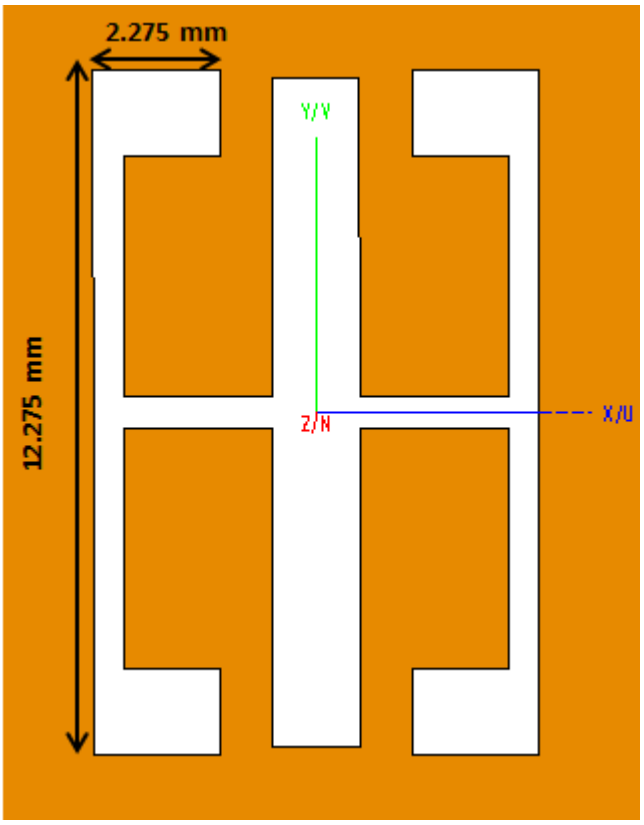

Figure 4-24: C-shape slot

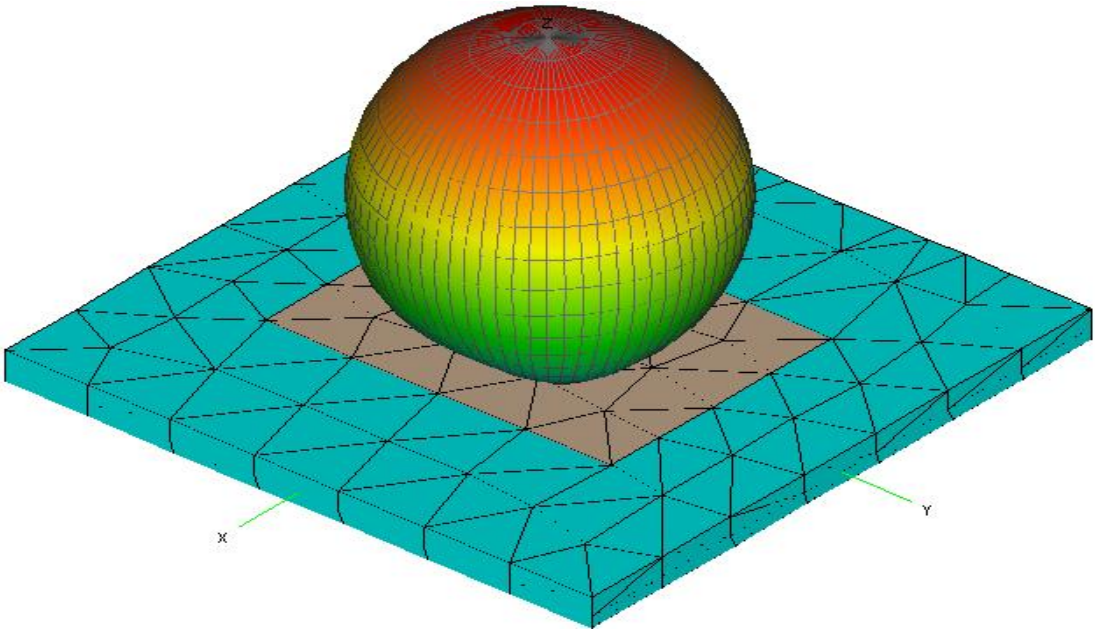

Figure 4-25: 3-D Radiation pattern of C-shaped slot in FEKO

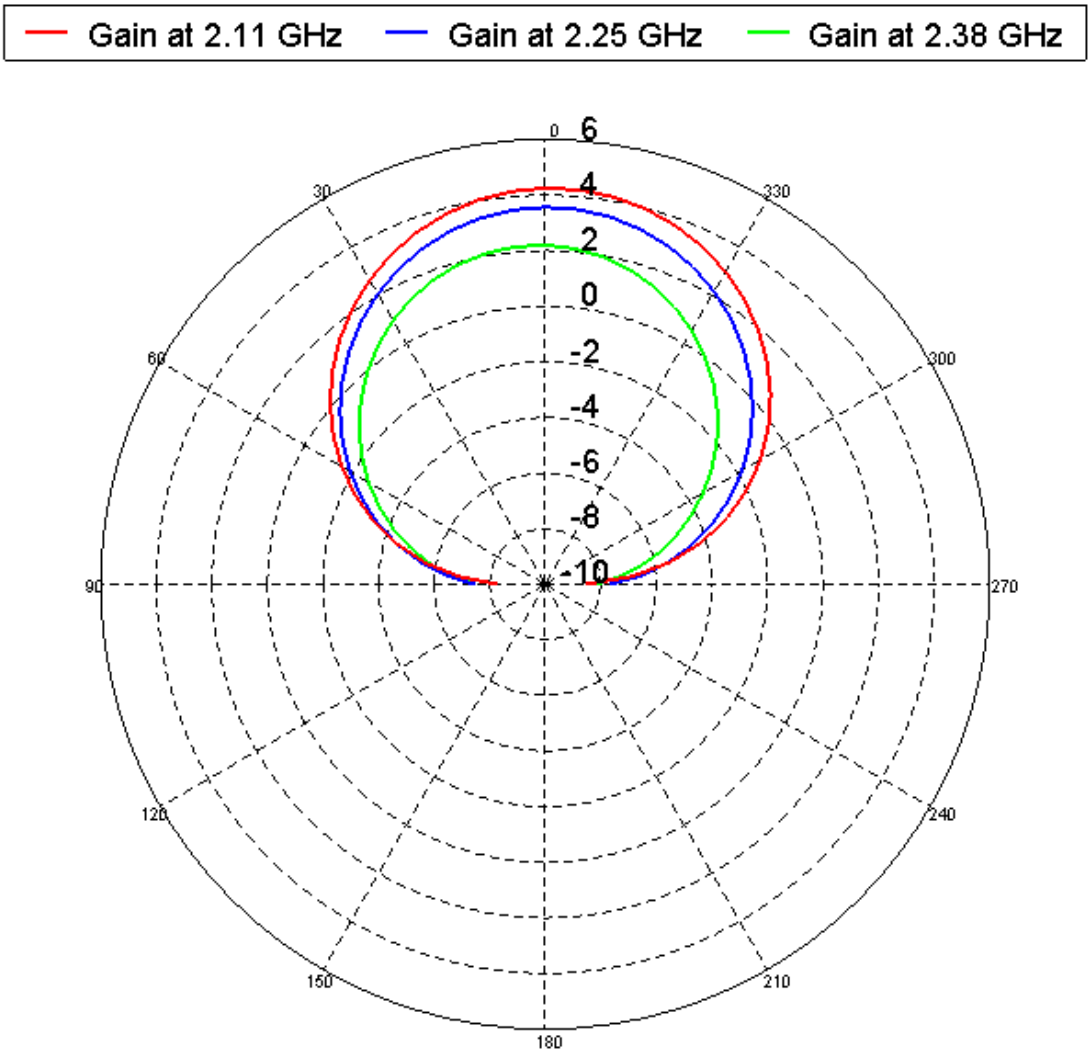

Figure 4-26: Gain value for C-shaped slot in x-y plane

4.4.4.3 Plus-Shape Slot

Gain at frequencies 2.11, 2.25 GHz and 2.38 GHz was achieved by using the Plus-Shape slot. The structure of the slot is explained clearly in Figure 4.27. Figure 4.29 shows the value of the gain at each frequency.

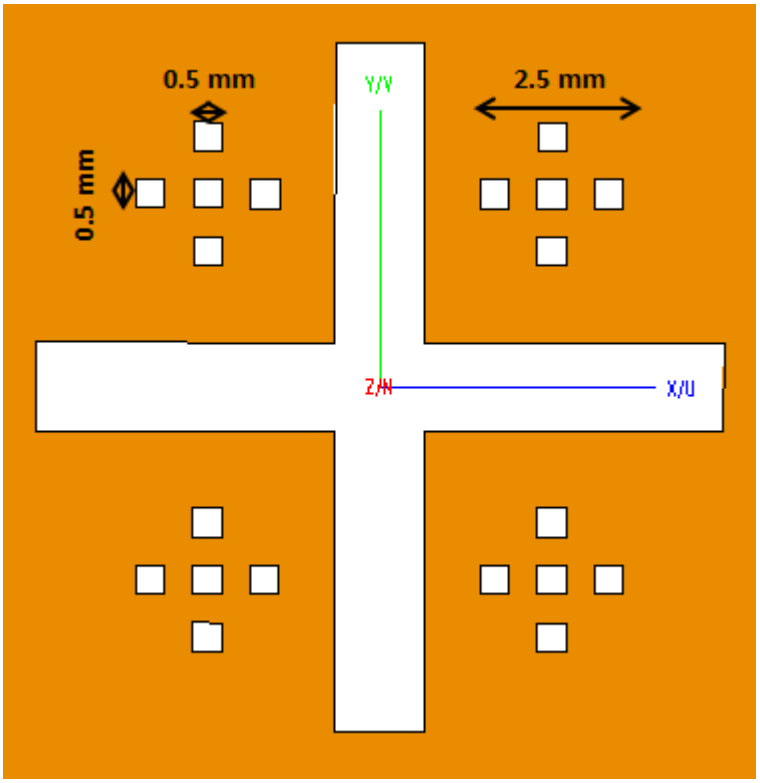

Figure 4-27: Plus-shaped slot

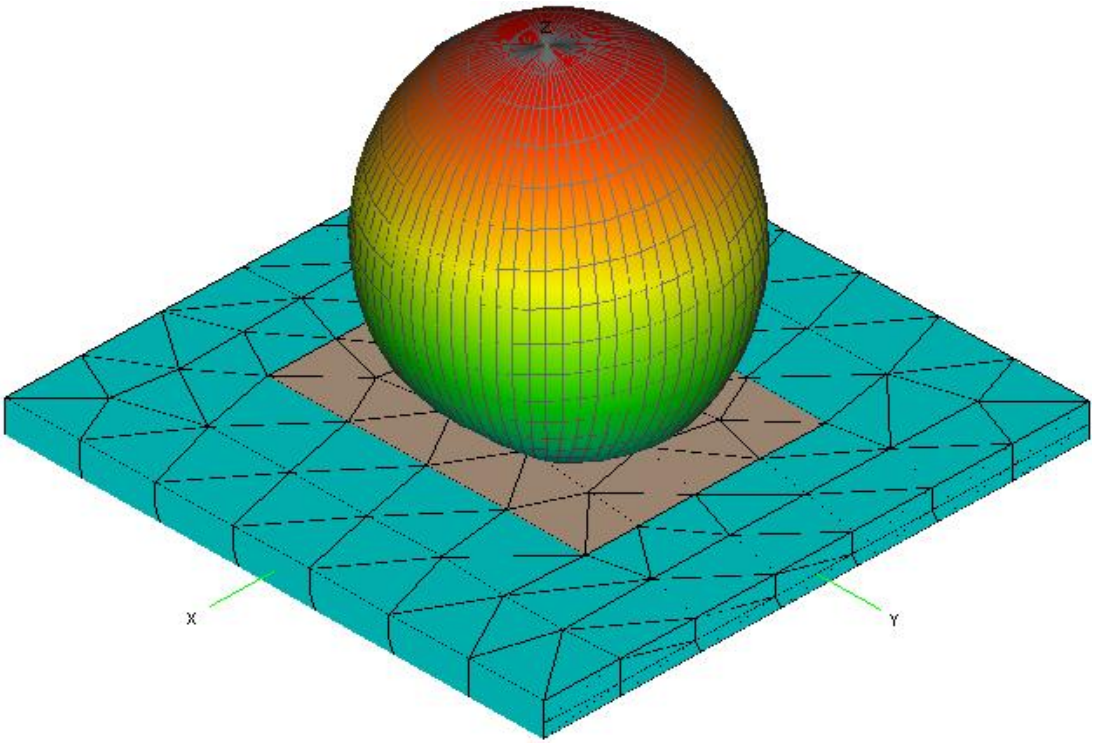

Figure 4-28: 3-D Radiation pattern of the plus-shaped slot in FEKO

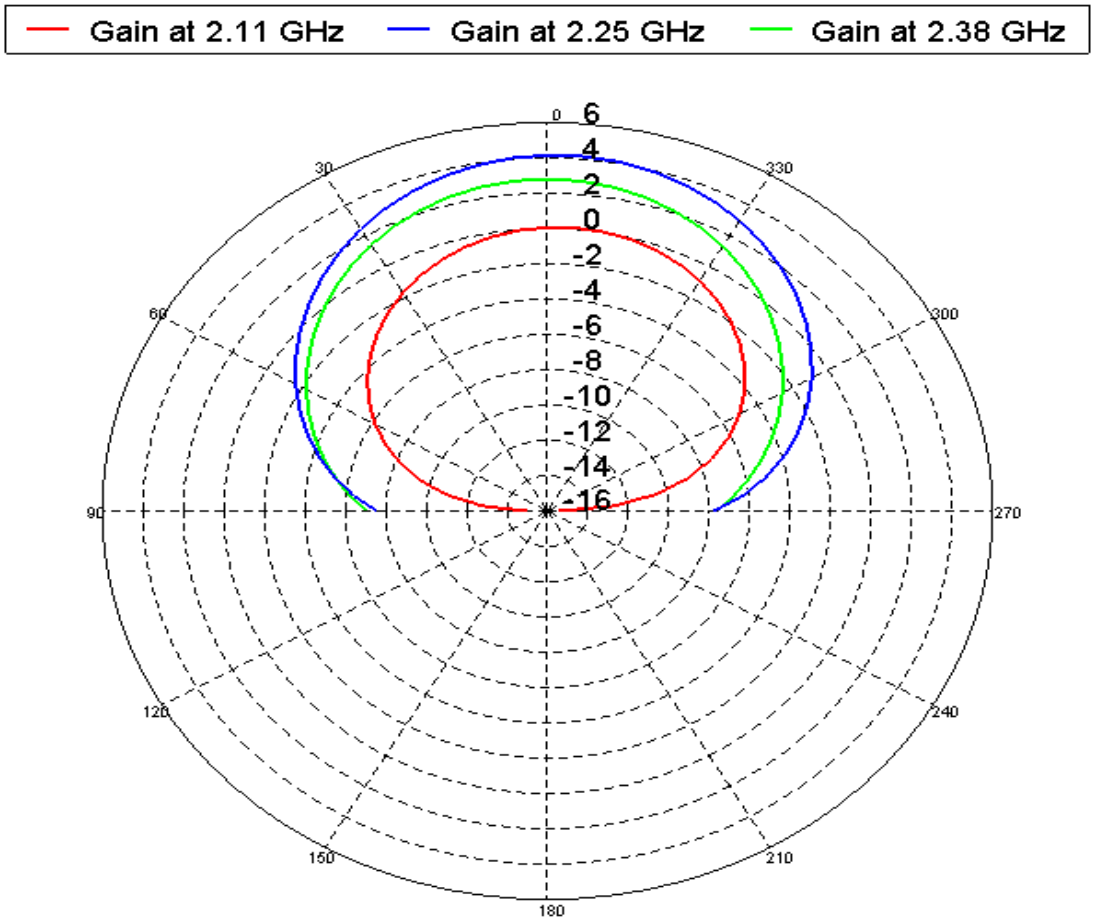

Figure 4-29: Gain values for plus-shaped slot in x-y plane

All the results are listed in the Table 4.7:

Table 4-7: Gain at different shapes of ground aperture

Rectangular slot	**Frequency (GHz)**	2.11	2.25	2.38
	Gain (dB)	2.4	4	2.7
Phi-shape slot	**Frequency (GHz)**	2.11	2.25	2.38
	Gain (dB)	4.3	3.6	2.5
C-shape slot	**Frequency (GHz)**	2.11	2.25	2.38
	Gain (dB)	4.2	3.6	2.2
Plus-shape slot	**Frequency (GHz)**	2.11	2.25	2.38
	Gain (dB)	0.1	4.2	2.8

It is observed that, the maximum gain at frequency 2.11 GHz was obtained by using phi-shape slot which is equal to 4.3 dB, while the maximum gain at 2.25 GHz and 2.38 GHz were achieved by using plus-shape slot which are equal to 4.2 and 2.8 respectively.

Chapter 5

PATCH ARRAY ANTENNA

This technological trend has focused much effort into the design of a microstrip patch antenna. The objective of this study is to design, and simulate an inset fed rectangular microstrip patch antenna based on FEKO software with four element array. Patch array, consists of a number of patch elements which are combined with transmission lines to improve the performance of the antenna.

Yahya S. H. Khraisat (January, 2012) designed a 4 element rectangular microstrip patch antenna with high gain for 2.4 GHz applications [27]. In the beginning, he set the antenna as a single patch, and after checked the results for antenna features; such as return losses and gain, he turned it to 2 X 1 array. Finally, 4 X 1 array was designed to have better antenna performance at element distances equal to 2λ. All the results of literature study are shown as in the Table 5.1.

Table 5-1: Literature results of a single patch, (2 X 1) array patch and (4 X 1) array patch at 2.4 GHz

Case	S-parameter (dB)	Gain (dB)
Single	-16.624	5.1877
2X1 array	-9.5	9.186
4X1 array	-22	13.2

5.1 Analysis and Design of a Single Microstrip Patch Antenna

In this thesis, a new designs is suggested for at 2 GHz applications. The element distances are reduced to 0.72λ. Figure 5.1 shows that the single patch at 2 GHz, Transmission Line model is used to analyze the patch antenna which was designed by using FEKO software with dimensions (L X W), the Relative permittivity (ε_r) and substrate thickness (h). The infinity ground plane is applied in this design. Microstrip line inset feed $L_f X W_f$ is used to excite the antenna. Table 5.2 shows all design parameters.

Table 5-2: Single patch antenna design parameters

Parameter	**Value**
Operating frequency (f_o)	2 GHz
Patch width (W)	59.29 mm
Patch length (L)	49.78 mm
Feed line width (W_f)	4.977 mm
Feed line length (L_f)	30 mm
Relative permittivity (ε_r)	2.2
Substarte thickness (h)	1.65 mm

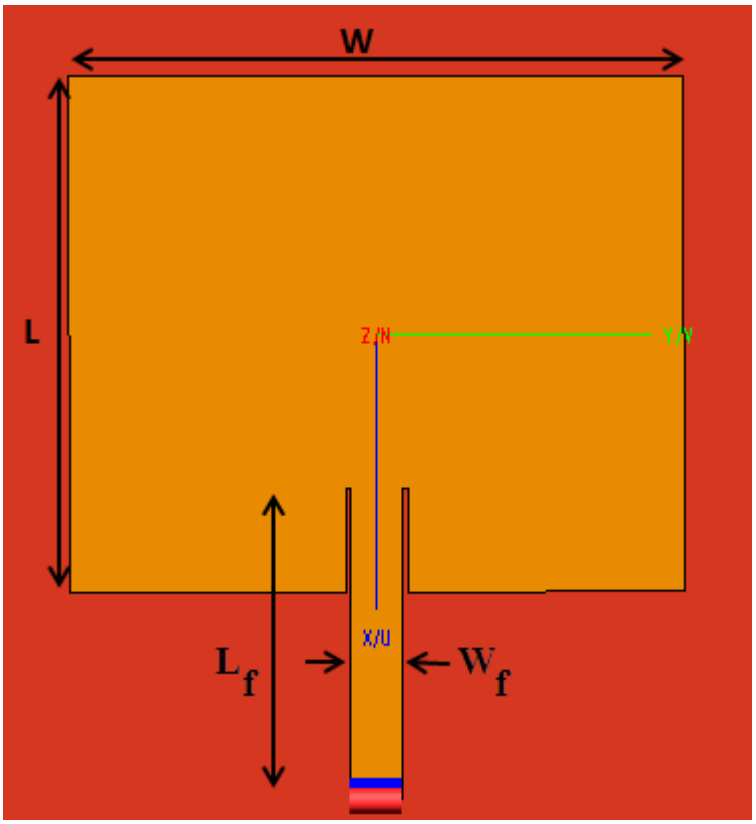

Figure 5-1: Single patch antenna at 2 GHz in FEKO

From the output results of a single patch antenna, the value of a return loss at 2.01 GHz is -8.70 dB and the gain is 7.1 dB.

5.2 Patch Array (2 X 1)

In this case, two elements of patch antenna were used to improve the radiation parameters as shown in Figure 5.2. A transmission line is used to connect the patches as a network.

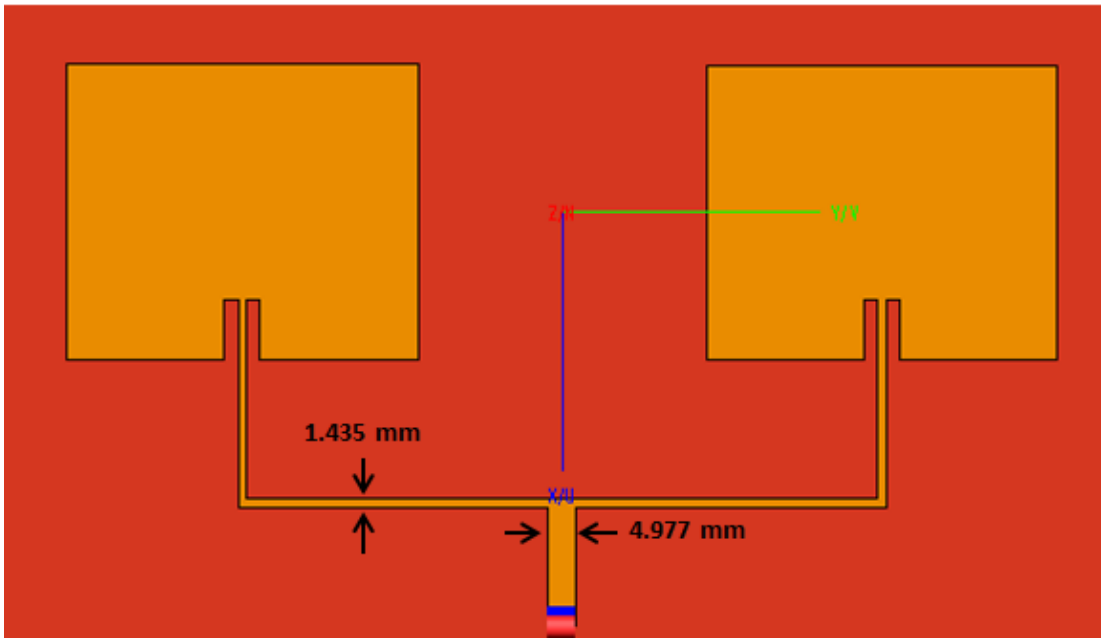

Figure 5-2: Patch array (2 X 1) in FEKO

It is possible to observe that the value of the return loss is reduced to -26.78 dB at 2 GHz and the antenna gain is improved by 3.2dB.

5.3 Patch Array (4X 1)

Finally, four element array was used as shown in Figure 5-3.

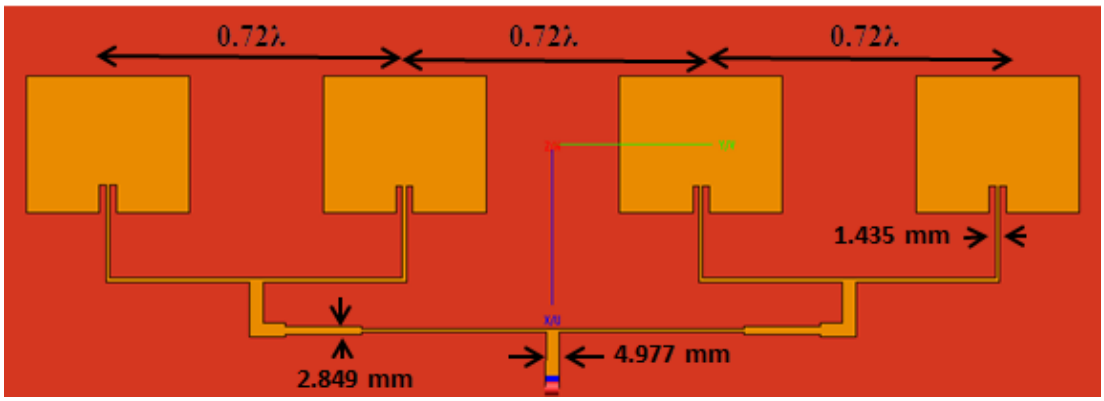

Figure 5-3: Patch array (4 x 1) in FEKO

Quarter wave transformer is used for matching the impedance between the transmission lines which have the length equal to $\left(\lambda_g / 4\right)$, the impedance of this transformer can be calculate by Equation 5.1:

$$Z_c = \sqrt{Z_1 Z_2} \tag{5.1}$$

The width of microstrip line can be calculated using Equations 5.2-5-4 shown below:

$$Z_o = \frac{60}{\sqrt{\varepsilon_e}} \ln\left(\frac{8H}{W} + \frac{W}{4H}\right)\Omega \qquad \text{if } \frac{W}{L} \leq 1 \tag{5.2}$$

$$Z_o = \frac{120\pi}{\sqrt{\varepsilon_e}} \left[\frac{1}{\left(\frac{W}{H}\right) + 1.393 + 0.667 \ln\left(\frac{W}{H} + 1.444\right)}\right]\Omega \qquad \text{if } \frac{W}{L} > 1 \tag{5.3}$$

$$\varepsilon_e = \frac{\varepsilon_r + 1}{2} + \frac{\varepsilon_r - 1}{2\sqrt{1 + \left(10H/W\right)}} \tag{5.4}$$

It can be observed from Figure 5.4 that, the return loss reduces gradually by increasing the number of patch elements, all the results are shown in Table 5.3.

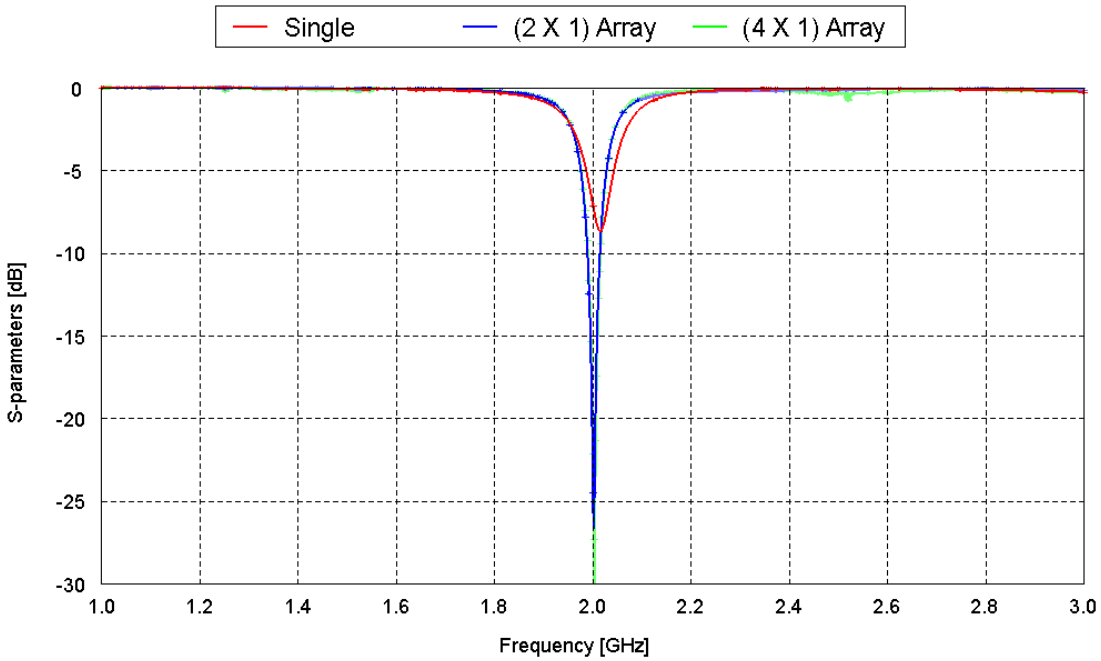

Figure 5-4: S-parameters of a single patch, (2 X 1) patch array and (4 X 1) patch array

A significant improvement was observed in the gain for 4X1 array elements as shown by Figure 5.5. The gain is improved from 7.1dB to 13.1dB and the return loss becomes -29.94 at 2 GHz. The results are summarized by Table 5.3.

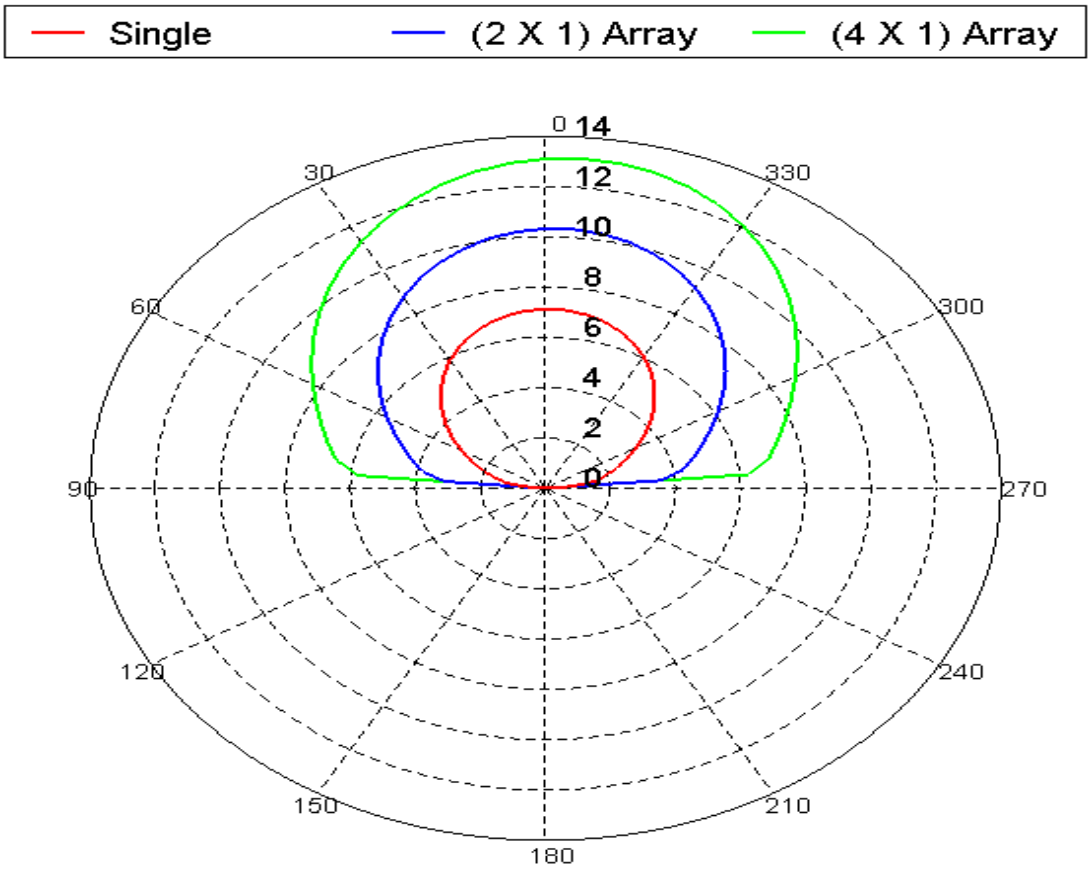

Figure 5-5: Antenna gain of single patch, (2 X 1) array patch and (4 X 1) array patch in x-y plane

Table 5-3: Summary results of a single patch, (2 X 1) array patch and (4 X 1) array patch at 2 GHz

Case	**Resonant frequency (GHz)**	**S-parameter (dB)**	**Gain (dB)**
Single	2.01	-8.70	7.1
2 X 1 array	2	-26.78	10.3
4 X 1 array	2	-29.94	13.1

Figures 5.6-5.8 demonstrates the 3D electric field patterns. The increase in the directivity of the pattern can be observed when the number of elements were increased.

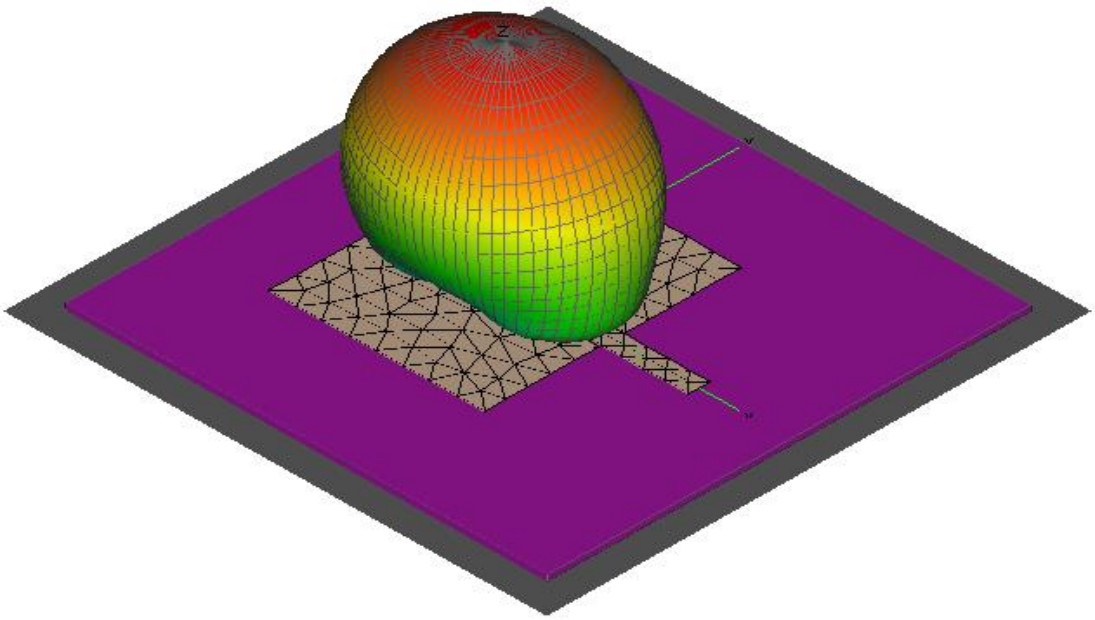

Figure 5-6: 3-D Radiation pattern of a single patch antenna

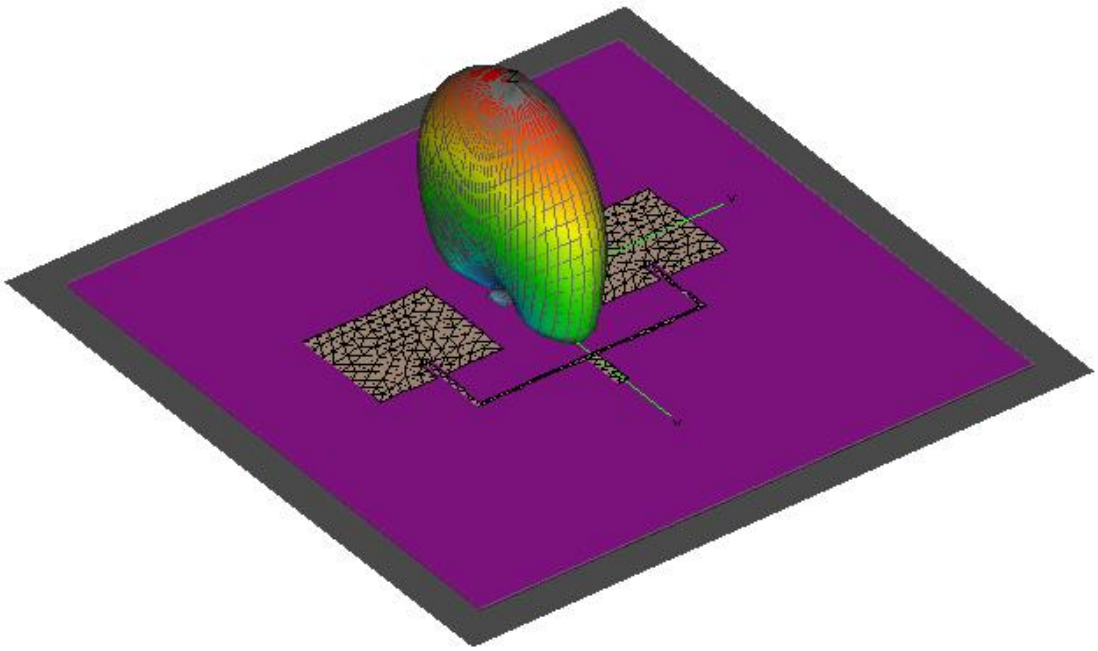

Figure 5-7: 3-D Radiation pattern of (2 X 1) array patch antenna

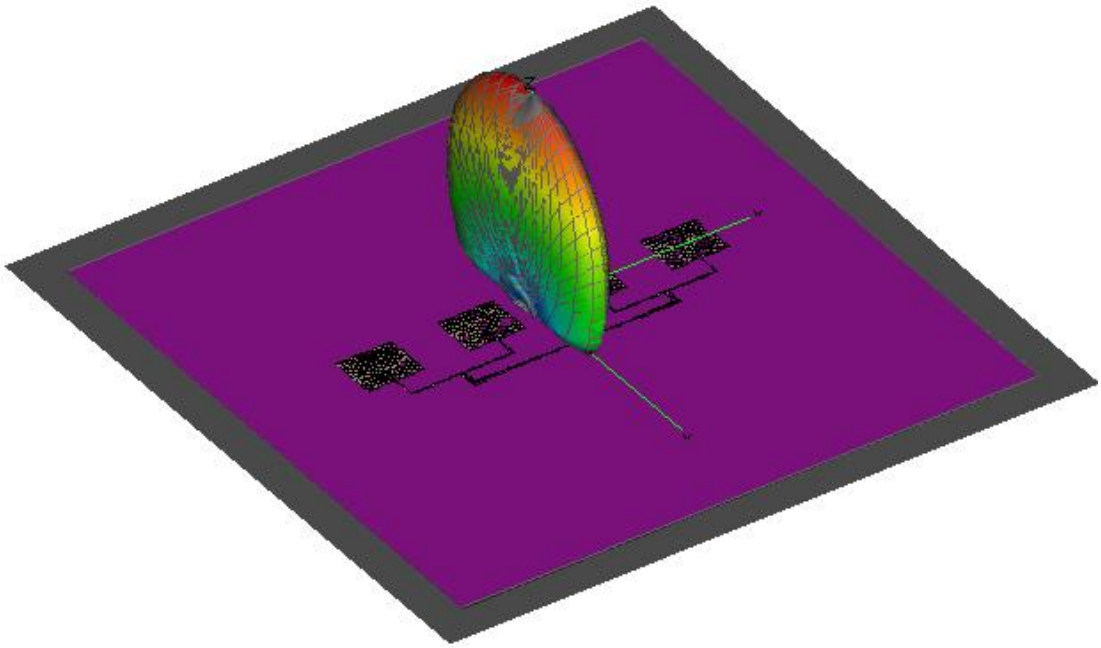

Figure 5-8: 3-D Radiation pattern of (4 X 1) array patch antenna

Chapter 6

CONCLUSION AND FUTURE WORK

6.1 Conclusion

In this thesis, microstrip patch antennas have been simulated in different structures by using FEKO software. The effective dielectric constant concept has been introduced, was simulated for different patch antenna structures. The resonant frequencies, for a single and multi-substrate layers and different patch geometries (circular, triangular and square) have been calculated based on the FEKO simulation results and compared with the published results.

For study and improve the antenna performance, slot antennas were proposed. They can be cut out of whatever surface they are to be mounted on. Triangular and square shaped slot antenna were stimulated by FEKO, and after the evaluation, it can observed that, the slot size was affected the value of effective permittivity, which was close to the published result for the triangular slot.

The resonance frequency of a rectangular patch antenna decreased gradually when the height of the triangular slot loading area at the one edge of radiating patch was increased because the current was lengthen which forced the current lines to bend. Also, different slot structures were applied inside the circular patch to improve the return loss, voltage standing wave ratio and the bandwidth. It was observed that the maximum bandwidth was 220 MHz and the return loss, voltage standing wave ratio (VSWR) was improved to -28.42 dB and 1.04 respectively as the maximum values compared to the conventional antenna.

Defected ground structure (DGS) is a technique used to solve the surface wave problem. In a rectangular patch antenna, four shapes of ground apertures (rectangular, phi-shape, c-shape and plus-shape) were considered to improve the gain. It was noted that the maximum values of gain are (4.3, 4.2 and 2.8) dB at resonant frequencies (2.11, 2.25 and 2.38) GHz respectively.

Due to the importance of the feed positions and types on the performance of antennas, FEKO was used to simulate two rectangular patch antennas with two types of feeding (coaxial cable and microstrip line feed). Single and dual band of frequencies were achieved in both cases at different feed positions.

Patch array is a topology used to increase the gain. In this thesis rectangular patch antenna was designed at 2 GHz based transmission line model, initially single patch element was simulated by FEKO software and the value of the gain at this time 7.1 dB, after it was transformed to 2X1 patch array and 10.3 dB was achieved. Finally the maximum value of the gain was realized in 4X1 patch array which was equal to 13.1 dB. It is concluded that the gain value increases when the number of patch elements is increased due to an increase in the electrical size of the antenna. Also, it is observed that in the study the value of return loss was improved gradually by increasing the patch elements up to -29.94 dB.

6.2 Future Work

In future work, new designs of triangular and circular patches array will be simulated and compared with the proposed design of rectangular patch array in this thesis to show the effects on the gain, bandwidth, return loss and other radiation parameters.

REFERENCES

[1] D. M. Pozar, "Microstrip Antennas," *Proc. IEEE*, vol. 80, no. 1, pp. 79-81, Jan 1992.

[2] J. Q. Howell, "Microstrip antennas," *IEEE APS Int. Symp. Digest*, pp. 177-180, 1972.

[3] R. E. Munson, "Conformal Microstrip Antennas and Microstrip Phased Arrays," *IEEE Transactions on Antennas and Propagation*, vol. 22, no. 1, pp. 74-78, Jan 1974.

[4] The antenna history [Online], http://www.antenna-theory.com/intro/history.php, Retrieved on Nov 2013.

[5] Constantine A. Balanis, *Antenna theory: Analysis and Design*. Hoboken: NJ: Wiley, 2005.

[6] MANIK GUJRAL, "Bandwidth Enhancement of Dual Patch Microstrip Antenna Array Using Dummy EBG Patterns on Feedline," NATIONAL UNIVERSITY OF SINGAPORE, Rourkela, Master's Thesis 2007.

[7] [Online], http://www.microwaves101.com/encyclopedia/antenna_ustrip.cfm, Retrieved on Nov 2013.

[8] Asad ullah Noor, "Design of Microstrip Patch Antennascat 5.8 GHz," Kapsch TrafficComm AB, Jönköping, Sweden, Master's Thesis.

[9] Vivekananda Lanka Subrahmanya, "Pattern Analysis of "The Rectangular Microstrip Patch Antenna"," University College of Boras, Boras, Master's Thesis January 2009.

[10] Ahmed Fatthi Alsager, "Design and Analysis of Microstrip Patch Antenna Arrays," University College of Borås, BORÅS, Master's Thesis 2011.

[11] Tanveer Kour Raina, "Design, Fabrication and Performance Evaluation of Micro-Strip Patch Antenna for Wireless Applications Using Aperture Coupled Feed," Thapar University, PATIALA, Master's Thesis 2012.

[12] Nikolova, "Transmission-Line Model. Design Procedure for A rectangular Patch. Cavity Model for A rectangular Patch," LECTURE 21: Microstrip Antennas – PART II 2010.

[13] Overview of FEKO [Online], http://feko.info/product-detail/overview-of-feko, Retrieved on Des 2013.

[14] Shubham Gupta and Shilpa Singh, "Bandwidth Enhancement in Multilayer Microstrip Proximity Coupled Array," in *International Journal of Electronics and Computer Science Engineering*, Mar 2012, pp. 287-293.

[15] Wen-Shan Chen and Fu-Mao Hsieh, "A broadband Design for a printed Isosceles Triangular Slot Antenna for Wireless Communications," in *Microwave Journal*, July 2005.

[16] S. Banik and M. Biswas, "The Resonant Frequency of a Circular Patch on Composite and Suspended Substrate," in *Antenna Test and Measurement Society*, 2012, pp. 1-4.

[17] David M. Pozar, *Microwave Engineering: Transmission Line and Waveguides*, 3rd ed.: WILEY, 2005, ch. 3.

[18] A. Sukla and M. Biswas, "Cad Model to Compute the Resonant Frequency of Cavity Backing Triangular Patch Antenna," in *Antenna Test and Measurement Society*, 2012, pp. 1-4.

[19] Samir Dev Gupta, Anvesh Garg and Anurag P.Saran, "Improvement in Accuracy for Design of Multidielectric Layers Microstrip patch Antenna," *International Journal of Microwave and Optical Technology*, vol. 3, no. 5, pp. 498-504, November 2008.

[20] M. Kirschning and R. H. Jansen, "Accurate Model for Effective Dielectric Constant of Microstrip with Validity up to Millimeter Wave Frequencies," *Electronics Letters*, vol. 18, pp. 272-273, 1982.

[21] Nitin Agarwal, D.C.Dhubkarya and Sanjay Garg, "Pattern Analysis of Rectangular Microstrip Antenna for 3G Frequency," *International Journal of Innovations in Engineering and Technology*, vol. 1, no. 4, pp. 72-76, Dec 2012.

[22] Ashish Kumar, "Rectangular Microstrip Patch Antenna using 'L' Slot Structure," *Journal of Research in Electrical and Electronics Engineering*, vol. 2, no. 2, pp. 15-18, March 2013.

[23] S.Bhunia, "Effects of Slot Loading on Microstrip Patch Antennas," *International Journal of Wired and Wireless Communications*, vol. 1, no. 1, pp. 1-6, October 2012.

[24] Sachin S. Khade and S.L.Badjate, "Modeling and Design of Annular Ring Microstrip Antenna," in *National Conference on Innovative Paradigms in Engineering and Technology, Proceedings Published by International Journal of Computer Applications*, 2012, pp. 18-21.

[25] Naveen Hemrajani, Sandhya Sharma, Rashid Hussain and Ravi Kumar, "Bandwidth Enhancement in Wireless Applications by using H-Shape Slot Microstrip Aperture Coupled Antenna," *Journal of Engineering Research and Applications*, vol. 2, no. 5, pp. 1932-1935, 2012.

[26] Meltem Yildirim, "Design of Dual Polarized Wideband Microstrip Antennas," Middle East Technical University, Northern Cyprus, Master's Thesis June 2010.

[27] Yahya S. H. Khraisat, "Design of 4 Elements Rectangular Microstrip Patch Antenna with High Gainfor 2.4 GHz Applications," *Modern Applied Science*, vol. 6, no. 1, pp. 68-74, January 2012.

APPENDICES

Appendix A: Band designations (Approximate)

Medium frequency	300 KHz to 3 MHz
High frequency (HF)	3 MHz to 30 MHz
Very high frequency (VHF)	30 MHz to 300 MHz
Ultra high frequency (UHF)	300 MHz to 3 GHz
L band	1-2 GHz
S band	2-4 GHz
C band	4-8 GHz
X band	8-12 GHz
Ku band	12-18 GHz
K band	18-26 GHz
Ka band	26-40 GHz
U band	40-60 GHz
V band	50-75 GHz
E band	60-90 GHz
W band	75-110 GHz
F band	90-140 GHz

Appendix B: Roots Derivatives of Bessel functions

m\n	**n=1**	**n=2**	**n=3**	**n=4**	**n=5**
m=0	3.8317	7.0155	10.1734	13.3236	16.4706
m=1	1.8411	5.3314	8.5363	11.7060	14.8635
m=2	3.0542	6.7061	9.9694	13.1703	16.3475
m=3	4.2011	8.0152	11.3459	14.5858	17.7887
m=4	5.3175	9.2823	12.6819	15.9641	19.1960
m=5	6.4156	10.5198	13.9871	17.3128	20.5755
m=6	7.5012	11.7349	15.2681	18.6374	21.9317
m=7	8.5778	12.9323	16.5293	19.9418	23.2680
m=8	9.6474	4.1155	17.7740	21.2290	24.5871
m=9	10.7114	15.2867	19.0045	22.5013	25.8912
m=10	11.7708	16.4478	20.2230	23.7607	27.1820